Oxo, Imido, and Borollide Complexes of Tantalum and Zirconium

Thesis by

Roger W. Quan

In Partial Fulfillment of the
Requirements for the Degree of
Doctor of Philosophy

Division of Chemistry
and Chemical Engineering

California Institute of Technology
Pasadena, California

1994
(Submitted November 1. 1993)

For Dad, Mom, William, Feng, and Tony

I shall pass through this world but once.
Any good that I can do, or any kindness that I can show
another human being, let me do it now and not defer it.
For I shall not pass this way again.

Author unknown

First, I want to thank John Bercaw for giving me the opportunity to work in the group. John is a great advisor and leader for the group, providing the optimal situation for a graduate student to grow and learn from him, other graduate students and post-docs within the group.

Other members of the Caltech faculty and staff who have helped during my stay include Bill Schaefer, Dick Marsh, and Larry Henling for solving the crystal structures which are shown in these chapters. Fenton Harvey assisted in all of the analyses. Joe Ziller at the Univerisity of California-Irvine solved the second structure in Chapter 3 and Terry Burkhardt at Exxon obtained the GPC data for the polyethylene samples in Chapter 4.

Former and current Bercaw group members have been instrumental in my learning and experience here. LeRoy Whinnery was a guiding hand during my initial experiences with handling reactions on the vacuum line. Pam Shapiro was a source of inspiration through candidacy. In 213, Donnie Cotter worked on the line with me and put up with me listening to Pirate Radio until he could stand it no more and left to work with Sharad!!! (Just kidding.) Without Bryan Coughlin, it would have been quite different working here. During our five years here, it seems like I was always asking Bryan questions about life, love, and the pursuit of a Ph.D. My other classmate, Eric Kelson, helped with the electrochemistry described in Chapter one. Andy Kiely has been a great vaccum line mate and coach of the Hogs this last year, allowing me playing time at third base and continuing the Bryan tradition of letting me bat lead-off. (Bo knows enough chemistry for another Ph.D, Andy!!!) Another 213 companion, Bob Blake provided the lab with easy listening tapes which included Van Halen, Scorpions and Metallica. Rock on!! Howie rules, Bob!! Sharad Hajela made coffee many mornings during the writing of this document while Mike Abrams (Coffee Czar) provided the beans. Tim Herzog kept me on my toes when he came to bat during batting practice while Shannon Stahl was the recipient of a "few" high throws to first base.

The group has also been fortunate to have some outstanding post-docs here. John Power seemed to always have a reference for you if you needed one. Gui Bazan started the project described in Chapter 4 by introducing the ligand to both scandium and zirconium. Helpful discussions with Jon Mitchell on imido chemistry provided insight into its chemistry. Finally,

Eugene Mueller shocked me by seemingly writing as much as I did when he read my thesis chapters.

Outside of the group, Sunney Chan has been a second father for me. Laura Mizoue has been a great dinner companion and a great friend as well. A special thanks to Gary, Nancy and Benjamin Shreve for providing a place to go to for Thanksgiving dinner. Others in the Lewis group have provided a source of relaxation and fun, especially during my last year here. Paul Laibinis has been a great roommate. How can one not miss Colby Stanton's "Are you busy?", Ming Tan's promptness (NOT!) on dinner and movie excursions, or Janet Kesselman's threat to dump a glass of water on you (of course for a good reason!!).

Financial support for this work was provided by the National Science Foundation.

Abstract: The preparation of reactive oxo, imido, and borollide complexes on tantalum and zirconium will be described. Metathesis of $Cp^*_2Ta(=O)Cl$ with $AgPF_6$ afforded $[Cp^*_2TaF_2][PF_6]$, which presumably formed from P-F activation of $PF6^-$. When $AgSO_3CF_3$ was used, $[Cp^*_2Ta(=O)][SO_3CF_3]$ was isolated; however, it was unreactive toward styrene, methane, or benzene. Exposure to water resulted in the 1,2-addition product, $[Cp^*_2Ta(OH)_2][SO_3CF_3]$. Finally, treating $Cp^*_2Ta(=O)H$ with $[Ph_3C][B(C_6F_5)_4]$ afforded $[Cp^*_2Ta(=O)][B(C_6F_5)_4]$. Even with this non-coordinating counterion, the complex was found to be surprisingly unreactive. To prepare an imido complex, treating Cp^*TaCl_4 with four equivalents of lithium anilide affords $Cp^*Ta(=NPh)(NHPh)_2$. This complex reacts readily with substituted anilines to generate $Cp^*Ta(=NPh')(NHPh')_2$ and with alcohols such as pinacol to afford $Cp^*Ta(OCMe_2CMe_2O)_2$, products whereby both the imido and amido groups are exchanged. Exposing $Cp^*Ta(=NPh)(NHPh)_2$ to CO_2 resulted in the isolation of $Cp^*Ta(OCONPh)(\eta^2\text{-}OCONHPh)_2$ with both the formal [2+2] addition of CO_2 across the imido group and insertion of CO_2 into the amido group. Finally, bis-imido complexes were prepared by treating $Cp^*Ta(=NPh)(NHPh)_2$ to one equivalent of HCl to yield $Cp^*Ta(=NPh)_2$ or by treating Cp^*TaCl_4 with four equivalents of lithium 2,6-diisopropylanilide to yield $Cp^*Ta(=NPh'')_2$. The borollide ligand, $(C_4H_4BN^iPr_2)^{2-}$, ligand is introduced by treating Cp^*ZrCl_3 with one equivalent of $Li_2(C_4H_4BN^iPr_2)\cdot THF$ to generate $Cp^*(C_4H_4BN^iPr_2)ZrCl\cdot LiCl$. This complex contains a η^5-coordinated borollide ligand, as shown by an X-ray crystal structure analysis. Alkylation and arylation with trimethylsilylmethyllithium, benzylpotassium or phenyllithium yielded $Cp^*(C_4H_4BN^iPr_2)ZrR$ complexes. These catalysts polymerizes ethylene, but only oligomerizes α-olefins. In addition, $Cp^*(C_4H_4BN^iPr_2)ZrCl\cdot LiCl$ has been found to exhibit the formal heterolytic cleavage of HCl and CH_3I, affording $Cp^*(C_4H_4BNH^iPr_2)ZrCl_2$ and $Cp^*(C_4H_4BN(CH_3)^iPr_2)ZrCl(I)$, respectively. Finally, treatment of $Cp^*(C_4H_4BN^iPr_2)ZrCl\cdot LiCl$ with $LiNH^tBu$ generated the zwitterionic complex, $Cp^*(C_4H_4BNH^iPr_2)Zr{=}N^tBu$.

TABLE OF CONTENTS

LIST OF FIGURES

LIST OF TABLES

Chapter 1

Heterogeneous and Homogeneous Oxo and Imido Complexes

Abstract: A brief introduction to transition metal oxo and imido complexes is provided as background to Chapters 2 and 3.

Metal oxo and imido complexes have been prepared to model both important industrial processes and enzymatic reactions. Industrially, the oxidation of organic substrates is important in the conversion of feedstock hydrocarbons to profitable chemicals. For example, four million tons of aldehyde is produced annually from alkenes by the Wacker Process.[1]

$$CH_2{=}CH_2 \xrightarrow[CuCl_2,\ H_2O]{PdCl_2/\ O_2} CH_3\overset{\overset{O}{\|}}{C}\text{-}H$$

The mechanism of this catalytic process has been thoroughly investigated and, interestingly, oxygen is not directly involved in oxidizing ethylene.[2] Rather, ethylene coordinates to $PdCl_2$ and nucleophilic attack by water results in a palladium hydroxyethyl complex. The resulting palladium species is reoxidized by a process mediated by cuprous chloride with oxygen as the co-oxidant.[3]

On the other hand, the oxidation of propene to acrolein by the heterogeneous metal-oxo catalyst, Bi_2O_3/MoO_3, is not well understood.

$$CH_3CH{=}CH_2 + O_2 \xrightarrow[400^{\circ}C]{Bi_2O_3/\ MoO_3} CH_2{=}CH\text{-}\overset{\overset{O}{\|}}{C}H$$

An oxo species is believed to be involved since stoichiometric conversion with Bi_2O_3/MoO_3 is possible . The currently accepted mechanism is shown in Scheme I. The initial formation of an allyl species is followed by the formal addition reaction to the molybdenum-oxo bond, resulting in **3**. The catalytic cycle is then completed by loss of acrolein and re-oxidation of the surface molybdenum by oxygen.

Scheme I

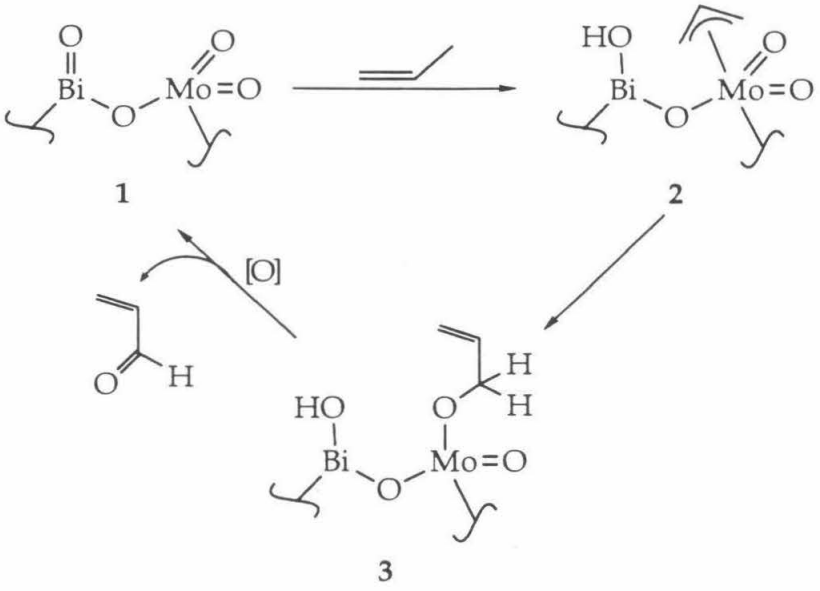

The related ammoxidation of propene to acrylonitrile can be accomplished using the bismuth molybdate catalyst that is used to synthesize acrolein. This methodology is used in the production of 8 billion pounds of acrylonitrile each year in the United States.

$$CH_3CH{=}CH_2 + O_2 + NH_3 \xrightarrow[400^{o}C]{Bi_2O_3/\ MoO_3} CH_2{=}CH{-}C{\equiv}N$$

The proposed mechanism for the conversion is similar to that for the acrolein synthesis (Scheme I) except that ammonia reacts with surface oxo groups to form imido moieties. In fact, several models of the proposed intermediates have been prepared which are capable of simulating some of the steps in the catalytic cycle.[4]

Another important industrial process is the commercial conversion of butane and butene to maleic anhydride, which is utilized in the manufacture of resins, food additives and pharmaceuticals. Employing a vanadium phosphorous oxide catalyst, 1.3 billion pounds of maleic anhydride is produced annually.[5] The exact nature of the catalyst remains elusive, though a vanadium oxo species is the expected precursor. This uncertainty is typical of heterogeneous catalytic processes in which mechanistic studies are generally difficult.

In nature, enzymes utilize metal-oxo moieties in which the reaction center is embedded in a protein matrix. Though the protein is important in the enzyme's biological activity and stability, understanding the chemistry of the reaction site is thus more challenging. One example is cytochrome P-450 which catalyzes important biological processes such as steroid metabolism and drug detoxification. Cytochrome P-450 contains an iron heme which has been shown to use either dioxygen or oxygen-transfer reagents to form an iron (V) oxo species. It is this iron moiety which is capable of transferring an oxygen atom to various substrates. The related horseradish peroxidase also employs an oxo species formed from hydrogen peroxide or an alkyl hydroperoxide in its catalytic oxidations. Model systems for both of these enzymes have recently been prepared.[6]

Examples of oxidations mediated by homogeneous metal-oxo complexes include the cis-hydroxylation of olefins,[7] epoxidation of olefins,[8] C-H activation of alkanes,[9] and oxygen transfer reactions.[10] (Figure 1)

Figure 1. Representative examples of homogeneous oxidation reactions.

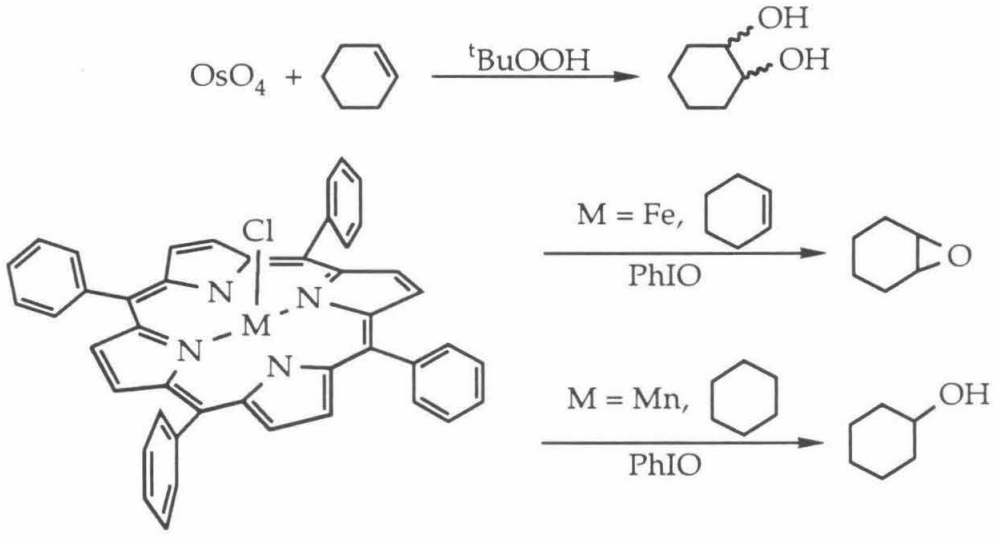

While a metal-oxo bond is intimately involved in the formation of the diols, the epoxidations and C-H activation reactions by the iron and manganese porphyrins are postulated to employ high oxidation state metal-oxo species. These two porphyrin complexes model the iron (V) oxo heme species of cytochrome P-450.

Homogenous reactions with imido complexes have been prepared for the oxyamination of olefins,[11] azirdinations[12] and imide exchange of carbodiimides.[13]

Figure 2. Representative examples of homogeneous metal imido mediated reactions.

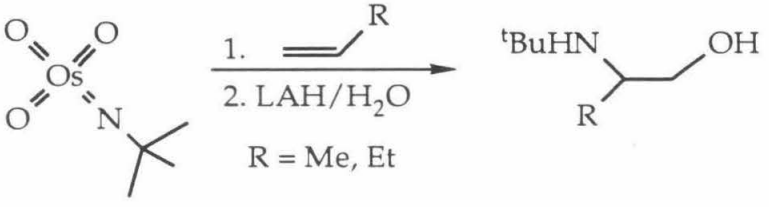

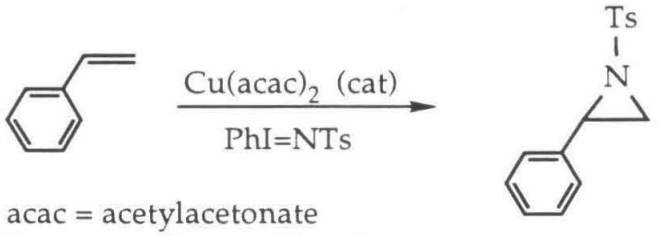

acac = acetylacetonate
Ts = *para*-toluenesulfonyl

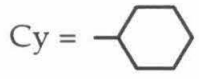

In summary both the oxo and imido metal complexes exhibit the ability to mediate important reactions. Chapters 2 and 3 present the preparation of oxo and imido complexes of an early transition metal. These compounds contain a basic heteroatom group (oxo or imido) attached directly to an electrophilic metal center. Chapter 4 presents the synthesis of electrophilic zirconium borollide complexes with a basic amine group that is not coordinated to the metal.

References

1. (a) Crabtree, R. H. *The Organometallic Chemistry of the Transition Metals.* John Wiley and Sons. New York, 1988. (b) Collman, J. P.; Hegedus, L. S.; Norton, J. R.; Finke, R. G. *Principle and Applications of Organotransition Metal Chemistry.* University Science Books. Mill Valley, California, 1987.

2. For a discussion on the lack of late metal transition metal oxo complexes, see: Mayer, J. M. *Comments Inorg. Chem.* **1988**, *8*, 125.

3. (a) Bäckvall, J. E.; Akermark, B. Ljunggren, S. O. *J. Am. Chem. Soc.* **1979**, *101*, 2411. (b) Stille, J. K.; Divakaruni, R. *J. Organomet. Chem.* **1979**, *169*, 239.

4. (a) Maata, E. A.; Du, Y.; Rheingold, A. L. *J. Chem. Soc., Chem. Commun.* **1990**, 756. (b) Maata, E. A.; Du, Y. *J. Am. Chem. Soc.* **1988**, *110*, 8249. (c) Rhodes, L. F.; Venanzi, L. M. *Inorg. Chem.* **1987**, *26*, 2692. (d) Chan, D. M. -T.; Fultz, W. C.; Nugent, W. A.; Roe, D. C.; Tulip, T. H. *J. Am. Chem. Soc.* **1985**, *107*, 251.

5. Centi, G.; Trifori, F.; Ebner, J. R.; Franchetti, V. M. *Chem. Rev.* **1988**, *88*, 55.

6. (a) McMurry, T. J.; Groves, J. T. In *Cytochrome P-450* Ortiz de Montellano, P. R., Ed.; Plenum: New York, 1986, Chapter 1.

7. (a) Akashi, K.; Palermo, R. E.; Sharpless, K. B. *J. Org. Chem.* **1978**, *43*, 2063. (b) Sharpless, K. B.; Williams, D. R. *Tetrahedron Letters* **1975**, *35*, 3045.

8. (a) see reference 6a (b) White, P. W. *Biorganic Chemistry* **1990**, *18*, 440. (c) Gunter, M. J.; Turner, P. *Coordination Chemistry Reviews* **1991**, *108*, 115.

9. (a) Groves, J. T.; Kruper, W. J.; Haushalter, R. C. *J. Am. Chem. Soc.* **1980**, *102*, 6375. (b) Hill, C. L.; Schoudt, B. C. *J. Am. Chem. Soc.* **1980**, *102*, 6374. (c) Groves, J. T.; Nemo, T. E.; Myers, R. S. *J. Am. Chem. Soc.* **1979**, *101*, 1032.

10. Holm, R. H. *Chem. Rev.* **1987**, *87*, 1401.

11. (a) Sharpless, K. B.; Patrick, D. W.; Truesdale, L. K.; Biller, S. A. *J. Am. Chem. Soc.* **1975**, *97*, 2305. (b) Patrick, D. W.; Truesdale, L. K.; Biller, S. A.; Sharpless, K. B. *J. Org. Chem.* **1978**, *43*, 2628. (c) Herranz, E.;

Sharpless, K. B. *J. Org. Chem.* **1978**, *43*, 2544. (d) Herranz, E.; Biller, S. A.; Sharpless, K. B. *J. Am. Chem. Soc.* **1978**, *100*, 3596.

12. (a) Allain, E. J.; Hager, L. P.; Deng, L.; Jacobsen, E. N. *J. Am. Chem. Soc.* **1993**, *115*, 4415. (b) Pérez, P. J.; Brookhart, M.; Templeton, J. L. *Organometallics* **1993**, *12*, 261. (c) Evans, D. A.; Faul, M. M.; Bilodeau, M. T.; Anderson, B. A.; Barnes, D. M. *J. Am. Chem. Soc.* **1993**, *115*, 5328. (d) Evans, D. A.; Faul, M. M.; Bilodeau, M. T. *J. Org. Chem.* **1991**, *56*, 6744. (e) Mahy, J.-P.; Bedi, G.; Battioni, P.; Mansuy, D. *J. Chem. Soc., Perkin Trans.* **1988**, *22*, 1517.

13. Meisel, I.; Hertel, G.; Weiss, K. *J. Mol. Catal.* **1986**, *36*, 159.

Chapter 2

Cationic Tantalum Oxo Complexes

Abstract: The preparation of the reactive tantalum cation, $[Cp^*_2Ta{=}O]^+$ will be discussed. Metathesis of $Cp^*_2Ta(=O)Cl$ with $AgPF_6$ or $TlPF_6$ afforded $[Cp^*_2TaF_2][PF_6]$, which presumably formed from P-F activation of the counterion. When $SO_3CF_3^-$, a better non-coordinating anion, was used, $[Cp^*_2Ta(=O)][SO_3CF_3]$ was isolated. However, this cation was unreactive toward styrene, methane, or benzene, but exposure to water resulted in the 1,2-addition product, $[Cp^*_2Ta(OH)_2][SO_3CF_3]$. Finally, treating $Cp^*_2Ta(=O)H$ with $[Ph_3C][B(C_6F_5)_4]$ afforded $[Cp^*_2Ta(=O)][B(C_6F_5)_4]$. Even with this non-coordinating counterion, the complex was found to be surprisngly unreactive.

Introduction

Recent interest in the synthesis and reaction chemistry of metal ligand multiple bonds has been sparked by the successful modeling of some of the reactions described in Chapter 1.[1] The lack of reactivity of many early transition metal-oxo complexes lies in the propensity of these metal-oxo bonds to assume triple bond character.

I **II**

Comparing the potential reactivities of the two resonance forms, the oxygen atom of **II** is expected to be more nucleophilic and the metal center of **II** is expected to be more electrophilic than in **I**. Design of reactive early transition metal oxo complexes should therefore, included features that strongly favor resonance form **II**. Since the oxo ligand generally manifests maximal π-bonding to a metal, complexes intended to exhibit resonance **II**'s character are formidable design challenges.

Recently, Wigley[2] introduced the term "π-loaded" to describe situations in which the number of potential π interactions with the ligands exceed the capacity of the metal, resulting in a formal electron count exceeding eighteen on the metal. Two such complexes are $(OC)W(RC{\equiv}CR)_3$ and $Os(=NR)_3$. The inertness of these "20 electron" complexes is attributed to the "extra" lone pair residing on a ligand-based molecular orbital.[3,4]

Due to their electronic properties, the bent metallocenes provide a unique opportunity to study metal-oxo bond that have little triple bond character. As described by Hoffmann,[5] the cyclopentadienyl-metal bond is comprised of one σ and two π interactions with three frontier orbitals located in the wedge between the cyclopentadienyl rings. The $1a_1$ molecular orbital is a d_{z^2}-like orbital; the b_2 molecular orbital is a d_{xz} orbital; and the $2a_1$ molecular orbital is a p_x-s hybrid-like orbital (Figure 1).

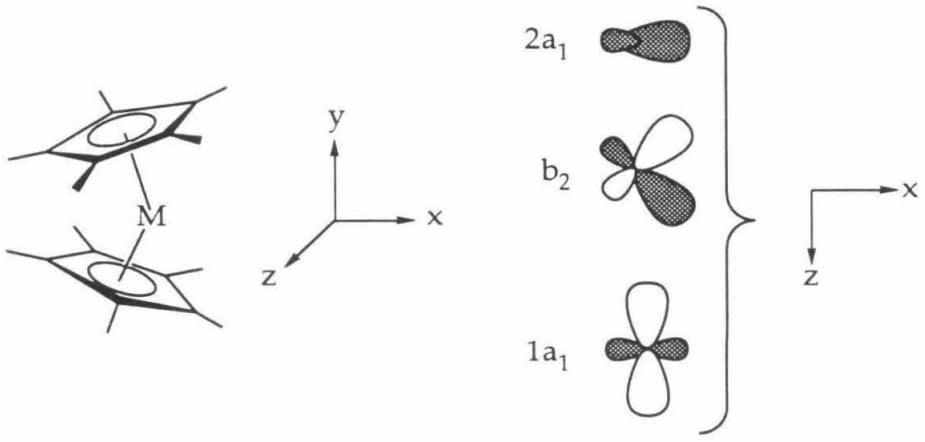

Figure 1. Frontier molecular orbitals of bent metallocenes.

An oxo or imido ligand forms one σ bond with the $2a_1$ orbital and one π bond with the b_2 orbital. However, the orbital from the oxygen or nitrogen that is available for a second π bond is orthogonal to the $1a_1$ orbital. For this reason, oxo or imido groups will be two electron donors in bent metallocene complexes with one (imido) or two (oxo) lone pairs residing on the heteroatom. Bent metallocene oxo complexes, therefore, will ideally fulfill our design of a complex with resonance form **II** character.

For a d^2 bent metallocene, the lone pair of electrons are localized in the $1a_1$ orbital and the metal is expected to be nucleophilic. Indeed, Geoffroy has shown that the d^2 tungsten metallocene complex, $Cp_2W{=}O$ (**1**),[6] undergoes formal [2+2] addition reactions with carbonyl groups, ketenes and isocyanates (Scheme I).[7]

Scheme I

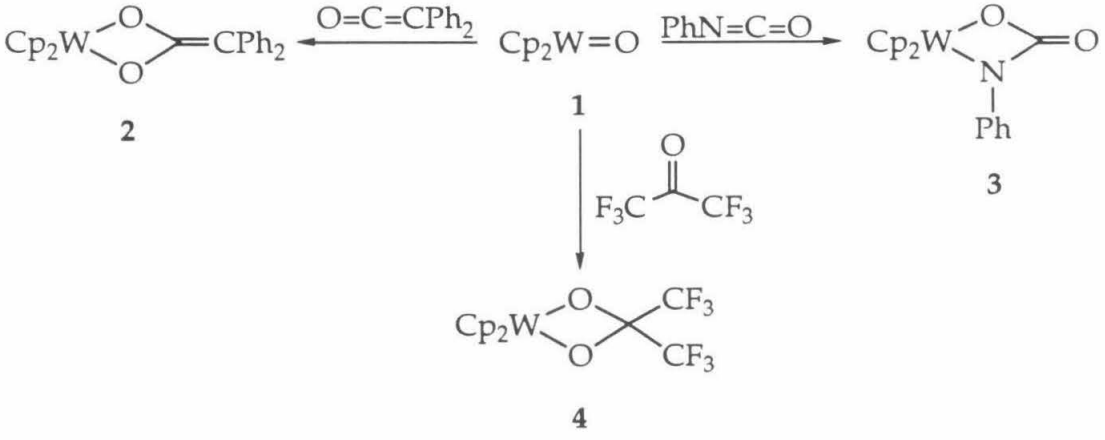

Though the mechanism of the reaction is unknown, the conversion of the oxo complex (**1**) to the metallacycle (**3**) may proceed either by a concerted [2+2] cycloaddition through the transition state **A** or by nucleophilic attack of the oxo moiety to form **B** followed by ring closure (Scheme II).

Scheme II

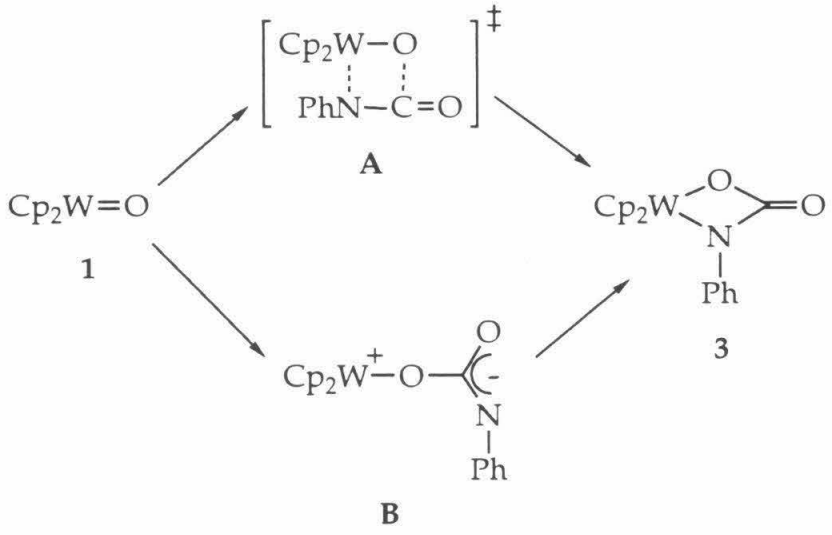

Interestingly, the only cycloaddition product observed with phenylisocyanate is that with a W-N bond. This result implies either a preference for transition state **A** or W-N bond formation from the closure in **B**. Both of these processes result in the reduction of bond order for the C=N bond, which is weaker than the C=O bond.

Previous work in this group[8] has shown that the d^2 complex $Cp^*_2W{=}O$ (**6**) also contains a reactive oxo group. The W=O bond stretch occurs at 860 cm^{-1}, indicative of a weak metal oxo bond. Typical metal-oxo stretches range from 800-1000 cm^{-1}, so this tungsten-oxo bond stretch is indicative of a low W=O bond order. The lack of triple bond character and, thus, nucleophilicity at the oxygen atom is borne out in the reactivity of the complex which reacts with TMSCl and HBF_4 to afford **7** and **8** respectively. (Scheme III)

Scheme III

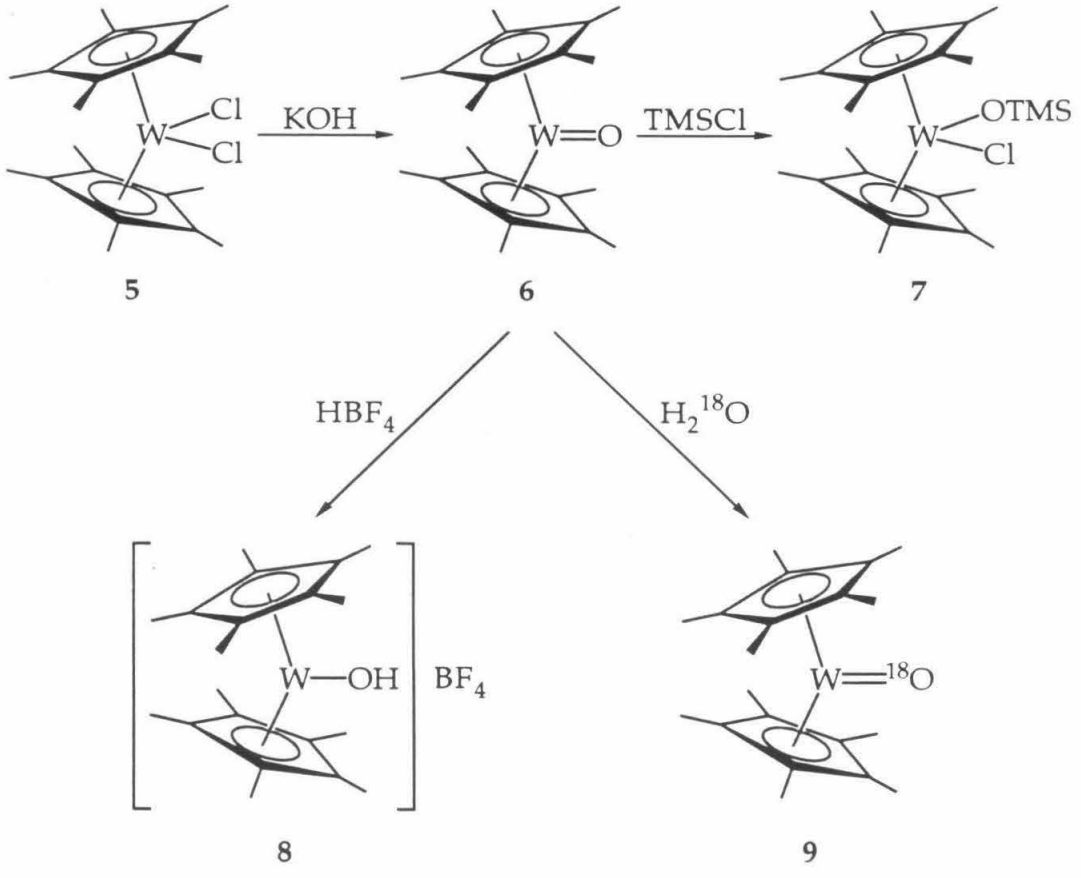

Interestingly, **6** undergoes oxo-exchange with labelled water. The reaction proceeds by a 1,2-addition/elimination pathway via the dihydroxide intermediate.

$$Cp^*_2W={}^{16}O + H_2{}^{18}O \rightleftharpoons \left[Cp^*_2W\begin{matrix}{}^{18}OH\\{}^{16}OH\end{matrix}\right] \rightleftharpoons Cp^*_2W={}^{18}O + H_2{}^{16}O$$

The syntheses of early transition metal reactive d^0 metal oxo, imido,[9] alkylidene,[10] phosphido,[11] and sulfido[12] complexes have been achieved. These electrophilic complexes are expected to encourage σ coordination of the substrate prior to its reaction.[13] Recently, Bergman[14] has provided evidence for the transient 16 electron intermediate [Cp^*_2Zr=O] (**12**) by the thermolysis of $Cp^*_2Zr(OH)Ph$ (**10**) or the deprotonation of $Cp^*_2Zr(OH)(OSO_2CF_3)$ (**11**).

Evidence of its intermediacy is provided by trapping **12** with either a nitrile or acetylene. (Scheme IV)

Scheme IV

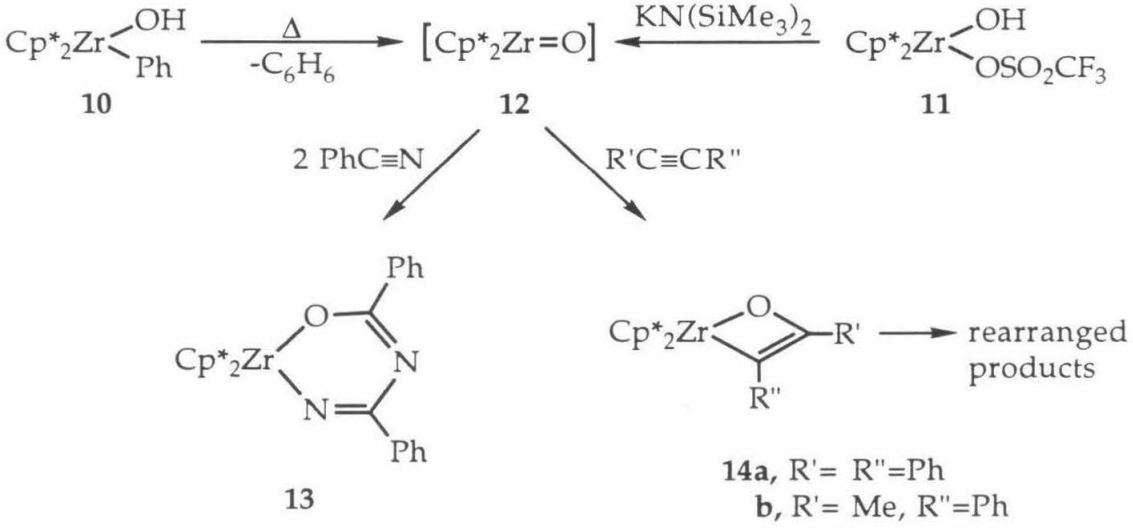

In the presence of benzonitrile, the observed product is a six-membered metallacycle (**13**), which presumably arises from an initial cycloaddition step followed by the insertion of a second equivalent of the nitrile. Substituted acetylenes afford an oxametallacycle (**14**), which rearranges when heated at higher temperatures. Parkin[15] has confirmed this claim by preparing $Cp^*_2Zr(=O)(NC_5H_5)$ (**15**) from the oxidation of $Cp^*_2Zr(CO)_2$ with N_2O in pyridine; **15** was found to undergo similar [2+2] cycloaddition chemistry. The crystal structure of the related $(\eta^5\text{-}C_5Me_4Et)_2Zr(O)(NC_5H_5)$ shows a Zr=O bond length of 1.80 Å, which is shorter than other Zr-O single bonds. The infrared absorption of 780 cm^{-1} is low in energy for metal-oxo bonds and indicates a bond with very little triple bond character.

Scheme V

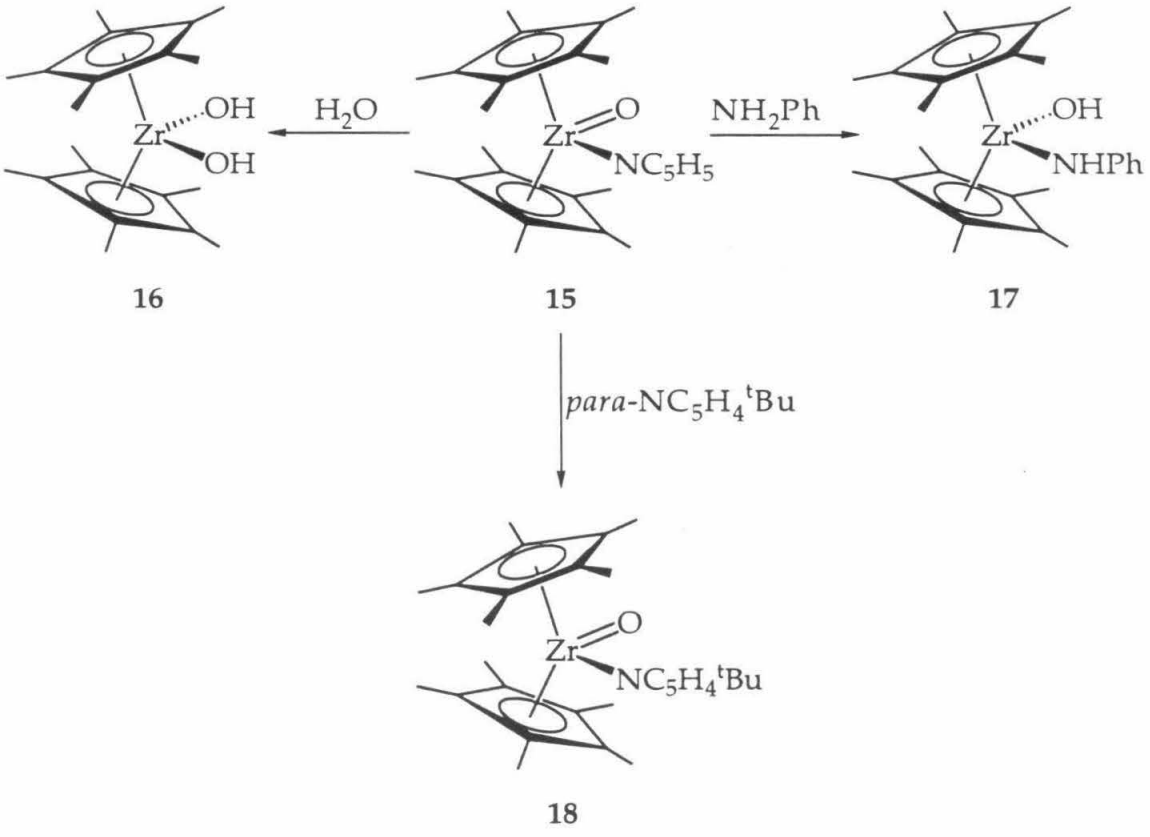

Furthermore, **15** readily undergoes 1,2-addition chemistry with water and aniline across the reactive metal-oxo bond to afford the dihydroxy (**16**) and hydroxyamido (**17**) complexes. Interestingly, the pyridine adduct (**18**) is labile to substitution by other Lewis bases such as 4-*tert*-butylpyridine, suggesting the formation of [$Cp^*_2Zr{=}O$] as an intermediate from the dissociation of pyridine.

In another example of 1,2-addition, the complex $Cp^*_2Ta(=^{18}O)H$ was found to undergo exchange of the oxo group with $D_2{}^{16}O$ without exchange of the hydride group.[16]

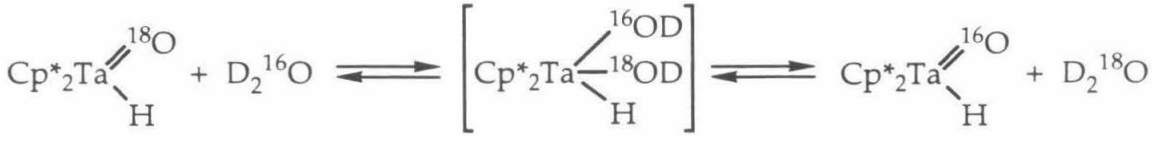

The oxygen exchange reaction does not proceed by initial α-migration to form [Cp^*_2TaOH] followed by the oxidation addition of water since this would also necessarily involve exchange of the hydride on $Cp^*_2Ta(=O)H$.

While Bergman has demonstrated that the transient [$Cp^*_2Zr=O$] undergoes [2+2] addition with diphenylacetylene and isocyanates, the isoelectronic [$Cp_2Zr=N^tBu$] fragment activates the C-H bond on benzene (see Chapter 3). Since the two complexes also differ in their ancillary ligand, one with Cp and the other with Cp*, direct comparisons of the two complexes are difficult. For this reason we have been interested in studying the reactivity of both the $[Cp^*_2Ta=O]^+$ and $[Cp^*_2Ta=NR]^+$ cations. With a formal positive charge on the metal, the cations are expected to be more reactive. This chapter presents the efforts in the synthesis of the $[Cp^*_2Ta=O]^+$ species.

Results and Discussion

The preparation of a $[Cp^*_2Ta{=}O]^+$ species was attempted by two strategies: (1) metathesis of chloride from $Cp^*_2Ta(=O)Cl$ with silver salts and (2) hydride abstraction from $Cp^*_2Ta(=O)H$ by a trityl salt.

Scheme VI

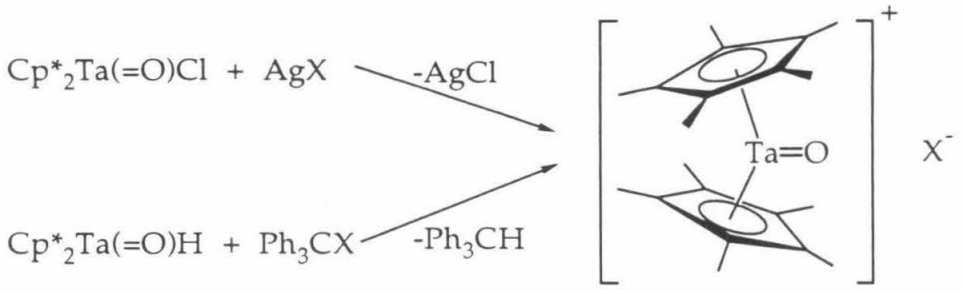

The choice of the counterion, X^-, is expected to be crucial since a coordinating anion is anticipated to reduce the reactivity while a non-coordinating anion should result in a maximally reactive species. Indeed, it might be too unstable to isolate.[17]

In order to investigate the metathesis reactions, an efficient synthetic route to $Cp^*_2Ta(=O)Cl$ was needed. Previous work in this group has demonstrated that $Cp^*_2Ta(=O)Cl$ can be prepared in low yield from $Cp^*_2TaCl_2$ and hydrogen peroxide.[18] Substituting iodosylbenzene for H_2O_2 afforded an alternate route to $Cp^*_2Ta(=O)Cl$ in high yield. When $Cp^*_2TaCl_2$ was added to a THF solution of iodosylbenzene over 1% sodium amalgam; the yield of $Cp^*_2Ta(=O)Cl$ was 75%.[19]

$$Cp^*_2TaCl_2 \xrightarrow[THF]{Na/Hg,\ PhIO} Cp^*_2Ta(=O)Cl$$

19

Initial metathesis reactions with silver tetraphenylborate resulted in complex mixtures of products. Hexafluorophosphate was predicted to be an innocent counterion (one not expected to interact with the tantalum center). To test this prediction, $Cp^*_2Ta(=O)Cl$ was treated with thallium hexafluorophosphate. A yellow solid was isolated in less than 50% yield and it was crystallographically determined to be $[Cp^*_2TaF_2][PF_6]$ (**20**) (Figure 2).

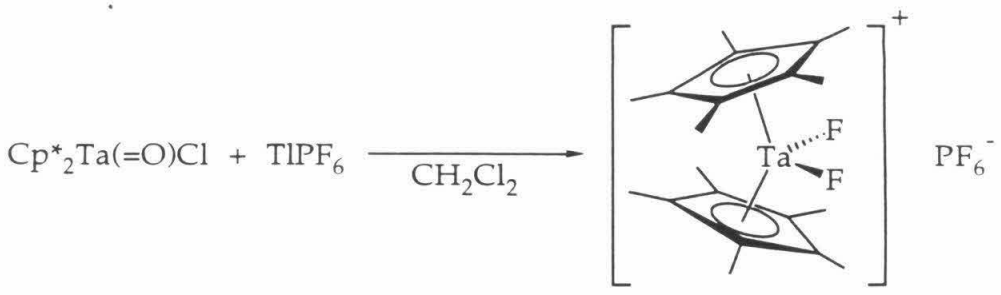

20

Presumably, $[Cp^*_2Ta{=}O][PF_6]$ was transiently formed by the metathesis of $Cp^*_2Ta(=O)Cl$, but subsequent P-F activation of the counterion by the highly electrophilic cation produced $[Cp^*_2TaF_2][PF_6]$.[20]

In order to circumvent this problem, triflate was the next logical counterion to try. Treatment of $Cp^*_2Ta(=O)Cl$ with $AgSO_3CF_3$ afforded a solid, $[Cp^*_2Ta(=O)][SO_3CF_3]$, **21**, which was spectroscopically characterized.

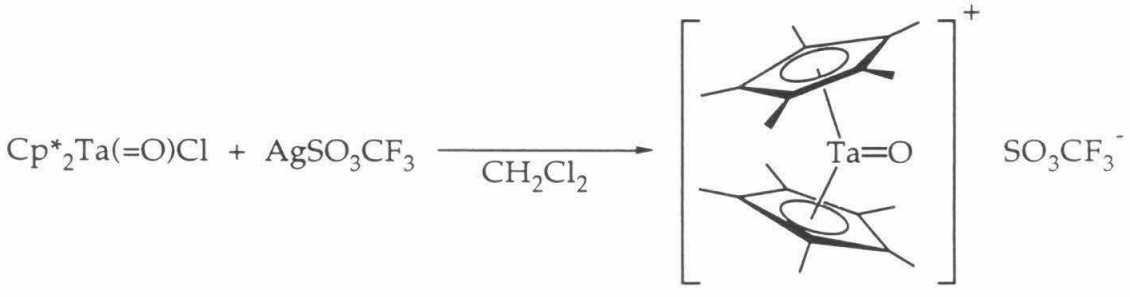

21

The complex is surprisingly soluble in benzene, methylene chloride, and tetrahydrofuran, suggesting that **21** dissociates in polar solvents and remains undissociated in nonpolar solvents. When the complex was prepared in tetrahydrofuran, $[Cp^*_2Ta(=O)(THF)][SO_3CF_3]$ was isolated but the solvent was easily removed by heating the solid *in vacuo*.

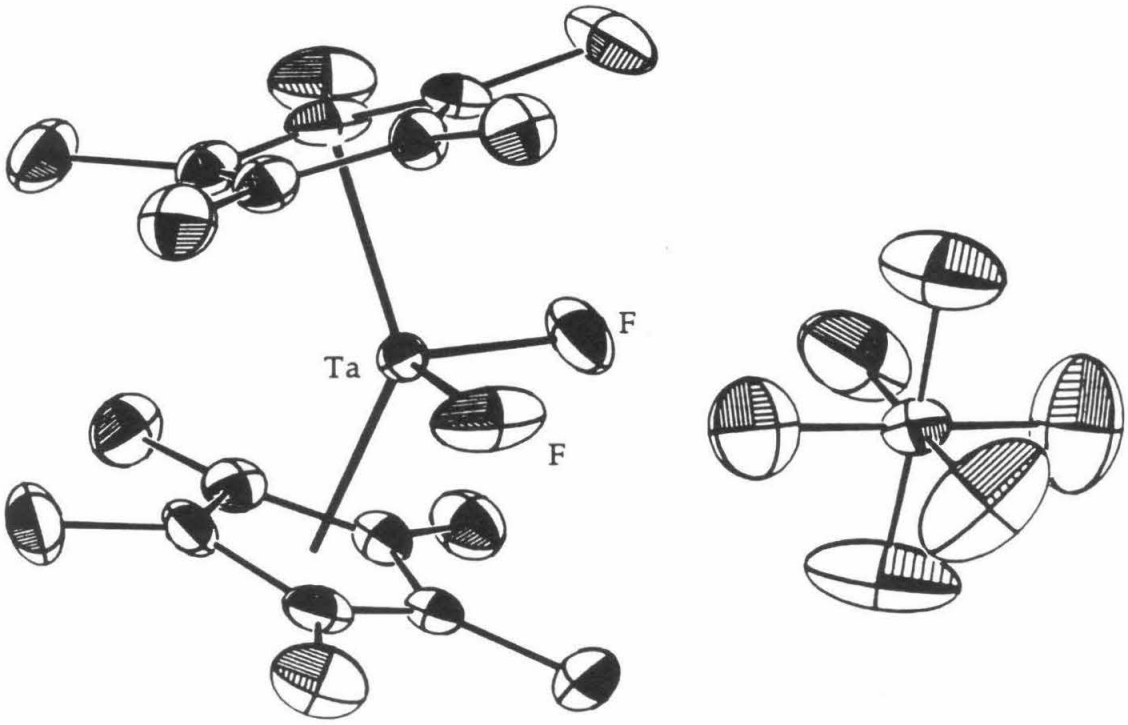

Figure 2. ORTEP diagram of $[Cp^*_2TaF_2]PF_6$ (**20**)

While growing crystals of **21**, two different types of crystals were observed and both were determined by X-ray crystallography.[21] The ORTEP diagrams for both crystalline products (**22** and **23**) are shown in figures 3 and 4.

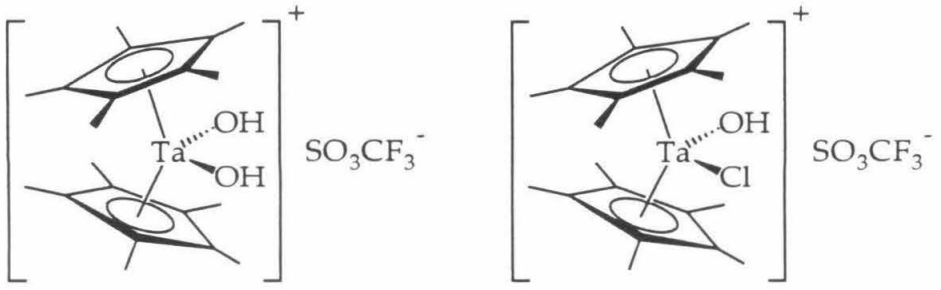

22 **23**

Complex **22** is the expected product from the 1,2- addition of H_2O across the Ta=O moiety of $[Cp^*_2Ta(=O)][SO_3CF_3]$. Water in the solvent during crystallization accounts for the isolation of **22**. On the other hand, **23** is probably the result of $Cp^*_2Ta(=O)Cl$ reacting with minute amounts of HSO_3CF_3 present during the generation of **21**. This protonation reaction has been demonstrated independently. When $Cp^*_2Ta(=O)Cl$ was treated with HSO_3CF_3, the product was determined to be $[Cp^*_2Ta(OH)(Cl)][SO_3CF_3]$ (**23**) by its ^1H NMR spectrum.

$$Cp^*_2Ta(=O)Cl \underset{NEt_3}{\overset{HSO_3CF_3}{\rightleftharpoons}} [Cp^*_2Ta(OH)(Cl)]^+[SO_3CF_3]^-$$

23

This protonation of the Ta=O bond is reversible, since treatment of **23** with triethylamine cleanly affords $Cp^*_2Ta(=O)Cl$.

Though reactive with water and HSO_3CF_3, **21** undergoes cycloaddition chemistry with neither styrene nor C-H activation of methane or benzene. As revealed in the crystal structures of both **22** and **23**, the triflate anion hydrogen bonds with the hydroxyl group of the cation portion of the complex, indicating that triflate is not a completely innocent counterion and may be coordinated to the tantalum center in **21**. A coordinate triflate in **21** would reduce its reactivity toward substrates.

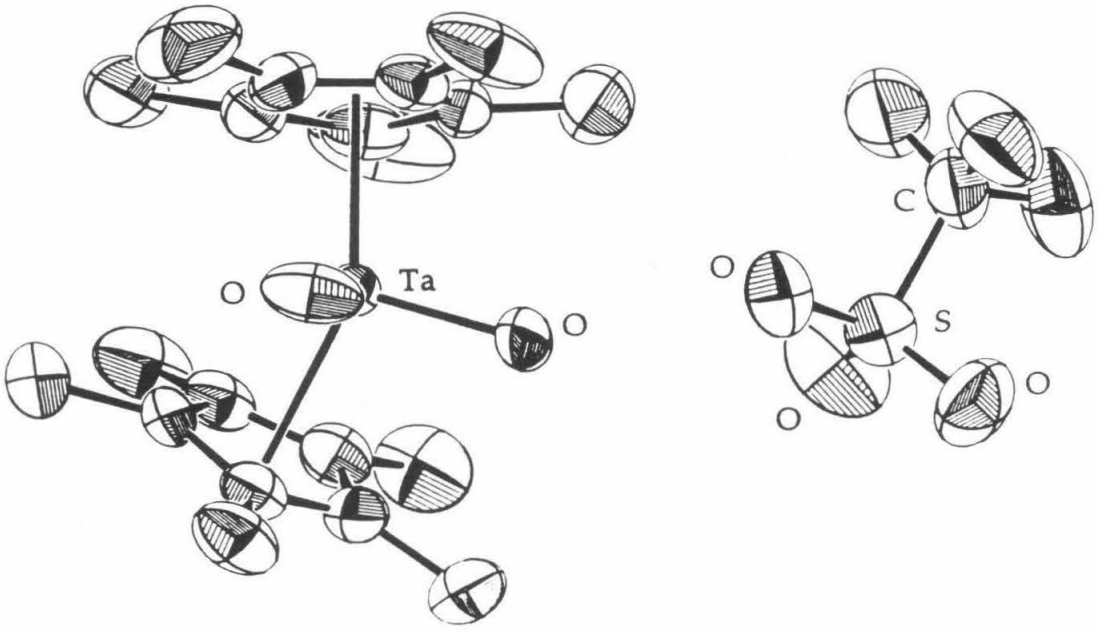

Figure 3. ORTEP diagram of $[Cp^*_2Ta(OH)_2][SO_3CF_3]$ (**22**)

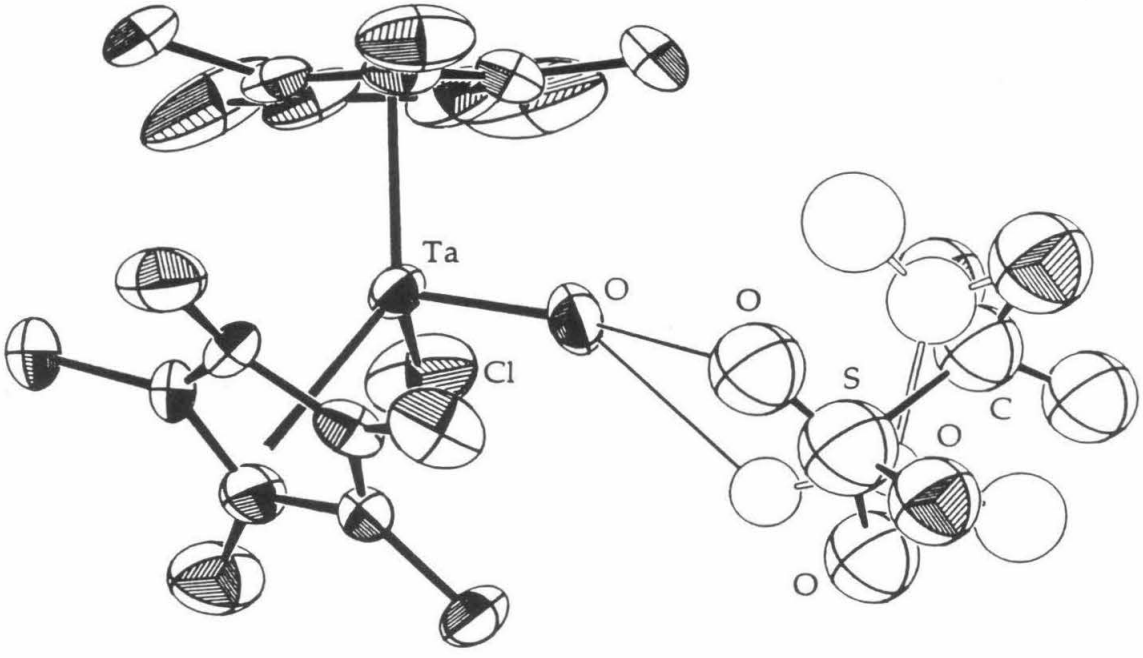

Figure 4. ORTEP diagram of $[Cp^*_2Ta(OH)(Cl)][SO_3CF_3]$ (**23**)

The search of a truly innocent counterion continued with perfluorotetraphenylborate.[22] Treatment of $Cp^*_2Ta(=O)H$ with $[Ph_3C][B(C_6F_5)_4]$ in benzene afforded a green solid that exhibits an IR stretch at 980 cm^{-1}, which is indicative of a Ta=O bond. The product has been preliminarily determined to be $[Cp^*_2Ta(=O)][B(C_6F_5)_4]$, **24**.

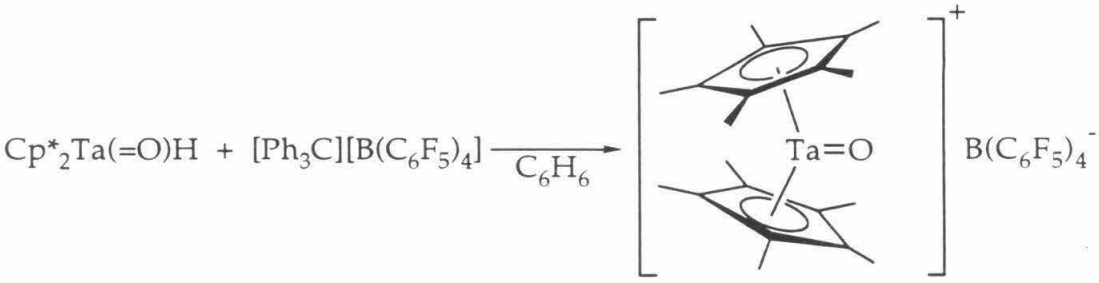

24

This compound was surprisingly unreactive with benzene at 120°C though the counterion is not expected to be coordinated to the cation.

In order to better understand the reaction chemistry of $Cp^*_2Ta(=O)Cl$ and $Cp^*_2Ta(=NPh)H$, the Ta-O and Ta-N bond orders in these complexes were probed. Therefore, the electrochemistry of both oxo and imido complexes were obtained. An irreversible oxidative peak at 1.06 volts (versus SCE) dominates the cyclic voltammogram of $Cp^*_2Ta(=O)Cl$ in acetonitrile. This result precludes the oxidation of $Cp^*_2Ta(=O)Cl$ by silver (I). Interestingly, the electrochemistry of $Cp^*_2Ta(=NPh)H$ and $Cp^*_2Ta(=NPh)I$ (**25**) exhibited irreversible oxidative waves at 30 millivolts and 560 millivolts (versus SCE). This is consistent with the oxidation of both complexes with Ag^+ salts. The electrochemistry and solution chemistry results are both in agreement with a molecular orbital representation in which the second lone pair of the nitrogen is not strongly bonded to the tantalum center. In addition, the photoelectron spectroscopy[23] of $Cp^*_2Ta(=O)X$ (X = H, Cl, CH_3, Ph, OCH_3) and $Cp^*_2Ta(=NPh)Y$ (Y = H, I) support a molecular orbital description in which the second metal-π interaction for the $[Cp^*_2Ta{=}X]^+$ fragment contains anti-bonding character. This molecular orbital is much higher in energy in the imido complexes when compared to the metal-oxo orbital and is consistent with the reactive nature of the imido ligand in the $[Cp^*_2Ta{=}X]^+$ fragment.

Conclusion

During the preparation of $[Cp^*_2Ta{=}O]^+$, the counterion has been found to be crucial to its isolation. With PF_6^-, P-F bond activation led to the isolation of $[Cp^*_2TaF_2]PF_6$. Triflate anion proved to be less problematic. $[Cp^*_2Ta{=}O][SO_3CF_3]$ was isolated from the metathesis reaction, though the 1,2-addition of water to afford $[Cp^*_2Ta(OH)_2][SO_3CF_3]$ was a significant side reaction. Finally, when $Cp^*_2Ta(=O)H$ was treated with $[Ph_3C][B(C_6F_5)_4]$, $[Cp^*_2Ta{=}O][B(C_6F_5)_4]$ was isolated and found to be surprisingly unreactive. These results agree with other findings that oxo complexes tend to be much less reactive than the isostructural imido complexes.[24] The strong metal-oxo bond undoubtedly accounts for the observed inertness of these compounds.

Experimental

General Considerations. All manipulations were performed using glovebox or high vacuum line techniques.[25] Solvents were dried over $LiAlH_4$ or Na/benzophenone and stored under vacuum over "titanocene."[26] Benzene-d_6 , tetrahydrofuran-d_8, and methylene chloride-d_2 were dried over activated molecular sieves (4Å, Linde) and stored over "titanocene" or Na/benzophenone. Argon and nitrogen gases were passed over MnO on vermiculite and activated sieves. Iodosylbenzene[27] was prepared as previously described. Silver triflate and thallium hexafluorophosphate were purchased from Aldrich and used without further purification.

Many reactions were surveyed by NMR spectroscopy. Any experiment described herein but not explicitly listed below was carried out in a sealed NMR tube using ~0.7 mL of the NMR solvent with the appropriate reagents.

$Cp^*_2Ta(=O)Cl$ (19). A large high pressure glass reaction vessel was charged with 2.5 g (11 mmol) iodosylbenzene, 25.9 g of 1% sodium amalgam, and 5.01 g (9 mmol) $Cp^*_2TaCl_2$. Approximately 100 mL THF was then condensed on the solids at -78°C. The reaction vessel was agitated for three days with the resultant solution appearing grayish white. The solution was filtered through Celite to remove the mercury and then transferred to a 100 mL round bottom flask equipped with a swivel frit assembly. The volatiles were removed *in vacuo*. Toluene was then condensed on the solid and the suspension was filtered to afford (3.48 g, 6.92 mmol) a white solid, **29**. Yield = 77%.

$[Cp^*_2TaF_2]PF_6$ (20). A high pressure glass reaction vessel was charged with 460 mg (0.92 mmol) $Cp^*_2Ta(=O)Cl$ and 320 mg (0.92 mmol) $TlPF_6$. Approximately 20 mL of methylene chloride was condensed on the solids at -78°C and the resultant solution was heated at 80°C for three days. The violet solution was then transfered to a 100 mL round bottom flask fitted with a swivel frit assembly. A white solid was filtered and the filtrate was concentrated. Toluene was added to the solution and filtration afforded 267 mg (0.42 mmol) of a yellow solid, **20**. Yield = 46%. Analysis : Calculated (Found) C: 37.87 (37.50); H: 4.77 (4.70).

[$Cp^*_2Ta{=}O][SO_3CF_3]$ (21). A 50 mL round bottom flask was charged with 903 mg (1.80 mmol) $Cp^*_2Ta(=O)Cl$ and 462 mg (1.80 mmol) silver triflate. A swivel frit assembly was attached and approximately 40 mL methylene chloride was condensed on the solids at -78°C. The resultant solution was allowed to warm slowly to room temperature and then stirred for 90 minutes. Filtration of a gray solid yielded an orange filtrate from which the volatiles were removed *in vacuo*. The solid was washed with petroleum ether to afford 468 mg (0.76 mmol) of a light brown solid, **21**. Yield = 42%. IR spectroscopy (KBr, cm^{-1}): 1271.6, 1143.7, 1160.4, 1031.7, 980.3, 856.0, 637.1. Analysis : Calculated (Found) C: 40.91 (38.79); H: 4.91 (4.60).

[$Cp^*_2Ta(=O)][B(C_6F_5)_4]$ (24). A 50 mL round bottom flask was charged with 200 mg (0.43 mmol) $Cp^*_2Ta(=O)H$ and 394 mg (0.43 mmol) $[Ph_3C][B(C_6F_5)_4]$ and a swivel frit assembly was attached. Approximately 20 mL benzene was condensed on the solids at -78°C, and the solution was stirred at room temperature overnight. The volatiles were removed *in vacuo* and the solid was washed with petroleum ether to afford 355 mg (0.31 mmol) of a light green solid. Yield = 73%. IR spectroscopy (KBr, cm^{-1}): 1513.0, 1463.9, 1085.9, 979.9, 774.7, 756.2, 684.1, 669.7. IR spectroscopy (nujol mull, cm^{-1}): 1634.3, 1513.9, 1275.3, 1084.7, 979.7, 774.2, 756.0, 684.0, 661.4. Analysis : Calculated (Found) C: 46.10 (48.91); H: 2.64 (3.26).

$Cp^*_2Ta(=NPh)I$ (25). A high pressure glass vessel was charged with 795 mg (1.46 mmol) $Cp^*Ta(=NPh)H$. Approximately 75 mL toluene was condensed onto the solid at -78°C. Methyl iodide (250 µL, 4.02 mmol) was added *via* syringe against an argon flow. The reaction vessel was heated at 80°C for 48 hours, resulting in a red solution with a small amount of solid. This solution was transferred to a round bottom flask equipped with a swivel frit assembly. The solution was then concentrated and petroleum ether was added. Filtration afforded 701 mg (1.05 mmol) of **25** as an orange solid. Yield = 72%. IR spectroscopy (nujol mull, cm^{-1}): 1161.4, 1063.4, 1019.2. Analysis : Calculated (Found) C: 46.65 (46.51); H: 5.27 (5.41); N: 2.09 (1.80).

X-Ray Crystal Structure Determination of $[Cp^*_2TaF_2]PF_6$ (20).

The ORTEP drawing of $[Cp^*_2TaF_2]PF_6$ is shown in figure 2. A yellow crystal was mounted in a greased capillary and then centered on a CAD-4 diffractometer. Unit cell parameters and an orientation matrix were obtained by a least squares calculation from the setting angles of 25 reflections with $15^o < \theta < 17^o$. The data were corrected for absorption. Coordinates of the tantalum atom were obtained from a Patterson map; locations of the other non-hydrogen atoms were determined from successive structure factor-Fourier calculations. Calculations were performed with programs of the CRYM Crystallographic Computing System and ORTEP. Scattering factors and corrections for anamalous scattering were taken from a standard reference.[28]

Electrochemistry of $Cp^*_2Ta(=O)Cl$, $Cp^*_2Ta(=NPh)H$ and $Cp^*_2Ta(=NPh)I$.

The electrochemical results were obtained on a BAS 100A Electrochemical Analyzer using two compartment sample cells. All the experiments were performed under an argon or nitrogen atmosphere utilizing a $Ag^+/AgCl$ reference electrode and platinum gauze as an auxiliary electrode. For a typical experiment, 4-6 mg of the complex was added with approximately 340 mg of *tert*-butylammonium perchlorate or *tert*-butylammonium hexafluorophosphate. The $Cp^*_2Ta(=O)Cl$ data were acquired in acetonitrile while the $Cp^*_2Ta(=NPh)H$ and $Cp^*_2Ta(=NPh)I$ data were acquired in THF.

Table I. ^{1}H NMR Spectral Data for complexes **19 - 25**.

Compound	Assignment	δ (ppm)	J (Hz)
$Cp^*2Ta(=O)Cl$ **(19)** in C_6D_6	$C_5(CH_3)_5$	1.85 (s)	
$[Cp^*_2TaF_2]PF_6$ **(20)** in CD_2Cl_2	$C_5(CH_3)_5$	2.23 (s)	
$[Cp^*_2TaF_2]PF_6$ **(20)** in THF-d_8	$C_5(CH_3)_5$	2.28 (s)	
$[Cp^*_2Ta{=}O]SO_3CF_3$ **(21)** in CD_2Cl_2	$C_5(CH_3)_5$	2.04 (s)	
$[Cp^*_2Ta{=}O]SO_3CF_3$ **(21)** in C_6D_6	$C_5(CH_3)_5$	1.78 (s)	
$[Cp^*_2Ta{=}O]B(C_6F_5)_4$ **(24)** in THF-d_8	$C_5(CH_3)_5$	2.18 (s) 10.92 13.05	
$Cp^*_2Ta(=NPh)I$ **(25)** in THF-d_8	$C_5(CH_3)_5$ *para*-C_6H_5 *ortho*-C_6H_5 *meta*-C_6H_5	2.08 (s) 6.33 (t) 6.40 (d) 6.90 (t)	 7.20 7.50 7.50

Table II. ^{19}F NMR Spectral Data for complexes **20 - 24**.

Compound	Assignment	δ (ppm)	J (Hz)
$[Cp^*_2TaF_2]PF_6$ **(20)** in CD_2Cl_2	Ta-*F* P-*F*	23.57 73.20	 707
$[Cp^*_2TaF_2]PF_6$ **(20)** in THF-d_8	P-*F* Ta-F	18 -73.96	 707
$[Cp^*_2Ta{=}O]SO_3CF_3$ **(21)** in CD_2Cl_2	CF_3	-76.92	
$[Cp^*_2Ta{=}O]SO_3CF_3$ **(21)** in C_6D_6	CF_3	-77.19	
$[Cp^*_2Ta{=}O]B(C_6F_5)_4$ **(24)** in THF-d_8		-129.51 -161.87 -165.35	

Table III. ^{13}C NMR Spectral Data for complexes **19 - 25**.

Compound	Assignment	δ (ppm)
$Cp^*_2Ta(=O)Cl$ **(19)**	$C_5(CH_3)_5$	11.31
in C_6D_6	$C_5(CH_3)_5$	129.24
$[Cp^*_2TaF_2]PF_6$ **(20)**	$C_5(CH_3)_5$	10.72
in CD_2Cl_2	$C_5(CH_3)_5$	129.53
$[Cp^*_2Ta=O]SO_3CF_3$ **(21)**	$C_5(CH_3)_5$	11.51
in CD_2Cl_2	$C_5(CH_3)_5$	122.58
$[Cp^*_2Ta=O]SO_3CF_3$ **(21)**	$C_5(CH_3)_5$	11.24
in C_6D_6	$C_5(CH_3)_5$	121.15
$[Cp^*_2Ta=O]B(C_6F_5)_4$	$C_5(CH_3)_5$	11.12
(24) in THF-d_8	$C_5(CH_3)_5$	121.14
	aromatic	135.49
	aromatic	137.68
	aromatic	138.75
	aromatic	140.75
	aromatic	147.52
	aromatic	150.83
$Cp^*_2Ta(=NPh)I$ **(25)**	$C_5(CH_3)_5$	13.33
in THF-d_8	aromatic	117.40
	aromatic	118.14
	$C_5(CH_3)_5$	118.95
	aromatic	128.44
	aromatic	160.28

Table IV. ^{31}P NMR Spectral Data for complex **20**.

Compound	Assignment	δ (ppm)	J (Hz)
$[Cp^*_2TaF_2]PF_6$ **(20)**	PF_6	18	
in CD_2Cl_2	PF_6	110.65	713

References

1. (a) Nugent, W. A.; Haymore, B. L. *Coord. Chem. Rev.* **1980**, *31*, 123. (b) Nugent, W. A.; Mayer, J. M. *Metal-Ligand Multiple Bonds*, John Wiley and Sons, New York, 1988.

2. Huber, S. R.; Baldwin, T. C.; Wigley, D. E. *Organometallics* **1993**, *12*, 91.

3. (a) Tate, D. P.; Augl, J. M.; Ritchey, W. M.; Ross, B. L.; Grasselli, J. G. *J. Am. Chem. Soc.* **1964**, *86*, 3261. (b) Tate, D. P.; Augl, J. M. *J. Am. Chem. Soc.* **1963**, *85*, 2174.

4. Schofield, M. H.; Kee, T. P.; Anhaus, J. T.; Schrock, R. R.; Johnson, K. H.; Davis, W. M. *Inorg. Chem.* **1991**, *30*, 3595. (b) Anhaus, J. T.; Kee, T. P.; Schofield, M. H.; Schrock, R. R. *J. Am. Chem. Soc.* **1990**, *112*, 1642.

5. Lauher, J. W.; Hoffmann, R. *J. Am. Chem. Soc.* **1976**, *98*, 1729.

6. Green, M. L. H.; Lynch, A. H.; Swan, M. G. *J. Chem. Soc., Dalton Trans.* **1972**, 1445.

7. (a) Pilato, R. S.; Housemekerides, C. E.; Jernakoff, P.; Rubin, D.; Geoffroy, G. L.; Rheingold, A. L. *Organometallics* **1990**, *9*, 2333. (b) Jernakoff, P.; Geoffroy, G. L.; Rheingold, A. L.; Geib, S. J. *J. Chem. Soc., Chem. Commun.* **1987**, 1610.

8. Parkin, G.; Bercaw, J. E. *Polyhedron* **1988**, *7*, 2053.

9. See introduction of Chapter 3.

10. (a) Fryzuk, M. D.; Mao, S. S. H.; Zaworotko, M. J.; MacGillivray, L. R. *J. Am. Chem. Soc.* **1993**, *115*, 5336. (b) Fryzuk, M. D.; Mao, S. S. H.; Zaworotko, M. J.; MacGillivray, L. R. Abstract 293. 206th National ACS Meeting, Chicago, Illinois, 1993. (c) Finch, W. C.; Anslyn, E. V.; Grubbs, R. H. *J. Am. Chem. Soc.* **1988**, *110*, 2406. (d) Howard, T. R.; Lee, J. B.; Grubbs, R. H. *J. Am. Chem. Soc.* **1980**, *102*, 6876. (e) Tebbe, F. N.; Parshall, G. W.; Reddy, G. S. *J. Am. Chem. Soc.* **1978**, *100*, 3611.

11. (a) Hou, Z.; Breen, T. L.; Stephan, D. W. *Organometallics* **1993**, *12*, 3158. (b) Ho, J.; Hou, Z.; Drake, R. J.; Stephan, D. W. *Organometallics* **1993**, *12*, 3145. (c) Ho, J.; Hou, Z.; Drake, R. J. Stephan, D. W. Abstracts 72 and 74. 206th ACS National Meeting, Chicago, Illinois, 1993. (d) Hou, Z.; Stephan, D. W. *J. Am. Chem. Soc.* **1992**, *114*, 10088.

12. (a) Brunner, H.; Kubicki, M. M.; Leblanc, J-C.; Moise, C.; Volpato, F.;

Wachter, J. *J. Chem. Soc., Chem. Commun.* **1993**, 851. (b) Nelson, J. E.; Parkin, G.; Bercaw, J. E. *Organometallics* **1992**, *11*, 2181.

13. Crabtree, R. H. *Angew. Chem. Int. Ed. Engl.* **1993**, *32*, 789.

14. (a) Carney, M. J.; Walsh, P. J.; Hollander, F. J.; Bergman, R. G. *Organometallics* **1992**, *11*, 761. (b) Carney, M. J.; Walsh, P. J.; Bergman, R. G. *J. Am. Chem. Soc.* **1990**, *112*, 6426. (c) Carney, M. J.; Walsh, P. J.; Hollander, F. J.; Bergman, R. G. *J. Am. Chem. Soc.* **1989**, *111*, 8751.

15. Howard, W. A.; Waters, M.; Parkin, G. *J. Am. Chem. Soc.* **1993**, *115*, 4917.

16. Parkin, G.; Bercaw, J. E. *J. Am. Chem. Soc.* **1989**, *111*, 391.

17. Strauss, S. H. *Chem. Rev.* **1993**, *93*, 927.

18. van Asselt, A., Ph. D. Thesis, California Institute of Technology, 1987.

19. For a better synthesis of $Cp^*_2Ta(=O)Cl$ see: Antonelli, D. M.; Schaefer, W. P.; Parkin, G.; Bercaw, J. E. Submitted manuscript to *J. Organomet. Chem.*

20. Jordan, R. F.; Dasher, W. E.; Echols, S. F. *J. Am. Chem. Soc.* **1986**, *108*, 1718.

21. Quan, R. W.; Bercaw, J. E.; Schaefer, W. P. *Acta. Cryst.* **1991**, *C47*, 2057.

22. (a) Lambert, J. B.; Zhang, S.; Stern, C. L.; Huffman, J. C. *Science* **1993**, *260*, 1917. (b) Hlatky, G. G.; Turner, H. W.; Eckman, R. R. *J. Am. Chem. Soc.* **1989**, *111*, 2728. (c) Turner, H. W. *European Patent Application* **1988** *277* 004. (d) Hlatky, G. G.; Turner, H. W. *European Patent Application* 1988 *277* 003. (e) Chien, J. C. W.; Tsai, W-M.; Raush, M. D. *J. Am. Chem. Soc.* **1991**, *113*, 8570. (f) Xinmin, Y.; Stern, C. L.; Marks, T. J. *J. Am. Chem. Soc.* **1991**, *113*, 3623.

23. Wright, I. N. ; Ph. D. thesis, Brasenose College, Oxford, 1991.

24. Antonelli, D. M.; Blake, R. E.; Bercaw, J. E. Unpublished results.

25. Burger, B.J.; Bercaw, J. E. In *Experimental Organometallic Chemistry*; Wayda, A. L., Darensbourg, M. Y. Eds.; ACS Symposium Series 357;

American Chemical Society, Washington, D. C. 1987.

26. Marvich, R. H.; Brintzinger, H. H. *J. Am. Chem. Soc.* **1971**, *93*, 2046.

27. Haltzman, H.; Sharefkin, J. G. *Organic Synthesis* vol. 43, 60.

28. International Tables for X-ray Crystallography, Volume IV, p. 71, p. 147; Birmingham, Kynoch Press, 1974.

Appendix 1. X-ray crystal structure data for $[Cp^*_2TaF_2][PF_6]$ (**20**).

Table V. Crystal and Intensity Collection Data for $[Cp^*_2TaF_2][PF_6]$ (**20**).

chemical formula	$C_{30}H_{30}F_8Ta$
crystal dimension, mm	all dimensions < 0.7 mm
crystal system	monoclinic
space group	$P2_1/c$
a,Å	11.582 (5)
b,Å	12.514 (6)
c, Å	15.712 (6)
β, deg	90.34 (3)
V, Å^3	2277.2 (17)
ρ_{calc}, g cm^{-3}	1.850
Z	4
λ,Å	0.711
μ, cm^{-1}	52.33
temp, ^oC	23
2θ rang, deg	3-50
no. of reflections measured, total	3996
R	0.053
GOF	2.65

Table VI. Final Heavy Atom Parameters for $[Cp^*_2TaF_2][PF_6]$ (20).
x, y, z and $U_{eq}{}^a \times 10^4$

Atom	x	y	z	U_{eq}
Ta	7753(.4)	2672(.3)	4843(.3)	417(1)
F1	7052(8)	2373(6)	3776(5)	1109(28)
F2	9122(6)	3342(6)	4484(6)	1191(30)
Cp1	6394(9)	4120(8)	4590(7)	492(27)
Cp2	7333(10)	4592(8)	4953(8)	591(33)
Cp3	7504(11)	4137(9)	5793(8)	645(34)
Cp4	6557(9)	3457(9)	5943(7)	507(27)
Cp5	5914(9)	3423(9)	5196(7)	518(27)
Cp6	7442(9)	980(8)	5594(8)	500(28)
Cp7	7707(10)	725(8)	4714(8)	565(32)
Cp8	8862(9)	1073(7)	4574(7)	456(26)
Cp9	9315(8)	1503(8)	5330(7)	448(25)
Cp10	8452(9)	1461(8)	5953(6)	468(25)
Me1	5921(11)	4371(10)	3736(8)	717(36)
Me2	8165(13)	5409(10)	4552(11)	993(50)
Me3	8438(13)	4493(12)	6425(10)	973(47)
Me4	6162(12)	3137(12)	6822(8)	844(41)
Me5	4775(10)	2857(11)	5060(10)	822(40)
Me6	6381(12)	565(11)	6031(9)	853(41)
Me7	6920(12)	159(11)	4110(9)	878(42)

Table VI. (Continued)

Atom	x	y	z	U_{eq}
Me8	9500(11)	990(10)	3747(8)	736(37)
Me9	10521(10)	1893(10)	5451(9)	713(34)
Me10	8677(11)	1620(11)	6899(8)	771(39)
P	12667(3)	2420(3)	2766(2)	580(7)
F3	13308(10)	3482(9)	2883(9)	1740(47)
F4	12943(10)	2434(10)	1767(7)	1583(44)
F5	13811(9)	1820(10)	2942(7)	1586(40)
F6	11531(8)	3067(10)	2600(8)	1729(44)
F7	12007(10)	1342(9)	2637(8)	1735(47)
F8	12381(9)	2352(12)	3705(7)	1786(50)

[a] $U_{eq} = \frac{1}{3} \sum_i \sum_j [U_{ij}(a_i^* a_j^*)(\vec{a}_i \cdot \vec{a}_j)]$

Table VII. Anisotropic Displacement Parameters for $[Cp^*_2TaF_2][PF_6]$ (20).

Atom	U_{11}	U_{22}	U_{33}	U_{12}	U_{13}	U_{23}
Ta	556(3)	374(3)	323(2)	119(2)	69(2)	59(2)
F1	1802(83)	948(59)	571(45)	625(56)	−540(53)	−287(40)
F2	909(56)	715(52)	1959(96)	358(42)	793(59)	684(58)
Cp1	575(69)	515(66)	386(59)	−50(53)	−30(52)	−6(49)
Cp2	710(79)	316(57)	748(89)	164(53)	102(69)	36(53)
Cp3	777(91)	506(71)	651(81)	298(63)	−156(69)	−182(60)
Cp4	474(65)	536(67)	512(67)	137(52)	3(54)	−26(54)
Cp5	466(63)	549(68)	538(68)	99(51)	−17(53)	−29(54)
Cp6	518(69)	355(58)	629(74)	14(47)	81(57)	168(52)
Cp7	678(76)	313(55)	704(86)	84(55)	5(67)	24(54)
Cp8	574(67)	288(52)	505(63)	59(46)	35(53)	31(45)
Cp9	447(60)	361(54)	537(66)	−5(45)	−21(50)	52(48)
Cp10	543(66)	449(60)	410(59)	151(50)	−96(50)	44(47)
Me1	775(89)	760(90)	616(81)	116(69)	−116(69)	47(67)
Me2	1032(111)	482(79)	1465(146)	−59(76)	−28(106)	162(92)
Me3	1148(121)	845(106)	920(113)	181(88)	−431(100)	−298(86)
Me4	1047(105)	995(105)	492(73)	327(89)	184(72)	38(73)
Me5	554(75)	888(103)	1026(108)	−24(68)	83(73)	−34(87)
Me6	804(94)	815(97)	943(109)	10(75)	302(82)	372(83)
Me7	888(98)	724(92)	1019(113)	−221(75)	−338(88)	−189(82)
Me8	937(99)	678(84)	594(81)	144(71)	213(72)	−53(64)
Me9	601(74)	617(75)	921(96)	−48(63)	−25(68)	70(73)
Me10	947(98)	888(101)	478(72)	308(79)	9(68)	122(67)
P	548(16)	648(20)	546(18)	44(16)	68(14)	−69(15)
F3	1471(93)	1213(92)	2526(151)	−231(72)	−708(100)	−6(94)
F4	1560(94)	2263(139)	930(76)	−153(86)	291(70)	−27(76)
F5	1311(82)	1741(105)	1713(106)	597(77)	539(76)	786(91)
F6	1170(79)	1894(114)	2113(129)	642(79)	−777(85)	−744(105)
F7	1985(117)	1248(91)	1977(136)	−598(83)	555(103)	−307(87)
F8	1258(80)	3351(191)	751(65)	38(99)	252(61)	−49(87)

$U_{i,j}$ values have been multiplied by 10^4

The form of the displacement factor is:

$$\exp -2\pi^2(U_{11}h^2a^{*2} + U_{22}k^2b^{*2} + U_{33}\ell^2c^{*2} + 2U_{12}hka^*b^* + 2U_{13}h\ell a^*c^* + 2U_{23}k\ell b^*c^*)$$

Table VIII. Complete Distances and Angles for $[Cp^*_2TaF_2][PF_6]$ (**20**).

		Distance(Å)			Distance(Å)
Ta	-CpA	2.105	Me1	-H1M1	0.959
Ta	-CpB	2.119	Me1	-H2M1	0.946
Ta	-F1	1.896(8)	Me1	-H3M1	0.943
Ta	-F2	1.883(8)	Me2	-H1M2	0.948
Ta	-Cp1	2.432(11)	Me2	-H2M2	0.959
Ta	-Cp2	2.457(11)	Me2	-H3M2	0.950
Ta	-Cp3	2.383(12)	Me3	-H1M3	0.944
Ta	-Cp4	2.428(11)	Me3	-H2M3	0.944
Ta	-Cp5	2.396(11)	Me3	-H3M3	0.954
Ta	-Cp6	2.451(11)	Me3	-H4M3	0.951
Ta	-Cp7	2.446(11)	Me3	-H5M3	0.940
Ta	-Cp8	2.416(10)	Me3	-H6M3	0.951
Ta	-Cp9	2.445(10)	Me4	-H1M4	0.956
Ta	-Cp10	2.444(10)	Me4	-H2M4	0.941
Cp1	-Cp2	1.359(15)	Me4	-H3M4	0.953
Cp1	-Cp5	1.409(15)	Me5	-H1M5	0.955
Cp1	-Me1	1.480(16)	Me5	-H2M5	0.939
Cp2	-Cp3	1.450(17)	Me5	-H3M5	0.959
Cp2	-Me2	1.542(19)	Me5	-H4M5	0.962
Cp3	-Cp4	1.410(16)	Me5	-H5M5	0.943
Cp3	-Me3	1.529(19)	Me5	-H6M5	0.948
Cp4	-Cp5	1.386(15)	Me6	-H1M6	0.947
Cp4	-Me4	1.512(17)	Me6	-H2M6	0.946
Cp5	-Me5	1.512(17)	Me6	-H3M6	0.952
Cp6	-Cp7	1.454(16)	Me7	-H1M7	0.952
Cp6	-Cp10	1.430(15)	Me7	-H2M7	0.925
Cp6	-Me6	1.503(18)	Me7	-H3M7	0.969
Cp7	-Cp8	1.425(15)	Me8	-H1M8	0.950
Cp7	-Me7	1.490(18)	Me8	-H2M8	0.957
Cp8	-Cp9	1.403(14)	Me8	-H3M8	0.936
Cp8	-Me8	1.502(16)	Me9	-H1M9	0.942
Cp9	-Cp10	1.403(14)	Me9	-H2M9	0.954
Cp9	-Me9	1.492(16)	Me9	-H3M9	0.946
Cp10	-Me10	1.521(16)	Me10	-H1M1	0.932
P	-F3	1.547(12)	Me10	-H2M1	0.942
P	-F4	1.565(12)	Me10	-H3M1	0.971
P	-F5	1.563(12)			
P	-F6	1.517(12)			
P	-F7	1.533(13)			
P	-F8	1.604(12)			

Table VIII. (Continued)

			Angle(°)				Angle(°)
CpA	-Ta	-CpB	140.1	F8	-P	-F3	90.3(6)
F1	-Ta	-F2	100.3(4)	F5	-P	-F4	90.9(6)
CpA	-Ta	-F1	102.2	F6	-P	-F4	90.1(6)
CpA	-Ta	-F2	103.6	F7	-P	-F4	88.7(6)
CpB	-Ta	-F1	102.5	F8	-P	-F4	90.2(6)
CpB	-Ta	-F2	102.2	F6	-P	-F5	88.2(6)
Cp5	-Cp1	-Cp2	107.7(10)	F7	-P	-F5	179.4(7)
Me1	-Cp1	-Cp2	125.4(10)	F8	-P	-F5	89.1(6)
Me1	-Cp1	-Cp5	126.8(10)	F7	-P	-F6	92.3(7)
Cp3	-Cp2	-Cp1	108.4(10)	F8	-P	-F6	177.2(6)
Me2	-Cp2	-Cp1	128.1(11)	F8	-P	-F7	90.5(6)
Me2	-Cp2	-Cp3	123.3(11)	H2M1	-Me1	-H1M1	109.7
Cp4	-Cp3	-Cp2	106.6(10)	H3M1	-Me1	-H1M1	110.1
Me3	-Cp3	-Cp2	124.7(11)	H3M1	-Me1	-H2M1	111.2
Me3	-Cp3	-Cp4	128.0(11)	H2M2	-Me2	-H1M2	109.6
Cp5	-Cp4	-Cp3	107.0(10)	H3M2	-Me2	-H1M2	110.3
Me4	-Cp4	-Cp3	123.5(10)	H3M2	-Me2	-H2M2	109.5
Me4	-Cp4	-Cp5	126.9(10)	H2M3	-Me3	-H1M3	111.4
Cp4	-Cp5	-Cp1	109.9(9)	H3M3	-Me3	-H1M3	110.5
Me5	-Cp5	-Cp1	122.8(10)	H4M3	-Me3	-H1M3	59.8
Me5	-Cp5	-Cp4	126.8(10)	H5M3	-Me3	-H1M3	54.0
Cp10	-Cp6	-Cp7	106.9(9)	H6M3	-Me3	-H1M3	143.6
Me6	-Cp6	-Cp7	122.4(10)	H3M3	-Me3	-H2M3	110.4
Me6	-Cp6	-Cp10	129.4(10)	H4M3	-Me3	-H2M3	143.5
Cp8	-Cp7	-Cp6	106.4(9)	H5M3	-Me3	-H2M3	60.2
Me7	-Cp7	-Cp6	125.3(10)	H6M3	-Me3	-H2M3	53.6
Me7	-Cp7	-Cp8	128.2(10)	H4M3	-Me3	-H3M3	53.3
Cp9	-Cp8	-Cp7	109.5(9)	H5M3	-Me3	-H3M3	143.6
Me8	-Cp8	-Cp7	125.3(10)	H6M3	-Me3	-H3M3	59.5
Me8	-Cp8	-Cp9	125.2(9)	H5M3	-Me3	-H4M3	111.0
Cp10	-Cp9	-Cp8	108.2(9)	H6M3	-Me3	-H4M3	110.2
Me9	-Cp9	-Cp8	125.3(9)	H6M3	-Me3	-H5M3	111.1
Me9	-Cp9	-Cp10	126.4(9)	H2M4	-Me4	-H1M4	110.6
Cp9	-Cp10	-Cp6	109.0(9)	H3M4	-Me4	-H1M4	109.5
Me10	-Cp10	-Cp6	125.1(10)	H3M4	-Me4	-H2M4	110.9
Me10	-Cp10	-Cp9	124.0(9)	H2M5	-Me5	-H1M5	110.8
F4	-P	-F3	177.8(6)	H3M5	-Me5	-H1M5	109.2
F5	-P	-F3	91.3(6)	H4M5	-Me5	-H1M5	49.9
F6	-P	-F3	89.5(6)	H5M5	-Me5	-H1M5	62.8
F7	-P	-F3	89.2(6)	H6M5	-Me5	-H1M5	141.6

Table VIII. (Continued)

			Angle(°)
H3M5	–Me5	–H2M5	110.5
H4M5	–Me5	–H2M5	141.9
H5M5	–Me5	–H2M5	50.9
H6M5	–Me5	–H2M5	63.2
H4M5	–Me5	–H3M5	62.0
H5M5	–Me5	–H3M5	142.1
H6M5	–Me5	–H3M5	50.1
H5M5	–Me5	–H4M5	109.9
H6M5	–Me5	–H4M5	109.4
H6M5	–Me5	–H5M5	111.2
H2M6	–Me6	–H1M6	111.0
H3M6	–Me6	–H1M6	110.3
H3M6	–Me6	–H2M6	110.6
H2M7	–Me7	–H1M7	112.2
H3M7	–Me7	–H1M7	108.5
H3M7	–Me7	–H2M7	110.8
H2M8	–Me8	–H1M8	109.6
H3M8	–Me8	–H1M8	111.3
H3M8	–Me8	–H2M8	110.8
H2M9	–Me9	–H1M9	110.7
H3M9	–Me9	–H1M9	111.3
H3M9	–Me9	–H2M9	110.4
H2M1	–Me10	–H1M1	112.6
H3M1	–Me10	–H1M1	110.0
H3M1	–Me10	–H2M1	109.2

Table IX. Assigned Hydrogen Atom Parameters for $[Cp^*_2TaF_2][PF_6]$ (20).

	x, y and $z \times 10^4$			
Atom	x	y	z	B
H1M1	6558	4476	3358	6.8
H2M1	5479	5006	3769	6.8
H3M1	5466	3791	3549	6.8
H1M2	8897	5357	4822	9.4
H2M2	7857	6113	4633	9.4
H3M2	8232	5267	3960	9.4
H1M3	9168	4280	6222	9.2
H2M3	8272	4173	6954	9.2
H3M3	8398	5252	6468	9.2
H4M3	8927	4995	6151	9.2
H5M3	8857	3889	6604	9.2
H6M3	8054	4820	6890	9.2
H1M4	6821	2926	7150	8.0
H2M4	5635	2568	6773	8.0
H3M4	5808	3742	7081	8.0
H1M5	4864	2129	5230	7.8
H2M5	4554	2901	4485	7.8
H3M5	4210	3193	5414	7.8
H4M5	4575	2511	5585	7.8
H5M5	4853	2343	4625	7.8
H6M5	4200	3368	4919	7.8
H1M6	6419	−190	6039	8.1
H2M6	5720	803	5730	8.1
H3M6	6383	839	6596	8.1
H1M7	7360	−351	3801	8.3
H2M7	6563	651	3757	8.3
H3M7	6356	−221	4449	8.3
H1M8	10210	633	3852	7.0
H2M8	9649	1700	3548	7.0
H3M8	9041	614	3356	7.0
H1M9	10922	1393	5790	6.7
H2M9	10481	2568	5731	6.7
H3M9	10868	1969	4910	6.7
H1M10	9039	1014	7120	7.3
H2M10	7968	1766	7166	7.3
H3M10	9180	2236	6958	7.3

Chapter 3

[2+2] Cycloaddition, Insertion, and Substitution Reactions of Tantalum Imido and Amido Complexes

Abstract: The synthesis of reactive tantalum imido and amido complexes is described. Treatment of Cp^*TaCl_4 with four equivalents of lithium anilide affords $Cp^*Ta(=NPh)(NHPh)_2$. This complex reacts readily with substituted anilines to generate $Cp^*Ta(=NPh')(NHPh')_2$ and with alcohols such as pinacol to afford $Cp^*Ta(OCMe_2CMe_2O)_2$, products whereby both the imido and amido groups are exchanged. Exposing $Cp^*Ta(=NPh)(NHPh)_2$ to CO_2 resulted in the isolation of $Cp^*Ta(OCONPh)(\eta^2\text{-}OCONHPh)_2$ with both the formal [2+2] addition of CO_2 across the imido group and insertion of CO_2 into the amido group. Finally, bis-imido complexes were prepared by exposing $Cp^*Ta(=NPh)(NHPh)_2$ to one equivalent of HCl to afford $Cp^*Ta(=NPh)_2$ or by treating Cp^*TaCl_4 with four equivalents of lithium 2,6-diisopropylanilide to yield $Cp^*Ta(=NPh'')_2$ with Ph'' = 2,6-diisopropylphenyl.

Introduction

Since the first report of a transition metal imido complex forty years ago,[1] the number of complexes with this functional group has dramatically increased. The preparation of such complexes has been actively pursued because of the unique properties this ligand imparts to metal complexes. The imido group can act as a two or four electron donor and the metal valency can be deduced by the position of the substituent on the nitrogen.[2]

I II

As a four electron donor with an sp hybridized nitrogen atom, the M-N-R bond angle is expected to be 180°. For a two electron donor with a pair of electrons in a nitrogen sp^2 orbital, the M-N-R bond angle is expected to be 120°. All but one crystallographically characterized structures of terminal imido complexes have bond angles greater than 155°, suggesting that nearly all imido groups have triple-bond character. The imido moiety has been of major interest due to its potential in catalytic processes.[3] For example, metal-imido groups are important catalysts in the preparation of aziridines and amines.[4]

The great advantage of the imido group is the ability to control both the electronic and steric effects of the ligand. By using electron-donating or electron-withdrawing groups, the degree of π bonding and the strength of the π bond can be modulated. Furthermore, the steric bulk of the substituent on the nitrogen can also be used to adjust reactivity. For instance, bulky imido groups prevent dimerization reactions that lead to imido-bridged complexes. As one example, the Schrock alkylidene-imido complex (**1**) with the 2,6-di*isopropyl*phenyl imido group are stable, highly reactive catalysts for olefin metathesis.[5]

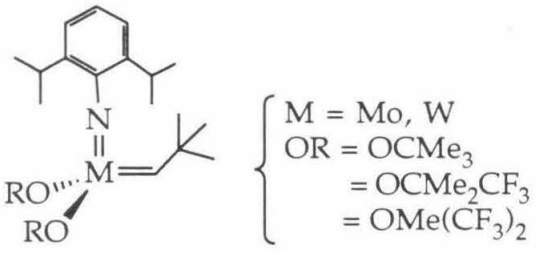

1

However, a change to a 2,6-di*methyl*phenylimido group results in decomposition of the complex; presumably, there are bimolecular decomposition pathways available with the less sterically bulky group.

Recently, several early transition metal complexes have been prepared which contain reactive imido groups. Wolczanski[6,7] has generated a series of coordinative unsaturated transition metal complexes with bulky silylamide ligands. It was shown that the thermolysis of the alkyl complex **2** led to C-H activation, presumably through the transient 14 electron imido complex **3**.[8] In benzene, **2a** produced **4** by the activation of the benzene C-H bond with concomitant loss of methane.

Scheme I

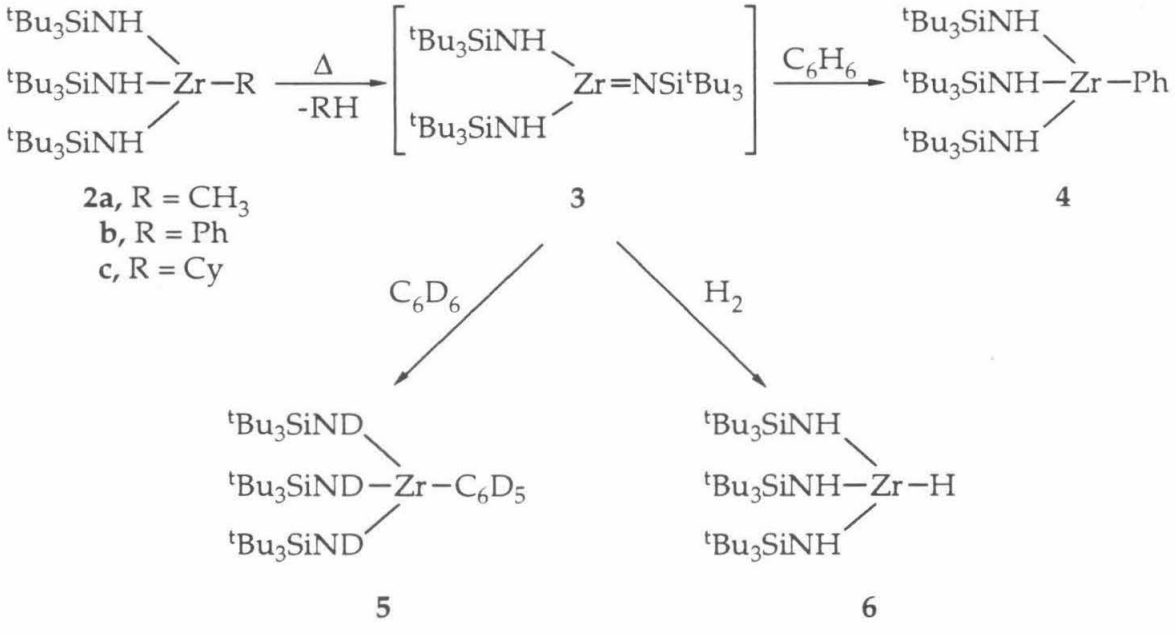

The intermediacy of a 14 electron bis(amido)imido complex **3** was confirmed when $(^tBu_3SiNH)_3ZrCH_3$ was thermolyzed in C_6D_6:

(^{t}Bu$_3$SiND)(^{t}Bu$_3$SiNH)$_2$ZrC$_6$D$_5$ and (^{t}Bu$_3$SiND)$_2$(^{t}Bu$_3$SiNH)$_2$ZrC$_6$D$_5$ appeared and then reacted further to afford **5**. Finally, methane activation was demonstrated by the thermolysis of (^{t}Bu$_3$SiNH)$_3$ZrCD$_3$ with CH$_4$. Complex **2a** was the sole organometallic species isolated and CD$_3$H was observed spectroscopically. The isolable titanium analog,[9] (^{t}Bu$_3$SiNH)$_2$Ti(=NSi^{t}Bu$_3$)(Et$_2$O), has also been found to undergo C-H activation of benzene. However, the related five-coordinate (Ar'O)$_2$Ti(=NPh)(py')$_2$ where Ar' = 2,6-diisopropylphenyl and py' = 4-pyrrolidinopyridine does not react with benzene or methane.[10] Presumably, with the weaker π-donation of the alkoxyl groups relative to the amido groups, the compound coordinates two nitrogen donors, leading to an unreactive complex.

Bergman[11] has provided evidence for the presence of the 16 electron [Cp$_2$Zr=NR] (**8**) as a transient species from the thermolysis of Cp$_2$Zr(NHR)CH$_3$ (**7**).

Scheme II

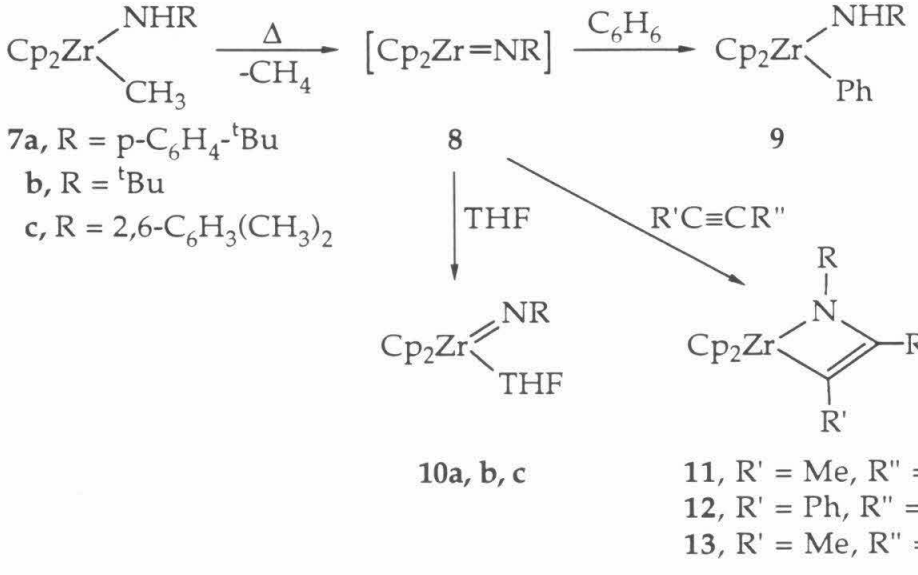

The intermediate imido species **8** is capable of C-H activation of benzene, and the highly electrophilic nature of the metal center is shown by its coordination with donor ligands such as THF, as shown in the crystallographically characterized complex **10b**. Though **10b** contains a linear Zr-N-C linkage which suggests that the imido group is acting as a 4 electron

donor, it does not necessarily follow that $Cp_2Zr(=NR)THF$ is a 20 electron complex.[12] Finally, thermolysis of the zirconium amido alkyls in the presence of alkynes results in the formation of azametallacyclobutenes (**11**, **12**, **13**). Exposure of these complexes to wet silica gel generates enamines that are hydrolyzed to ketones.

A low valent late transition metal complex that contains a terminal imido group is rare.[13] However, $Cp^*Ir{\equiv}N^tBu$ (**15**)[14] has been prepared and the crystal structure reveals a Ir-N bond distance of 1.71Å, which is typical of Ir-N triple bonds and the Ir-N-C linkage is nearly linear (bond angle of 177°). Furthermore, the imido complex does not coordinate acetonitrile or triphenylphosphine. These results indicate that **15** is an 18 electron complex; though it readily undergoes [2+2] cycloaddition reactions with carbon dioxide and isocyanides to form metallacycles such as **16**.

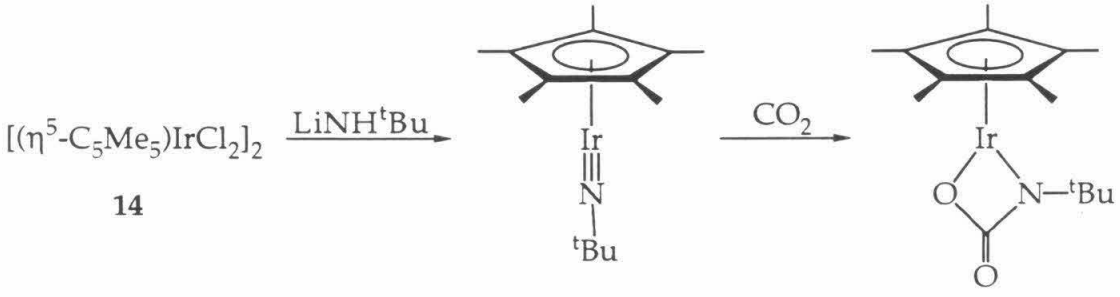

14 **15** **16**

Recently, a vanadium bisimido complex[15] has been proposed as an intermediate in the C-H activation of methane and benzene. The precursor alkyl complexes (**18**) are formed by treating $V(=NSi^tBu_3)(NHSi^tBu_3)Cl$ with an alkyllithium reagent.

17

18a, R' = Me
b, R' = nBu
c, R' = CH_2CMe_3
d, R' = CH_2SiMe_3

Subsequent thermolysis of **18a** in the presence of $^{13}CH_4$ resulted in the isotopically-labeled product **20**. The formation of CH_4, instead of CH_3D, when **18a** was heated in C_6D_6 indicates that the reaction does not proceed by a σ bond metathesis mechanism.[16] These results suggest that the 16 electron bis(imido)amido complex, $(RNH)V(=NR)_2$, is an intermediate in these reactions.

Scheme III

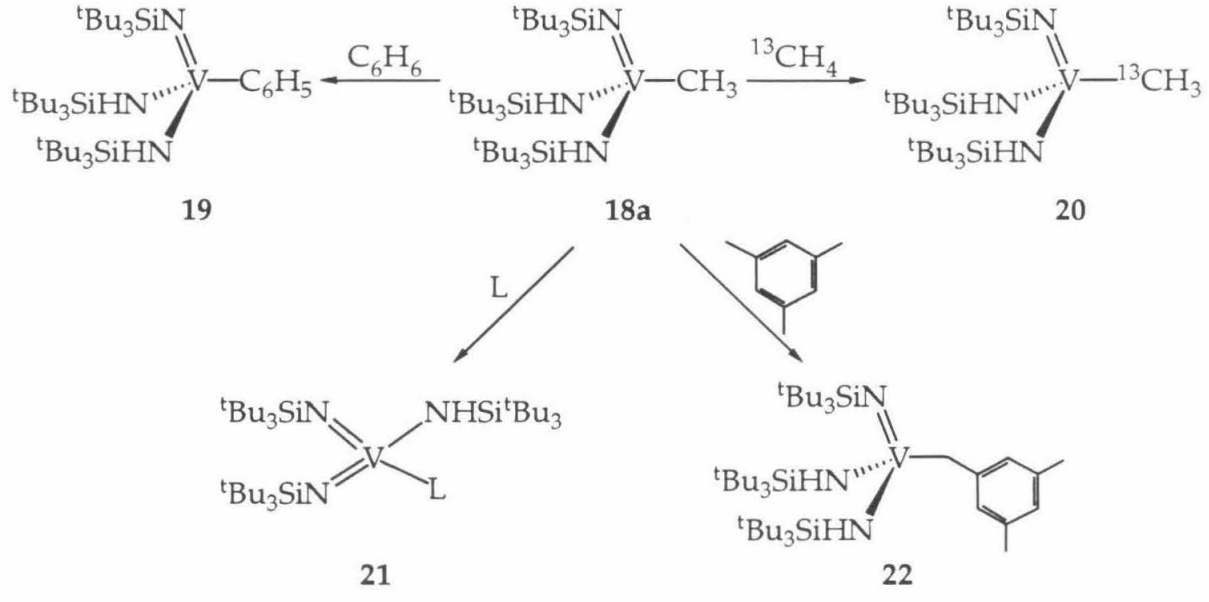

This intermediate can be trapped by diethyl ether, THF, or pyridine to form **21**. The steric influence of the *tert*-butylsilyl groups is demonstrated by C-H activation exclusively at the methyl groups of mesitylene to afford **22**.

Cyclopentadienyl complexes with imido groups have also been examined. Wigley[17] has synthesized a tungsten bisimido complex **24** that undergoes intramolecular C-H activation to form the "tuck-in" complex **26** (Scheme IV).

Scheme IV

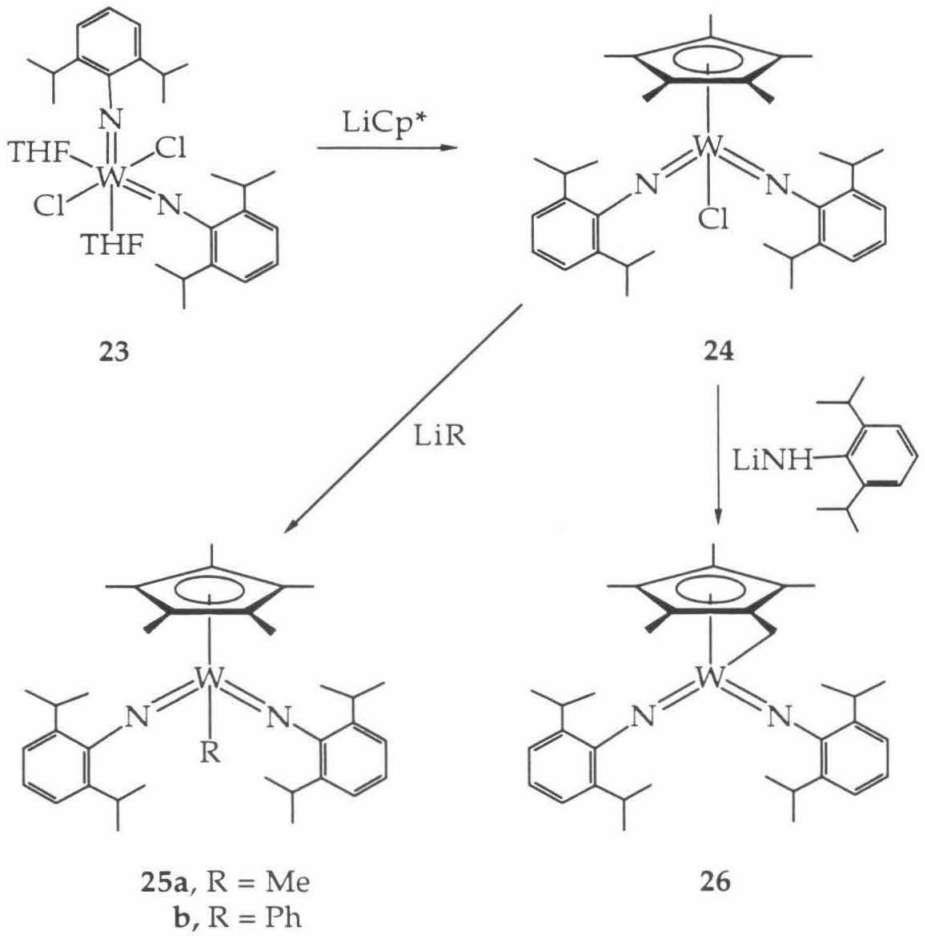

23 **24**

25a, R = Me
b, R = Ph

26

The conversion of **24** to **26** presumably proceeds via the intermediate shown in Scheme V. Interesting, under the reaction conditions employed for the preparation of **25, 26** is not observed even though loss of alkane is known to be facile.

Scheme V

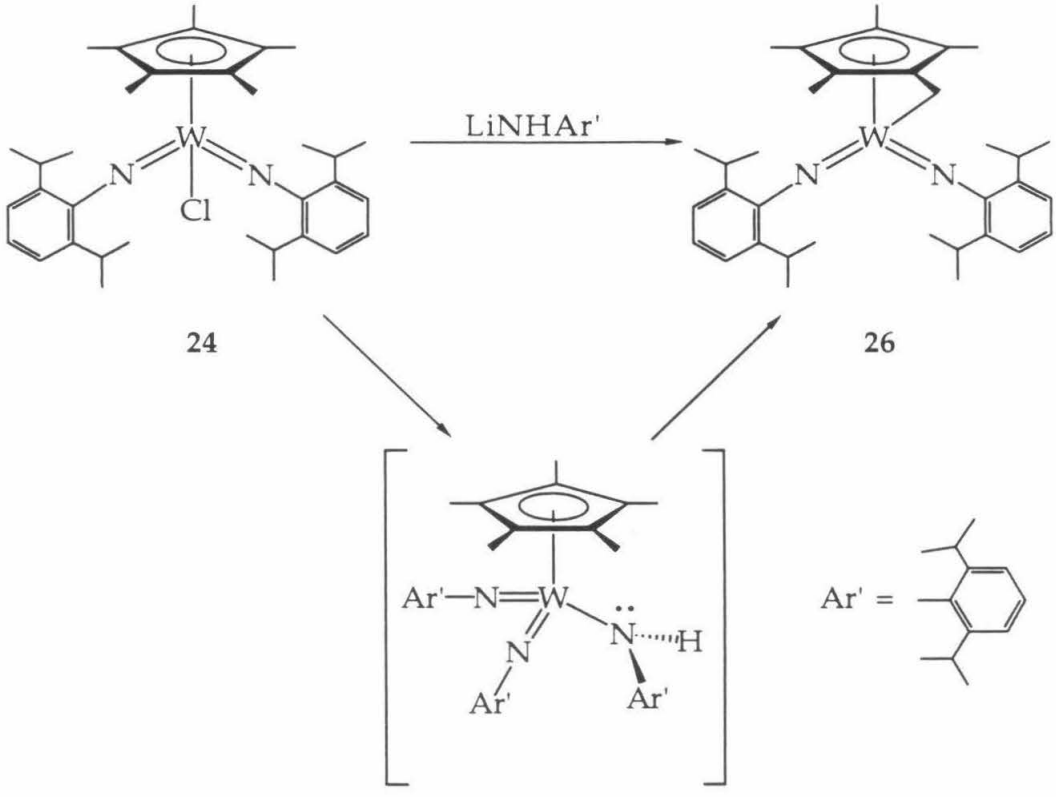

Complex **24** has been structurally characterized and contains linear phenylimido linkages (W-N-C_{ipso} = 168° and 171°). One of the W-Cp* ring carbon distances is short (2.33 Å) while the other four W-Cp* carbon distances are greater than 2.43 Å. Furthermore, the ring exhibits some electron localization to a 1,4-diene unit. This effect can be ascribed to a trans influence of the imido groups, resulting in a weakening of the double bond components of the η^5-C_5Me_5 ring.[18]

Schrock[19] has recently proposed that the 6 electron dianionic imido group is analogous to the 6 electron cyclopentadienide ligand. This line of reasoning leads to the question of whether the cyclopentadienyl group can be replaced by an imido group and what the effect of such a replacement would be on the reactivity of transition metal complexes.[20] Recently, several tungsten (IV) bisimido complexes were prepared, including $W(=NAr)_2(PMe_2Ph)_2$ (**27**) where Ar = 2,6-C_6H_3-*i*Pr_2.

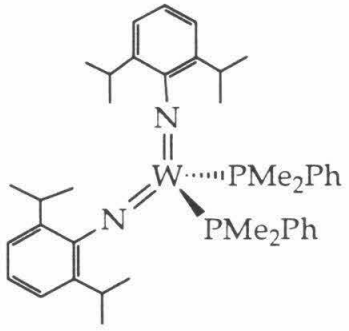

27

The four coordinate d^2 complex is pseudotetrahedral with linear imido groups and two metal-nitrogen π bonds for each imido moiety. With the 1 σ and 2 π interaction between the metal and each of the imido moieties, the $W(=NAr)_2$ is a 14 electron fragment and is both isolobal and isoelectronic with the Cp_2Hf fragment. Recently, Gibson[21] has carried out Fenske Hall calculations on the complex $CpNb(=NMe)Cl_2$ in order to compare it with the group 4 metallocenes, Cp_2MCl_2. Both the Cp and imido ligands are 1 σ, 2 π donors with the σ orbital of a_1 symmetry and the π orbitals of e_1 symmetry. The metallocene system has been previously studied by Hoffmann.[22] The Cp_2M fragment contains $1a_1$, b_2, and $2a_1$ symmetric frontier orbitals that contribute to the binding of ligands to the metal center.

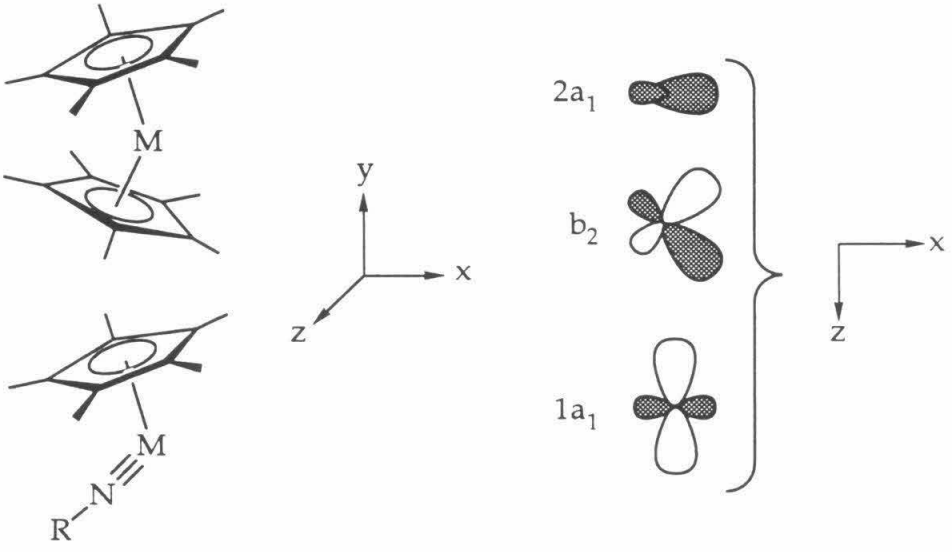

Figure 1. Frontier molecular orbitals for a bent metallocene and [Cp*M(=NR)] fragment.

When comparing the results from the Fenske Hall calculations for $CpNb(=NMe)Cl_2$ and Cp_2MCl_2, the frontier orbitals are similar in their molecular orbital compositions. The only significant difference lies in the $2a_1$ orbital of the imido complex, which exhibits a substantial amount of d_{xz} character.

Table I. Fenske Hall Frontier Orbital Contributions for $[Cp_2Zr]$ fragment

Orbital	% Contribution	
	Ligands	Metal
$1a_1$	11	84 d_{y^2}, 5 s
b_2	27	66 d_{yz}, 7p_y
$2a_1$	14	36 $d_{z^2-x^2}$, 33 s, 17 p_z

Table II. Fenske Hall Frontier Orbital Contributions for CpNb(=NR) fragment

Orbital	% Contribution	
	Ligands	Metal
$1a_1$	12	79 d_{y^2}, 9 s
b_2	41	57 d_{yz}, 2 d_{xy}
$2a_1$	24	23 $d_{z^2-x^2}$, 19 d_{xz}, 18s, 14 p_z, 2 p_x

The resultant orbital is directed out of the normal wedge of the bent metallocene and could result in differences in the reaction chemistry of metallocene and half-sandwich imido complexes.

The reactive imido complexes discussed in this introduction are electrophilic (12 to 16 electron metal centers) and many contain bulky ancillary ligands (*tert*-butylsilyl and 2,6-diisopropylphenyl) in order to prevent dimerization. Furthermore, the coordinative unsaturation of the metal plays a role in the reactivity of these complexes.[23] As mentioned in the introduction to chapter two, the goal was the preparation of "π-loaded"

complexes in which an oxo or imido group would not be maximally bonded to the metal center. Therefore, this chapter will describe the preparation and reaction chemistry of several complexes which contain the [Cp*Ta(=NR)] fragment. Specifically, the synthesis and reaction chemistry of $Cp^*Ta(=NPh)(NHPh)_2$ will be described, which contains both reactive imido and amido groups. Furthermore, the preparation of two bis-imido complexes will be presented.

Results and Discussion

The preparation of reactive tantalum imido complexes was attempted by treating readily available Cp^*TaCl_4[24] with trimethylsilyl amines and lithium amides or anilides. If a mono-imido complex (**28**) can be prepared, introduction of a second oxo, imido, or alkylidene group should be facile. (Scheme VI)

Scheme VI

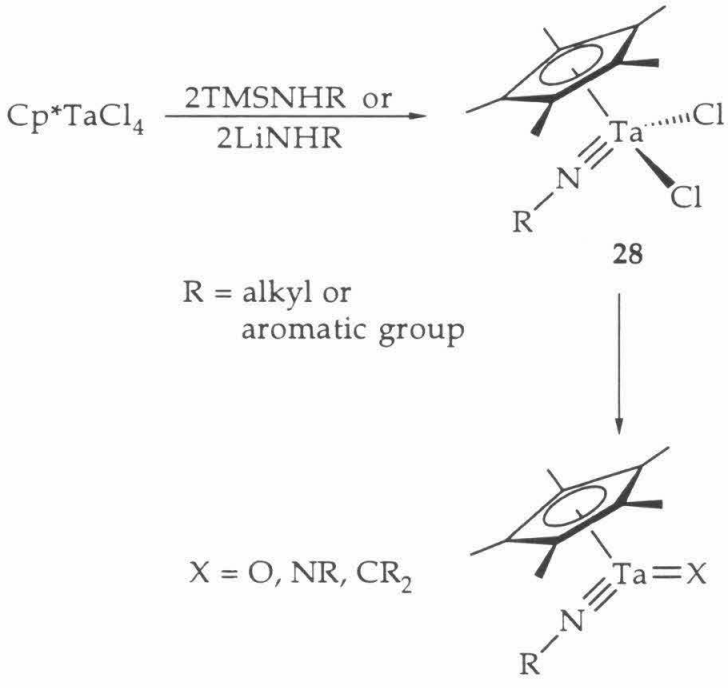

When Cp^*TaCl_4 was treated with two equivalents of trimethylsilyl-*tert*-butylamine, $Cp^*Ta(NH^tBu)Cl_3$ (**30**) was isolated as the only product.

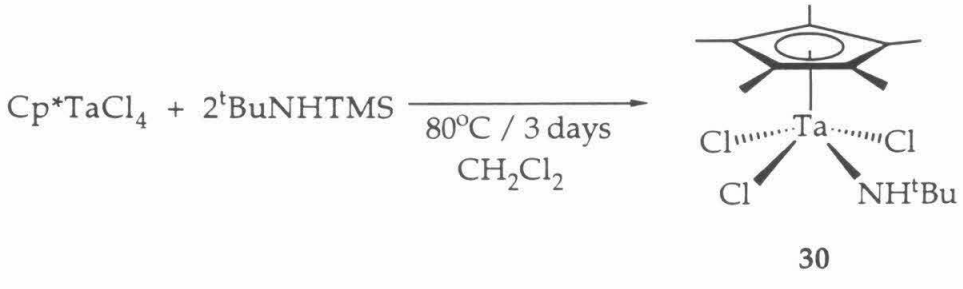

30

Similarly, when PhNHTMS was used, $Cp^*Ta(NHPh)Cl_3$ (**31**) was formed as the exclusive product. Recently, it has been reported that heating the reaction mixture at 80°C for 10 days affords the imido complexes, $Cp^*Ta(=NR)Cl_2$.[25] However, subsequent attempts to deprotonate $Cp^*Ta(NH^tBu)Cl_3$ or $Cp^*Ta(NHPh)Cl_3$ to generate imido complexes were unsuccessful.

Complexes with imido and amido functionalities were produced when lithium amides and anilides were employed. The complex $Cp^*Ta(=NPh)(NHPh)_2$ (**32**) was prepared by treating Cp^*TaCl_4 with four equivalents of lithium anilide in THF. A yellow product was isolated in good yield.

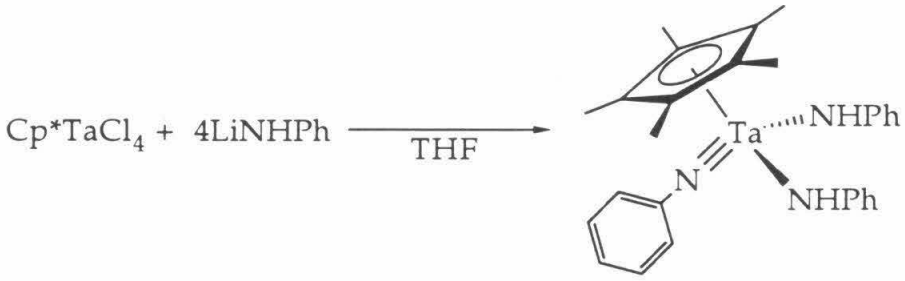

32

Complex **32** exhibited a singlet at 5.90 ppm for the equivalent amido protons. The ^{13}C NMR spectrum contains the appropriate number of peaks for one imido and equivalent amido groups. As is the case with $Mo(=NAr')_2(NHAr')_2$ (Ar' = 2, 6-diisopropylphenyl)[26], variable temperature NMR studies showed that proton transfer does not occur between an amido and imido group on the NMR time scale. The structure of **32** was determined by an X-ray diffraction study and an ORTEP drawing is shown in Figure 2. The Ta-N bond distance of 1.78Å for the imido group is typical for a triply bonded imido group (compare to $(Me_2N)_3Ta(NtBu)$ with 1.77Å and $(PEt_3)Cl(THF)_2Ta(NPh)$ with 1.77Å).[27,28] However, unlike the bis-imido complexes described in the introduction, the sole imido group of **32** does not exert a trans influence sufficient to effect a slippage of the Cp* ring to η^1,η^4- or η^2,η^3- coordination. The tantalum-Cp* ring carbon distances are within 0.1Å of each other, and no electron localization is evidenced by the Cp* carbon distances either.

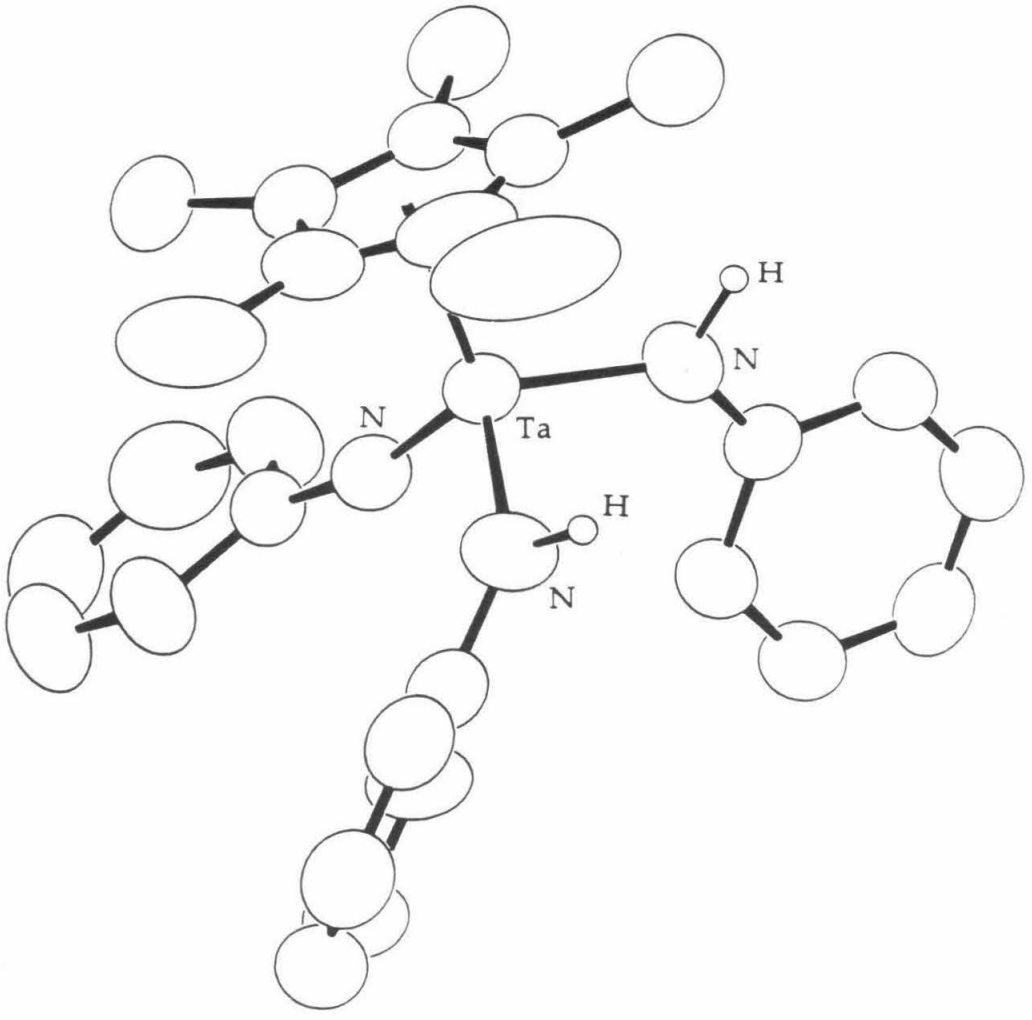

Figure 2. ORTEP diagram of $Cp^*Ta(=NPh)(NHPh)_2$ (**32**).

Table III. Selected distances (Å) and bond angles (deg) for $Cp^*Ta(=NPh)(NHPh)_2$ (**32**)

Distances			
Ta-Cp*	2.126 (3)	N2-C11	1.395 (6)
Ta-N1	1.784 (5)	N3-C21	1.395 (6)
Ta-N2	2.013 (5)	N2-HN2	0.974
Ta-N3	2.029 (5)	N3-HN3	0.972
N1-C1	1.383 (6)		

Bond Angles	
N1-Ta-Cp*	120.2 (2)
N2-Ta-N3	106.0 (2)
Ta-N1-C1	166.7 (4)
Ta-N2-C11	134.4 (3)
Ta-N3-C21	132.9 (3)

Initial attempts to expel a second equivalent of aniline to produce $Cp^*Ta(=NPh)_2$ were not successful. Thermolysis and the addition of donor compounds such as PMe_3 resulted in the observation of **32** with small amounts of decomposition. Also, neither C-H activation chemistry of benzene nor cycloaddition of ethylene or 2-butyne were observed. However, $Cp^*Ta(=NPh)(NHPh)_2$ does react with alcohols, amines, and water. Treatment of **32** with H_2O generates a complex (**34**) which had been previously prepared by another route.[29] Alcohols such as pinacol react with **32** to afford a product (**33**) in which both the imido and amido groups are replaced.[30] Finally, treating **32** with PCl_5 and $AlCl_3$ results in the isolation of Cp^*TaCl_4[31] (Scheme VII).

Scheme VII

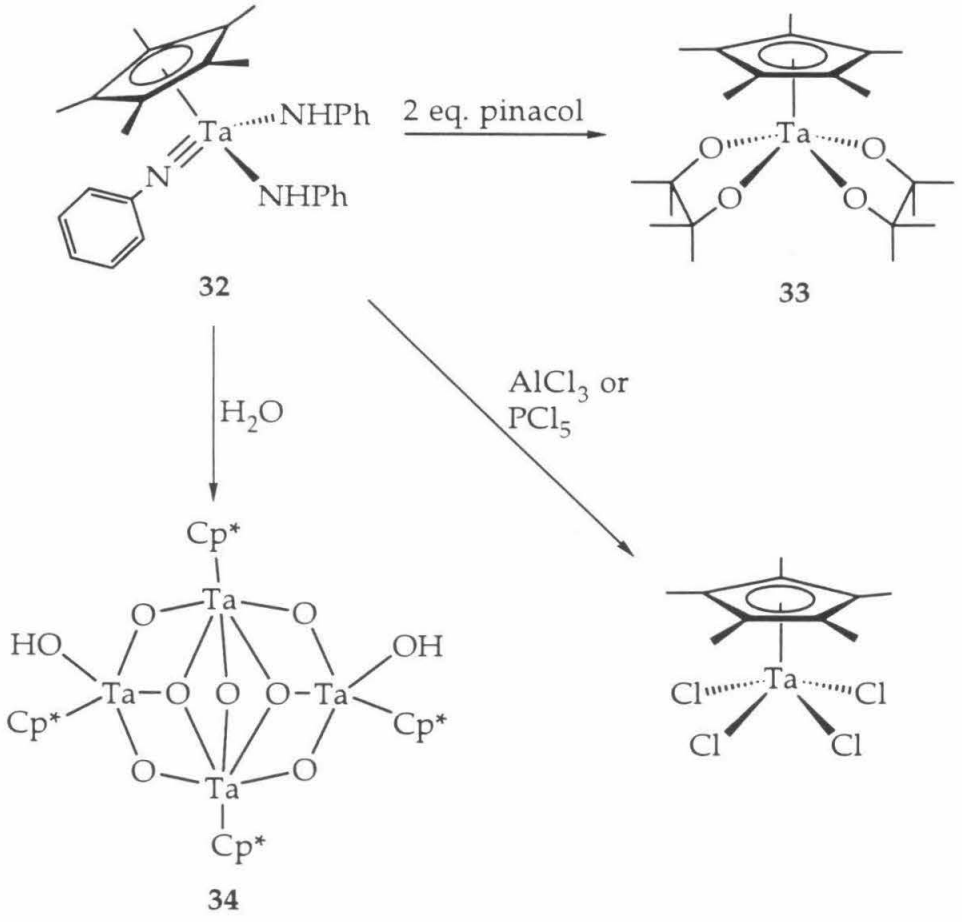

Amines afford new imido-amido complexes. Treating **32** with 20 equivalents of NH_2Ph' (Ph' = *p* -$NH_2C_6H_4X$, X = CH_3, OCH_3, NO_2, F) affords $Cp^*Ta(=NPh')(NHPh')_2$. With mono-, di- and tri- substituted products in the reaction mixture, the rates of the imido/amido transformation were difficult to quantitate. In addition, a large excess of the substituted anilines was necessary to drive the reaction to completion. However, the relative rates of the reactions suggest a mechanism for the imido-amido exchange in which there is a rate-determining pre-coordination of the amine prior to proton transfer. With electron-donating groups at the para position of the substituted aniline, the exchange was quite facile at room temperature. With an electron-withdrawing group at the para position, heating the reaction was necessary in order to drive the reaction to completion. These results are in agreement with the mechanisms shown in Schemes VIII and IX, which result in the exchange of both imido and amido groups.[32]

Scheme VIII

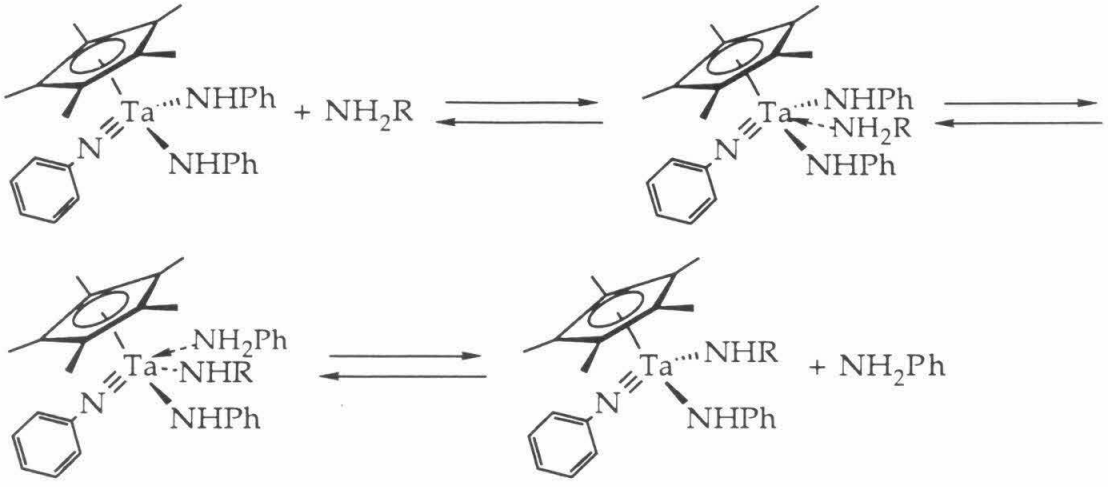

Scheme IX

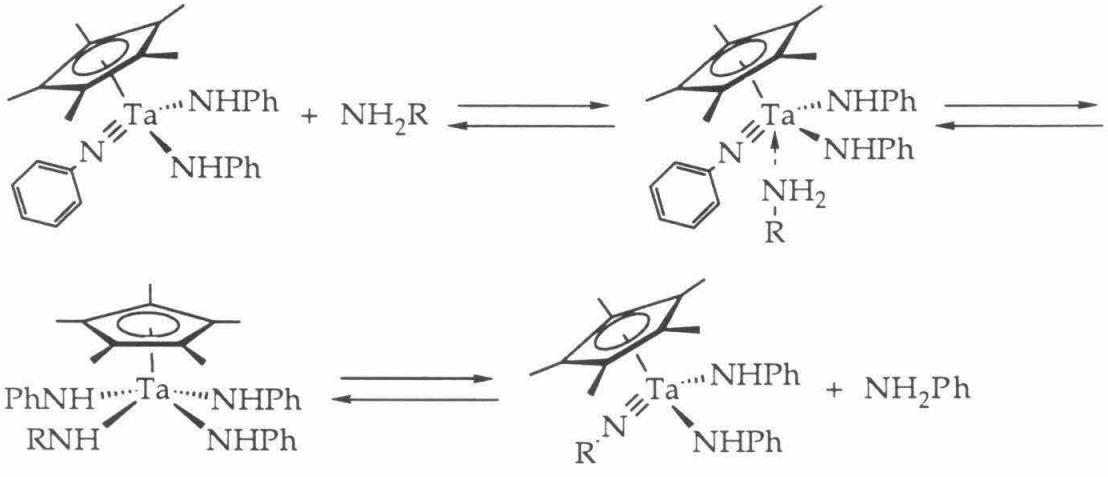

These results lead to the intriguing conclusion that coordination of the amine to what might be an eighteen electron metal center is required prior to proton transfer. The crystal structure and the ^{1}H NMR spectrum indicate that **32** contains equivalent amido groups. These exchange reactions indicate, however, that **32** can exist as a sixteen electron complex, therefore, without a dative bond from one of the amido groups. Once coordinated, the amine would be expected to undergo facile proton transfer, for the intermediate would contain a partial positive charge on the nitrogen and acidic protons.

In order to simplify the ^{1}H NMR spectra for the imido-amido exchange reaction with amines, Cp*Ta(=N-*p*-C_6H_4Me)(NH-*p*-$C_6H_4Me)_2$ was prepared.

Treatment of Cp^*TaCl_4 with 4 equivalents of *para*-toluidine gave **35** in high yield. Further studies with **35** to determine reaction rates with amines have not been attained.

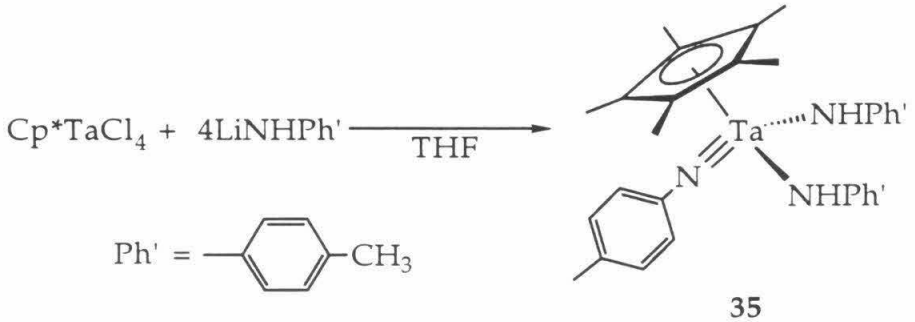

35

When **32** was treated with excess CO_2, both [2+2] addition of carbon dioxide across the imido group and insertion into the amido group affords **36**.[33] Complex **36** contains two η^2-carbamate groups from CO_2 insertion and the metallacycle from the formal [2+2] addition of a C=O bond of CO_2 with a tantalum imido bond.[34] The hapticity of the carbamates was confirmed by a X-ray structure analysis with the ORTEP drawing shown in Figure 3.

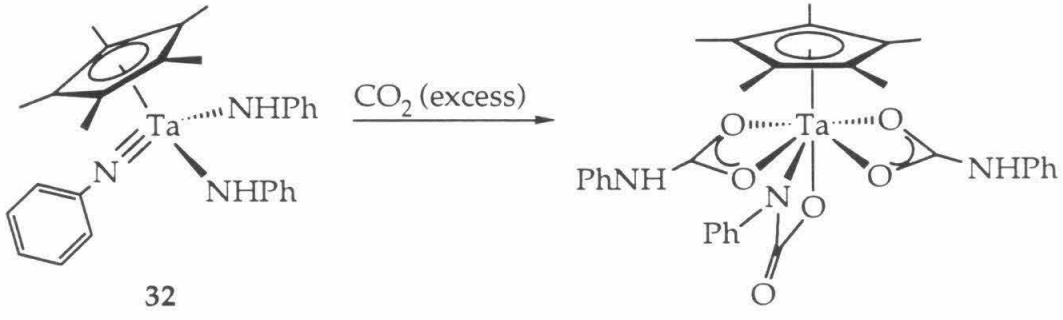

32 **36**

Interestingly, at room temperature, the ^1H NMR spectrum of **36** in THF-d_8 showed a broad singlet for the N-H resonances while the ^{13}C NMR spectrum exhibited four resonances in the carbonyl region. Cooling the sample resulted in more complex spectra. These observations can be attributed to a fluxional process involving either (1) a change in the hapticity of the carbamates or (2) C-N bond rotation of the carbamate groups or (3) a proton transfer from the η^2-carbamate to the O,N-metallacycle with rearrangements of both.

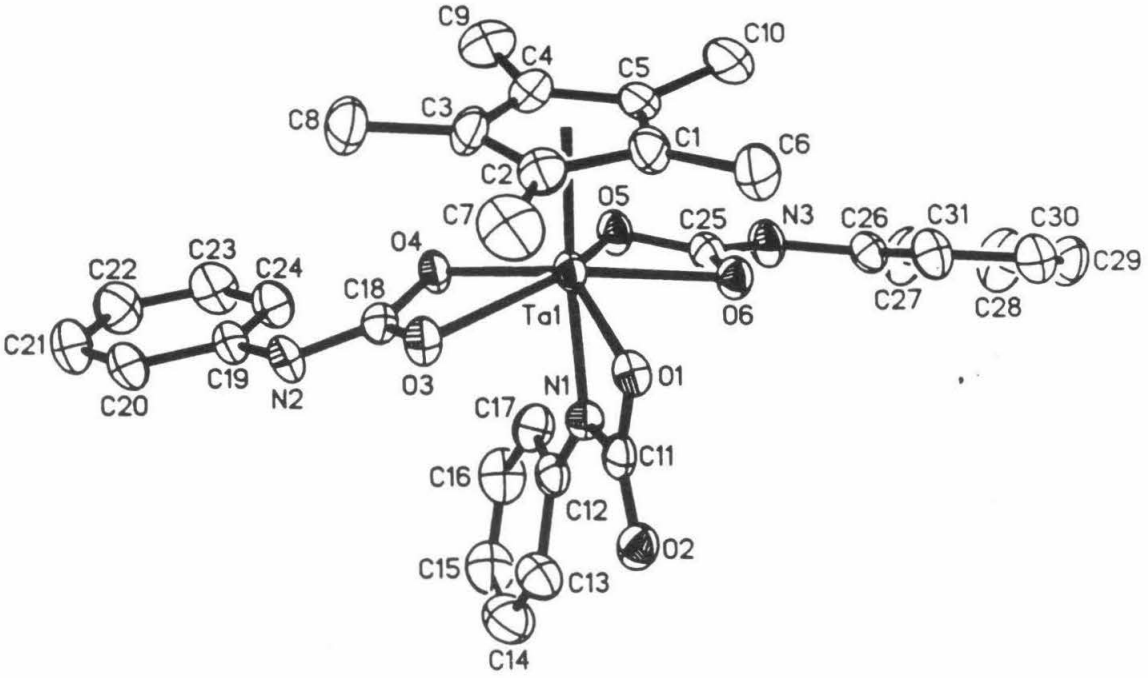

Figure 3. ORTEP diagram of Cp*Ta(OCONPh)(η^2-OCONHPh)$_2$ (**36**)

However, the rearrangements are probably assisted by THF. The complex was found to be insoluble in benzene, toluene and methylene chloride. The solid state infrared spectrum of **36** exhibited two peaks at 1571 and 1603 cm^{-1} which are characteristic of η^2-carbamates and two peaks at 1699 and 1655 cm^{-1} for the carbonyl group of the O,N-cyclometallacarbamate.[35,36]

The preparation of a bis-imido complex was attempted next. Neither thermolysis of **32** nor the addition of donor ligands such as THF and PMe_3 to **32** resulted in the loss of an equivalent of aniline. However, treatment of **32** with HCl resulted in the isolation of $Cp^*Ta(=NPh)_2$ (**37**) with the concomitant formation of $[NH_3Ph]Cl$.

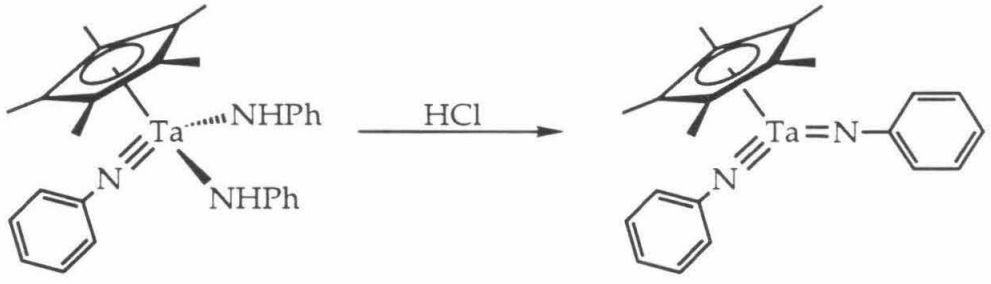

32 **37**

This complex is isostructural and isoelectronic to $[Cp_2Zr{=}N^tBu]$. However, **37** was found to be unreactive toward benzene when heated to 80°C. Further heating to 120°C only resulted in its decomposition. A solution molecular weight determination of **37** in benzene indicates that it is monomeric in solution. The infrared spectrum could be helpful since bridging imido stretches tend to be 50-100 cm^{-1} lower in energy than their terminal imido counterparts.[37] However, since the Ta-N and C-N stretches are coupled in **37**, it is difficult to access the infrared data here.

Finally, the crystal structure of $Cp^*Ta(=NPh')Cl_2$ where Ph' = 2,6-diisopropylphenyl suggested that the steric environment of the diisopropylphenyl group would not preclude reaction of Cp^*TaCl_4 with the lithium anilide to generate $Cp^*Ta(=NPh')Cl_2$. However, a complex isostructural to **32** would not be expected. This means that the loss of a second equivalent of 2,6-diisopropylaniline to form $Cp^*Ta(=NPh')_2$ is expected. When Cp^*TaCl_4 was treated with four equivalents of lithium 2,6-diisopropylanilide, a yellow solid was isolated (**38**).[38]

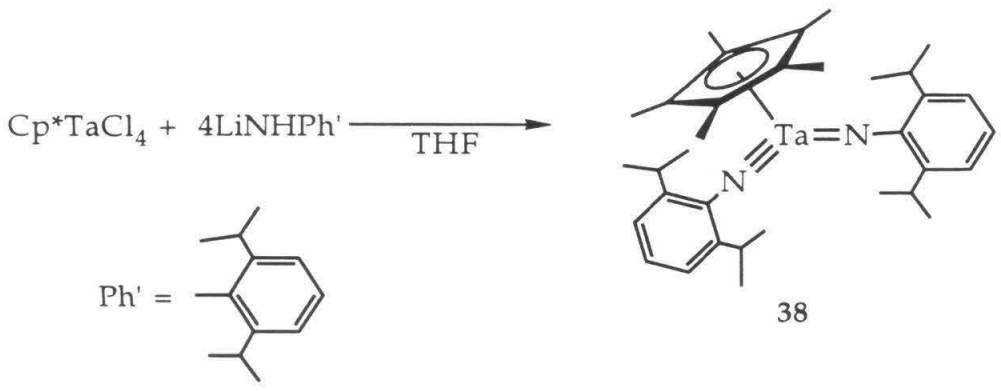

38

Conclusion

A series of tantalum imido complexes have been synthesized and contain both reactive imido and amido functional groups. $Cp^*Ta(=NPh)(NHPh)_2$ (**32**), which is prepared from Cp^*TaCl_4 and lithium anilide, contains imido and amido ligands that react with alcohols, amines, and water, resulting in the isolation of several novel tantalum species. Also, **32** was found to both insert CO_2 at the amido groups and undergo a cycloaddition at the imido group to form the crystallographically characterized $Cp^*Ta(OCONPh)(\eta^2\text{-}OCONHPh)_2$ (**36**). Finally, bis-imido complexes such as $Cp^*Ta(=NPh)_2$ (prepared by treating **32** with hydrochloric acid) or $Cp^*Ta(=NPh')_2$ where Ph' = 2,6-diisopropylphenyl (treating Cp^*TaCl_4 with lithium 2,6-diisopropylanilide) have not been a particularly reactive species.

Experimental

General Considerations. All manipulations were performed using glovebox or high vacuum line techniques.[39] Solvents were dried over $LiAlH_4$ or Na/benzophenone and stored under vacuum over "titanocene."[40] Benzene-*d6* and tetrahydrofuran-*d8*, were dried over activated molecular sieves (4Å, Linde) and stored over "titanocene" or Na/benzophenone. Argon and nitrogen gases were passed over MnO on vermiculite and activated sieves.

Many reactions were monitored by NMR spectroscopy. Any experiment described in this chapter but not explicitly listed below was carried out in a sealed NMR tube using ~0.7 mL of the NMR solvent with the appropriate reagents.

$Cp^*Ta(NH^tBu)Cl_3$ (30). A high pressure reaction vessel was charged with 1.53 g (3.34 mmol) Cp^*TaCl_4. On the vacuum line, 50 mL methylene chloride was condensed on the solid at -78°C. *Tert*-butyltrimethylsilylamine (1.50 mL, 1.13 g, 7.77 mmol) was added via syringe into the vessel under positive Ar flow. The reaction vessel with the homogeneous solution was heated at 80°C for 30 hours. The resultant solution and precipitate was transferred to a swivel frit assembly. Filtration affords 701 mg (1.42 mmol) of an orange solid. Yield = 43%. Analysis : Calculated (Found) C: 33.99 (34.99); H: 5.09 (5.38); N: 2.83 (2.75).

$Cp^*Ta(NHPh)Cl_3$ (31). Approximately 50 mL methylene chloride was condensed into a high pressure reaction vessel containing 9.88 g (21.6 mmol) Cp^*TaCl_4. This solution was transferred to a dry box where 7.17 g (43.3 mmol) phenyltrimethylsilylamine was added. This reaction mixture was then heated at 70°C for 2 weeks. The resultant orange-red solution was transferred to a swivel frit assembly. Filtration affords an orange solid (4.28 g, 8.32 mmol) which was then washed with methylene chloride. Yield = 39%. Analysis : Calculated (Found) C: 37.34 (34.56); H: 4.11 (3.86); N: 2.72 (2.71).

$Cp^*Ta(=NPh)(NHPh)_2$ (32). A 100 mL round bottom flask was charged with 8.05 g (17.6 mmol) Cp^*TaCl_4 and 6.97 g (70.4 mmol) lithium anilide. The flask was attached to a swivel frit assembly. Approximately 70 mL THF was condensed on the solids at -78°C and the solution was allowed to warm slowly to room temperature. The red solution was then stirred for another 20

hours. After removing the volatiles *in vacuo*, toluene was condensed on the solid and the lithium chloride was filtered. The toluene was then removed *in vacuo* and diethyl ether was condensed into the flask. Filtration affords 3.86 g (6.53 mmol) of a bright yellow solid. Yield = 37%. IR spectroscopy (nujol mull, cm^{-1}): 1558.9, 1592.8, 1347.2, 1249.1. Analysis : Calculated (Found) C: 56.85 (56.17); H: 5.45 (5.37); N: 7.10 (6.69).

$Cp^*Ta(OCMe_2CMe_2O)_2$ (33). A 100 mL round bottom flask was charged with 3.11 g (5.26 mmol) $Cp^*Ta(=NPh)(NHPh)_2$ and 1.23 g (10.4 mmol) pinacol. A swivel frit assembly was attached. Approximately 35 mL toluene was then condensed on the solids at -78°C. The resultant solution was stirred at -78°C for one hour at which the dry ice/acetone bath was removed and the volatiles were removed *in vacuo*. Then approximately 20 mL petroleum ether was added and a yellow solid (1.97 g, 3.59 mmol) was filtered. Yield = 68%. Analysis : Calculated (Found) C: 48.17 (48.13); H: 7.17 (6.94).

$Cp^*Ta(OCONPh)(\eta^2\text{-}OCONHPh)_2$ (36). A high pressure reaction vessel was charged with 705 mg (1.19 mmol) $Cp^*Ta(=NPh)(NHPh)_2$. Approximately 20 mL toluene was condensed on the solid at -78°C. Then approximately 3 equivalents of carbon dioxide was added at -196°C using a gas bulb. The resultant solution was allowed to warm to room temperature. The reaction vessel was placed on a device to shake the solution. Within the hour, the solution appeared orange and after 3 hours, an insoluble solid had appeared. After 22 hours, one atmospherere of carbon dioxide was introduced. After 48 hours, the solution and precipitate was transferred to a swivel frit assembly. Filtration affords a white product (408 g, 0.56 mmol) and washed with toluene and then petroleum ether. Yield = 47%. IR spectroscopy (KBr, cm^{-1}): 3292.2, 3057.8, 2913.7, 1699.2, 1654.5, 1603.5, 1570.9, 1500.3, 1490.0, 1438.7, 1326.1. Analysis : Calculated (Found) C: 51.46 (50.65); H: 4.46 (4.59); N: 5.81 (5.27).

$Cp^*Ta(=NPh)_2$ (37). A 50 mL round bottom flask was charged with 770 mg (1.30 mmol) $Cp^*Ta(=NPh)(NHPh)_2$. A swivel frit assembly was attached. Approximately 25 mL benzene was then condensed into the reaction vessel at -78°C followed by 1 equivalent of HCl from a lecture bottle using a gas bulb. The resulting solution was stirred for 3 days at room temperature. Then the volatiles were removed *in vacuo*, leaving a yellow solid. The product was

washed with petroleum ether and toluene to afford 150 mg (0.32 mmol) of **37**. Yield = 25%. IR spectroscopy (nujol mull, cm^{-1}): 1463.2, 1348.9, 1248.3. Analysis: Calculated (Found): C: 53.02 (48.01); H: 5.06 (4.65); N: 5.62 (4.90).

$Cp^*Ta(=NPh')_2$ (Ph' = 2,6-diisopropylphenyl) (38). A 100 mL round bottom flask was charged with 3.00 g (6.55 mmol) Cp^*TaCl_4 and 4.80 g (26.20 mmol) lithium 2,6-diisopropylanilide. A swivel frit assembly was attached. Approximately 50 mL THF was then condensed on the solids at -78°C at which the solution turned blue-green immediately. The resultant solution was then stirred at room temperature for 2 days. The volatiles were removed *in vacuo*. Petroleum ether was condensed onto the solids and the LiCl was filtered. Concentration and cooling the brown solution affords a yellow solid (714 mg, 1.07 mmol). Yield = 16%. IR spectroscopy (KBr, cm^{-1}): 2952.9, 2920.6, 1460.7, 1434.0, 1380.2, 1359.9, 1339.11, 1289.2, 1260.9, 1245.6, 1191.5, 933.4, 857.8, 799.0, 755.4. Analysis : Calculated (Found) C: 61.25 (61.14); H: 7.41 (7.70); N: 4.20 (3.81).

X-Ray Crystal Structure Determination of $Cp^*Ta(=NPh)(NHPh)_2$.
The ORTEP drawing of $Cp^*Ta(=NPh)(NHPh)_2$ is shown in figure 2 with important bond angles and distances in Table III. To obtain the structure, a yellow crystal was mounted in a greased capillary. The crystal was then centered on a CAD-4 diffractometer. Unit cell parameters and an orientation matrix were obtained by a least squares calculation from the setting angles of 25 reflections with $15^o < \theta < 17^o$. The data were corrected for absorption. Coordinates of the tantalum atom were obtained from a Patterson map; locations of the other non-hydrogen atoms were determined from successive structure factor-Fourier calculations. Calculations were done with programs of the CRYM Crystallographic Computing System and ORTEP with scattering factors and corrections for anamalous scattering taken from a standard reference.[41]

X-Ray Crystal Structure Determination of Cp*Ta(OCONPh)(η^2-OCONHPh)$_2$. The ORTEP drawing of Cp*Ta(OCONPh)[OC(=O)NHPh]$_2$ is shown in figure 3. To obtain the structure, a colorless crystal, obtained from cooling a THF/pentane solution, was oil-mounted on a glass fiber and transferred to the Synthex $P2_1$ diffractometer. The intensity data was collected at 163 K and corrected for absorption. The structure was solved by direct methods (SHELXTL) and refined by full-matrix least square techniques.

Table IV. ^{1}H NMR Spectral Data for complexes **30 - 38**.

Compound	Assignment	δ (ppm)	J (Hz)
$Cp^*Ta(NH^tBu)Cl_3$ **(30)** in CD_2Cl_2	NH-C(CH_3)$_3$	1.51 (s)	
	$C_5(CH_3)_5$	2.59 (s)	
	N-*H*	4.40 (s, br)	
$Cp^*Ta(NHPh)Cl_3$ **(31)** in C_6D_6	$C_5(CH_3)_5$	2.26 (s)	
	N-*H*	6.17 (s, br)	
	para-C_6H_5	6.82 (t)	7.20
	meta-C_6H_5	6.98 (t)	8.10
	ortho-C_6H_5	7.23 (d)	7.80
$Cp^*Ta(=NPh)(NHPh)_2$ **(32)** in C_6D_6	$C_5(CH_3)_5$	1.72 (s)	
	N-*H*	5.90 (s)	
	aromatic	6.8-7.5	
$Cp^*Ta(OCMe_2CMe_2O)_2$ **(33)** in C_6D_6	O-C-CH_3	1.27 (s)	
	O-C-CH_3	1.48 (s)	
	$C_5(CH_3)_5$	2.06 (s)	
$Cp^*Ta(NPhOCO)_2$ $(OCONHPh)_2$ **(36)** in THF-d_8	$C_5(CH_3)_5$	2.16 (s)	
	N(imido)-p-C_6H_5	6.51 (m, br)	
	N(imido)-m-C_6H_5	6.81 (t, br)	
	N(amido)-p-C_6H_5	6.99 (t)	7.50
	N(amido)-m-C_6H_5	7.23 (t)	8.40
	N(amido)-o-C_6H_5	7.33 (d)	7.50
	N(imido)-o-C_6H_5	7.52 (d)	9.60
	N-*H*	9.41 (s)	
$Cp^*Ta(=NPh)_2$ **(37)** in C_6D_6	$C_5(CH_3)_5$	1.79 (s)	
	aromatic	6.74-7.26	
$Cp^*Ta(=NPh')_2$ **(38)** in C_6D_6	N-CH-(CH_3)$_2$	1.21 (d)	6.90
	N-CH-(CH_3)$_2$	1.28 (d)	6.90
	N-CH-(CH_3)$_2$	1.34 (d)	6.60
	N-CH-(CH_3)$_2$	1.40 (d)	6.60
	$C_5(CH_3)_5$	1.91 (s)	
	N-C*H*-(CH_3)$_2$	3.56 (br)	
	N-C*H*-(CH_3)$_2$	4.01 (br)	
	aromatic	6.8-7.2	

Table V. ^{13}C NMR Spectral Data for complexes **30 - 38.**

Compound	Assignment	δ (ppm)
$Cp^*Ta(NH^tBu)Cl_3$ **(30)** in CD_2Cl_2	$C_5(CH_3)_5$	13.54
	$NH\text{-}C(CH_3)_3$	30.71
	$NH\text{-}C(CH_3)_3$	56.91
	$C_5(CH_3)_5$	133.76
$Cp^*Ta(NHPh)Cl_3$ **(31)** in CD_2Cl_2	$C_5(CH_3)_5$	13.56
	aromatic	122.72
	aromatic	125.82
	aromatic	128.55
	$C_5(CH_3)_5$	133.53
	aromatic	141.74
$Cp^*Ta(=NPh)(NHPh)_2$ **(32)** in C_6D_6	$C_5(CH_3)_5$	10.52
	aromatic	116.26
	aromatic	119.42
	aromatic	119.79
	aromatic	122.75
	aromatic	126.52
	aromatic	127.85
	aromatic	128.45
	aromatic	129.20
	aromatic	153.23
$Cp^*Ta(OCMe_2CMe_2O)_2$ **(33)** in C_6D_6	$C_5(CH_3)_5$	11.91
	$O\text{-}C\text{-}CH_3$	27.11
	$O\text{-}C\text{-}CH_3$	29.17
	$O\text{-}C\text{-}CH_3$	95.44
	$C_5(CH_3)_5$	121.28
$Cp^*Ta(NPhOCO)_2(OCONHPh)_2$ **(36)** in THF-d_8	$C_5(CH_3)_5$	10.06
	aromatic	119.94
	aromatic	120.32
	aromatic	121.69
	aromatic	124.31
	aromatic	124.94
	aromatic	127.96
	aromatic	129.67

Table V (Continued) ^{13}C NMR spectra

	aromatic	138.00
	aromatic	153.20
	aromatic	160.59
	aromatic	161.48
	aromatic	162.96
	aromatic	165.70
$Cp^*Ta(=NPh)_2$ **(37)** in C_6D_6	$C_5(CH_3)_5$	10.79
	aromatic	118.08
	$C_5(CH_3)_5$	120.52
	aromatic	122.20
	aromatic	123.33
	aromatic	126.28
	aromatic	129.02
	aromatic	152.06
$Cp^*Ta(=NPh')_2$ **(38)** in C_6D_6	$C_5(CH_3)_5$	10.92
	N-CH-$(CH_3)_2$	22.55
	N-CH-$(CH_3)_2$	23,73
	N-CH-$(CH_3)_2$	24.42
	N-CH-$(CH_3)_2$	25.56
	N-CH-$(CH_3)_2$	27.51
	N-CH-$(CH_3)_2$	28.33
	$C_5(CH_3)_5$	118.19
	aromatic	122.33
	aromatic	123.56
	aromatic	123.89
	aromatic	125.03
	aromatic	142.03
	aromatic	145.01

References

1. Clifford, A. F.; Kobayashi, C. S. Abstracts of the 130th National Meeting of the American Chemical Society, Atlantic City, New Jersey, September, 1956, p. 50R.

2. (a) Nugent, W. A.; Haymore, B. L. *Coord. Chem. Rev.* **1980**, *31*, 123. (b) Nugent, W. A.; Mayer, J. M. *Metal-Ligand Multiple Bonds*, John Wiley and Sons, New York, 1988.

3. See chapter 1.

4. The lone exception is $Mo(NPh)_2(S_2CNEt_2)_2$ from Haymore, B. L.; Maata, E. A.; Wentworth, R. A. D. *J. Am. Chem. Soc.* **1979**, *101*, 2063.

5. (a) Schrock, R. R.; DePue, R. T.; Feldman, J.; Yap, K. B.; Yang, D. C.; Davis, W. M.; Park, L.; Dimare, M.; Schofield, M.; Anhaus, J.; Walborsky, E.; Evitt, E.; Krüger, C.; Betz, P. *Organometallics*, **1990**, *9*, 2262. (b) Schaverien, C. J.; Dewan, J. C.; Schrock, R. R. *J. Am. Chem. Soc.* **1986**, *108*, 2771.

6. Cummins, C. C.; Baxter, S. M.; Wolczanski, P. T. *J. Am. Chem. Soc.* **1988**, *110*, 8731.

7. For other imido complexes, see:
(a) Hill, J. E.; Profilet, R. D.; Fanwick, P. E.; Rothwell, I. P. *Angew. Chem.* **1990**, *102*, 713. (b) Roesky, H. W.; Voelker, H.; Witt, M.; Noltemeyer, M. *Angew. Chem.* **1990**, *102*, 712.

8. For a theoretical treatment of C-H activation of group IV imido complexes, see: Cundari, T. R.; *J. Am. Chem. Soc.* **1992**, *114*, 10557.

9. Cummins, C. C.; Schaller, C. P.; Van Duyne, G. D.; Wolczanski, P. T.; Chan, A. W. E.; Hoffmann, R. *J. Am. Chem. Soc.* **1991**, *113*, 2985.

10. Hill, J. E.; Profilet, R. D.; Fanwick, P. E.; Rothwell, I. P. *Angew. Chem. Ent. Ed. Engl.* **1990**, *29*, 664.

11. (a) Walsh, P. J.; Hollander, P. J.; Bergman, R. G. *J. Am. Chem. Soc.* **1988**, *110*, 8729. (b) Walsh, P. J.; Baranger, A. M.; Bergman, R. G. *J. Am. Chem. Soc.* **1992**, *14*, 1708.

12. (a) Parkin, G.; van Asselt, A.; Leahy, D. J.; Whinnery, L.; Hua, N. G.; Quan, R. W.; Henling, L. M.; Bercaw, J. E. *Inorg. Chem.* **1992**, *31*, 82. (b) Jorgensen, K. A. *Inorg. Chem.* **1993**, *32*, 1521. (c) Osborne, J. H.; Rheingold, A. L.; Trogler, W. C. *J. Am. Chem. Soc.* **1985**, *107*, 7945.

13. Mayer, J. M. *Comments Inorg. Chem.* **1988**, *8*, 125.

14. (a) Glueck, D. S.; Wu, J.; Hollander, F. J.; Bergman, R. G. *J. Am. Chem. Soc.* **1991**, *113*, 2041. (b) Glueck, D. S.; Hollander, F. J.; Bergman, R. G. *J. Am. Chem. Soc.* **1989**, *111*, 2719.

15. de With, J.; Horton, A. D. *Angew. Chem. Int. Ed. Engl.* **1993**, *6*, 32,

16. Thompson, M. E.; Baxter, S. M.; Bulls, A. R.; Burger, B. J.; Nolan, M. C.; Santarsiero, B. D.; Schaefer, W. P.; Bercaw, J. E. *J. Am. Chem. Soc.* **1987**, *109*, 203.

17. Huber, S. R.; Baldwin, T. C.; Wigley, D. E. *Organometallics* **1993**, *12*, 91.

18. (a) Parkin, G.; Marsh, R. E.; Schaefer, W. P.; Bercaw, J. E. *Inorg. Chem.* **1988**, *27*, 3262. (b) Parkin, G.; Bercaw, J. E. *Polyhedron* **1988**, *7*, 2053.

19. (a) Williams, D. S.; Schrock, R. R. *Organometallics* **1993**, *12*, 1148. (b) Williams, D. S.; Anhaus, J. T.; Schofield, M. H.; Schrock, R. R.; Davis, W. M. *J. Am. Chem. Soc.* **1991**, *113*, 5480. (c) Williams, D. S.; Schofield, M. H.; Anhaus, J. T.; Schrock, R. R. *J. Am. Chem. Soc.* **1990**, *112*, 6728.

20. Other replacements for the cyclopentadienyl unit include the Kläui, tris-pyrazolylborate, and carborane ligands: (a) Kelson, E. P.; Henling, L. M.; Schaefer, W. P.; Labinger, J. A.; Bercaw, J. E. *Inorg. Chem.* **1993**, *32*, 2863. (b) Power, J. P.; Evertz, K.; Henling, L. M.; Marsh, R.; Schaefer, W. P.; Labinger, J. A.; Bercaw, J. E. *Inorg. Chem.* **1990**, *29*, 5058. (c) Kläui, W. *Angew. Chem. Int. Ed. Engl.* **1990**, *29*, 627. (d) Feng, X.; Bott, S. G.; Lippard, S. L. J. *Am. Chem. Soc.* **1989**, *111*, 8046. (e) Kläui, W.; Müller, A.; Eberspach, W.; Boese, R.; Goldberg, I. *J. Am. Chem. Soc.* **1987**, *109*, 164. (f) Grimes, R. M. *Chem. Rev.* **1992**, *92*, 251. (g) Trofimenko, S. *Chem. Rev.* **1993**, *93*, 943. (h) Calabrese, J. C.; Trofimenko, S.; Thompson, J. S. *J. Chem. Soc., Chem. Commun.* **1986**, 1122. (i) For recent work on tridentate ligands: Abstracts 289-297. 206th ACS National Meeting, Chicago, Illinois, 1993.

21. Williams, D. N.; Mitchell, J. P.; Poole, A. D.; Siemeling, U.; Clegg, W.; Hockless, D. C. R.; O'Neil, P. A. O.; Gibson, V. C. *J. Chem. Soc. Dalton. Trans.* **1992**, 739.

22. Lauher, J. W.; Hoffmann, R. *J. Am. Chem. Soc.* **1976**, *98*, 1729.

23. Schaller, C. P.; Bennett, J. L.; Wolczanski, P. T. Abstract 453. 204th ACS National Meeting, Washington, D. C., 1992.

24. (a) Gibson, V. C.; Bercaw, J. E.; Bruton, W. J., Jr.; Sanner, R. D. *Organometallics* **1986**, *5*, 976. (b) Sanner, R. D.; Bruton, W. J., Jr. *J. Organomet. Chem.* **1982**, *240*, 157.

25. Williams, D. N.; Mitchell, J. P.; Poole, A. D.; Siemeling, U.; Clegg, W.; Hockless, D. C. R.; O'Neil, P. A.; Gibson, V. C. *J. Chem. Soc., Dalton Trans.* **1992**, 739.

26. Bryson, N.; Youinou, M.-T.; Osborn, J. A. *Organometallics* **1991**, *10*, 3389.

27. Nugent, W. A.; Harlow, R. L. *J. Chem. Soc., Chem. Commun.* **1978**, 579.

28. Churchill, M. R.; Wasserman, H. J. *Inorg. Chem.* **1982**, *21*, 223.

29. Gibson, V. C.; Kee, T. P.; Clegg, W. *J. Chem. Soc. Chem. Commun.* **1990**, 29.

30. Michelman, R. I.; Andersen, R. A.; Bergman, R. G. *J. Am. Chem. Soc.* **1991**, *113*, 5100.

31 de With, J.; Horton, A. D. *Organometallics* **1990**, *9*, 2207.

32. Chan, D. M. -T.; Fultz, W. C.; Nugent, W. A.; Roe, D. C.; Tulip, T. H. *J. Am. Chem. Soc.* **1985**, *107*, 251.

33. (a) Simpson, R. D.; Bergman, R. G. *Organometallics* **1992**, *11*, 4306. (b) Hartwig, J. F.; Bergman, R. G.; Andersen, R. A. *J. Am. Chem. Soc.* **1991**, *113*, 6499. (c) Buhro, W. E.; Chisholm, M. H.; Martin, J. D.; Huffman, J. C.; Folting, K.; Streib, W. E. *J. Am. Chem. Soc.* **1989**, *111*, 8149. (d) Chisholm, M. H.; Extine, M.; Cotton, F. A.; Stults, B. R. *J. Am. Chem. Soc.* **1976**, *98*, 4683. (e) Chisholm, M. H.; Extine, M. W. *J. Am. Chem. Soc.* **1977**, *99*, 782. (f) Chisholm, M. H.; Extine, M. W. *J. Am. Chem. Soc.* **1977**, *99*, 792.

34. (a) Pilato, R. S.; Housmekerides, C. E.; Jernakoff, P.; Rubin, D.; Geoffroy, G. L.; Rheingold, A. L. *Organometallics* **1990**, *9*, 2333. (b) Jernakoff, P.; Geoffroy, G. L.; Rheingold, A. L.; Geib, S. J. *J. Chem. Soc., Chem. Commun.* **1987**, 1610. (c) reference 14.

35. (a) Chisholm, M. H.; Extine, M. W. *J. Am. Chem. Soc.* **1977**, *99*, 782. (b) Chisholm, M. H.; Extine, M. W. *J. Am. Chem. Soc.* **1977**, *99*, 792.

36. Cyclometallacarbamates are proposed as intermediates in the

preparation of imido complexes from metal oxo complexes and an isocyanate. See reference 2a for a review.

37. Danopoulos, A. A.; Wilkinson, G.; Hussainbates, B.; Hursthouse, M. B. *J. Chem. Soc., Dalton Trans.* **1991**, 269. (b) Green, M. L. H.; Hogarth, G.; Konidaris, P. C.; Mountford, P. *J. Chem. Soc., Dalton Trans.* **1990**, 3781.

38. Baldwin, T. C.; Huber, S. R.; Bruck, M. A.; Wigley, D. E. Manuscript submitted to *Inorg. Chem.* Recently, prepared [Li(THF)][Cp*Ta(=NPh')$_2$Cl] where Ph' = 2,6-diisopropylphenyl from Cp*TaCl$_4$ and lithium 2,6-diisopropylanilide in THF. Furthermore, the complex has been found to be rather unreactive.

39. Burger, B.J.; Bercaw, J. E. In *Experimental Organometallic Chemistry;* Wayda, A. L., Darensbourg, M. Y. Eds.; ACS Symposium Series 357; American Chemical Society, Washington, D. C. 1987.

40. Marvich, R. H.; Brintzinger, H. H. *J. Am. Chem. Soc.* **1971**, *93*, 2046.

41. International Tables for X-ray Crystallography, Volume IV, p. 71, p. 147; Birmingham, Kynoch Press, 1974.

Appendix 2. X-ray crystal structure data for $Cp^*Ta(=NPh)(NHPh)_2$ (**32**) and $Cp^*Ta(NPhOC)(OCONHPh)_2$ (**36**).

Table VI. Crystal and Intensity Collection Data for $Cp^*Ta(=NPh)(NHPh)_2$ (**32**).

chemical formula	$C_{28}H_{32}N_3Ta$
crystal dimensions, mm	0.53 X 1.05 X 1.35
crystal system	monoclinic
space group	$P2_1/c$
a,Å	12.343 (4)
b,Å	14.584 (6)
c, Å	15.104 (5)
β, deg	109.35 (2)
V, $Å^3$	2565.3 (16)
ρ_{calc}, g cm^{-3}	1.532
Z	4
λ,Å	0.711
μ, cm^{-1}	42.52
temp, °C	23
2θ rang, deg	2-48
no. of reflections measured, total	8700
no. of reflections measured, unique	4018
R	0.023
GOF	1.52

Table VII. Final Heavy Atom Parameters for Cp*Ta(=NPh)(NHPh)$_2$ (32).

x, y, z and U_{eq}[a] $\times 10^4$

Atom	x	y	z	U_{eq}
Ta	2537(.1)	668(.1)	4125(.1)	506
N1	1874(3)	1671(2)	4385(2)	551(9)
N2	4157(3)	1105(3)	4366(3)	701(11)
N3	2610(3)	−202(2)	5192(2)	633(10)
C1	1148(4)	2387(3)	4409(3)	515(11)
C2	1366(4)	3271(3)	4190(3)	728(14)
C3	621(6)	3974(4)	4200(4)	958(19)
C4	−347(6)	3813(5)	4414(4)	1004(20)
C5	−571(4)	2941(5)	4640(4)	981(18)
C6	171(4)	2233(3)	4641(3)	760(14)
C11	4694(4)	1959(3)	4534(3)	617(12)
C12	5524(4)	2182(4)	4123(3)	737(14)
C13	6073(4)	3012(4)	4276(4)	837(16)
C14	5809(5)	3646(4)	4835(4)	904(18)
C15	4988(5)	3451(4)	5244(4)	837(16)
C16	4439(4)	2615(3)	5106(3)	707(13)
C21	2752(3)	−63(3)	6138(3)	531(11)
C22	3031(4)	797(3)	6555(3)	621(12)
C23	3236(4)	908(3)	7501(3)	677(13)
C24	3156(4)	188(4)	8059(3)	706(13)

Table VII. (Continued)

Atom	x	y	z	U_{eq}
C25	2861(4)	−666(3)	7653(3)	707(13)
C26	2651(4)	−788(3)	6708(3)	601(12)
C31	2057(4)	−737(3)	3133(3)	699(14)
C32	2757(4)	−202(5)	2781(4)	822(16)
C33	2183(5)	629(4)	2464(3)	757(14)
C34	1106(4)	586(3)	2602(3)	643(12)
C35	1048(4)	−251(3)	3037(3)	594(12)
C36	2277(5)	−1709(4)	3475(4)	1187(22)
C37	3938(6)	−492(6)	2748(6)	1627(29)
C38	2576(6)	1400(5)	1961(4)	1448(25)
C39	174(5)	1295(4)	2279(4)	982(18)
C40	48(5)	−592(4)	3300(4)	960(17)

[a] $U_{eq} = \frac{1}{3} \sum_i \sum_j [U_{ij}(a_i^* a_j^*)(\vec{a}_i \cdot \vec{a}_j)]$

Table VIII. Anisotropic Displacement Parameters for Cp*Ta(=NPh)(NHPh)$_2$ (32).

Atom	U_{11}	U_{22}	U_{33}	U_{12}	U_{13}	U_{23}
Ta	526(1)	462(1)	479(1)	43(1)	96(1)	−81(1)
N1	579(22)	543(22)	494(19)	4(17)	128(17)	−25(16)
N2	592(24)	563(23)	890(28)	45(19)	166(21)	−173(20)
N3	823(27)	419(20)	611(23)	94(19)	177(20)	−73(17)
C1	614(28)	465(26)	429(22)	84(21)	122(20)	−40(18)
C2	958(37)	510(30)	763(31)	97(26)	349(28)	75(24)
C3	1429(59)	539(32)	827(38)	195(36)	266(40)	86(27)
C4	1116(52)	855(45)	878(41)	501(40)	111(37)	−110(34)
C5	730(36)	1103(49)	1141(46)	188(36)	353(33)	−210(40)
C6	837(36)	633(33)	854(35)	50(27)	341(30)	−23(25)
C11	508(27)	629(30)	616(27)	59(23)	56(22)	−15(23)
C12	623(31)	803(37)	702(31)	115(28)	107(25)	14(26)
C13	688(34)	923(42)	824(36)	−11(32)	150(28)	133(32)
C14	839(41)	709(38)	928(41)	−156(31)	−24(33)	88(32)
C15	826(38)	748(36)	821(35)	−39(30)	116(31)	−211(29)
C16	631(30)	769(34)	686(30)	−109(26)	171(25)	−248(26)
C21	474(26)	543(27)	515(26)	84(19)	81(20)	−47(20)
C22	715(30)	513(29)	595(27)	7(22)	164(23)	−22(21)
C23	741(33)	536(30)	674(30)	31(22)	125(25)	−106(22)
C24	735(33)	758(34)	556(28)	129(27)	120(25)	38(26)
C25	728(32)	670(31)	721(31)	56(27)	239(26)	120(27)
C26	597(27)	511(28)	654(28)	16(22)	154(22)	−22(22)
C31	785(34)	484(27)	623(27)	100(26)	−44(25)	−145(23)
C32	631(34)	1058(44)	726(34)	−38(32)	156(29)	−461(32)
C33	993(41)	749(34)	488(25)	−285(34)	191(26)	−151(26)
C34	693(30)	608(30)	510(24)	29(25)	41(22)	−77(23)
C35	544(28)	585(27)	531(25)	−65(23)	16(22)	−44(21)
C36	1445(56)	663(37)	981(42)	222(35)	−234(37)	−204(32)
C37	908(47)	2335(88)	1713(68)	−92(50)	533(48)	−1281(64)
C38	1856(72)	1654(67)	852(42)	−1023(57)	471(46)	−174(42)
C39	1117(46)	777(38)	748(34)	194(33)	−100(31)	25(28)
C40	771(36)	1125(46)	826(36)	−192(33)	51(29)	100(32)

$U_{i,j}$ values have been multiplied by 10^4

The form of the displacement factor is:

$$\exp -2\pi^2(U_{11}h^2a^{*2} + U_{22}k^2b^{*2} + U_{33}\ell^2c^{*2} + 2U_{12}hka^*b^* + 2U_{13}h\ell a^*c^* + 2U_{23}k\ell b^*c^*)$$

Table IX. Complete Distances and Angles for Cp*Ta(=NPh)(NHPh)$_2$ (32).

	Distance(Å)		Distance(Å)
Ta –Cp*	2.126(3)	N2 –HN2	0.974
Ta –N1	1.784(5)	N3 –HN3	0.972
Ta –N2	2.013(5)	C2 –H2	0.950
Ta –N3	2.029(5)	C3 –H3	0.947
Ta –C31	2.491(7)	C4 –H4	0.950
Ta –C32	2.484(6)	C5 –H5	0.952
Ta –C33	2.401(6)	C6 –H6	0.951
Ta –C34	2.395(5)	C12 –H12	0.949
Ta –C35	2.423(7)	C13 –H13	0.947
N1 –C1	1.383(6)	C14 –H14	0.947
N2 –C11	1.395(6)	C15 –H15	0.956
N3 –C21	1.395(6)	C16 –H16	0.951
C1 –C2	1.379(8)	C22 –H22	0.951
C1 –C6	1.382(7)	C23 –H23	0.951
C2 –C3	1.381(9)	C24 –H24	0.950
C3 –C4	1.357(9)	C25 –H25	0.952
C4 –C5	1.368(8)	C26 –H26	0.952
C5 –C6	1.381(7)	C36 –H36A	0.948
C11 –C12	1.401(8)	C36 –H36B	0.948
C11 –C16	1.392(6)	C36 –H36C	0.950
C12 –C13	1.370(8)	C37 –H37A	0.946
C13 –C14	1.362(8)	C37 –H37B	0.957
C14 –C15	1.380(7)	C37 –H37C	0.934
C15 –C16	1.376(6)	C38 –H38A	0.947
C21 –C22	1.395(6)	C38 –H38B	0.938
C21 –C26	1.395(7)	C38 –H38C	0.952
C22 –C23	1.377(7)	C39 –H39A	0.943
C23 –C24	1.369(7)	C39 –H39B	0.948
C24 –C25	1.383(6)	C39 –H39C	0.954
C25 –C26	1.374(6)	C40 –H40A	0.950
C31 –C32	1.393(8)	C40 –H40B	0.947
C31 –C35	1.399(8)	C40 –H40C	0.947
C31 –C36	1.503(10)		
C32 –C33	1.406(7)		
C32 –C37	1.534(9)		
C33 –C34	1.413(6)		
C33 –C38	1.523(7)		
C34 –C35	1.399(7)		
C34 –C39	1.503(7)		
C35 –C40	1.501(6)		

Table IX. (Continued)

	Angle(°)		Angle(°)
N1 -Ta -N2	101.6(2)	C38 -C33 -C32	126.8(4)
N1 -Ta -N3	103.9(2)	C38 -C33 -C34	125.2(4)
N1 -Ta -Cp*	120.2(2)	C35 -C34 -C33	107.8(4)
N2 -Ta -N3	106.0(2)	C39 -C34 -C33	125.3(4)
N2 -Ta -Cp*	112.7(2)	C39 -C34 -C35	126.8(4)
N3 -Ta -Cp*	111.1(2)	C34 -C35 -C31	107.9(5)
Ta -N1 -C1	166.7(4)	C40 -C35 -C31	125.9(5)
Ta -N2 -C11	134.4(3)	C40 -C35 -C34	126.1(5)
Ta -N3 -C21	132.9(3)	HN2 -N2 -C11	112.7
C2 -C1 -N1	121.3(5)	HN3 -N3 -C21	113.3
C6 -C1 -N1	120.7(4)	H2 -C2 -C1	119.3
C6 -C1 -C2	117.9(5)	H2 -C2 -C3	120.1
C3 -C2 -C1	120.6(6)	H3 -C3 -C2	119.1
C4 -C3 -C2	121.1(6)	H3 -C3 -C4	119.9
C5 -C4 -C3	119.1(6)	H4 -C4 -C3	120.3
C6 -C5 -C4	120.4(5)	H4 -C4 -C5	120.5
C5 -C6 -C1	120.8(4)	H5 -C5 -C4	119.8
C12 -C11 -N2	119.9(4)	H5 -C5 -C6	119.7
C16 -C11 -N2	122.4(4)	H6 -C6 -C1	119.4
C16 -C11 -C12	117.7(5)	H6 -C6 -C5	119.7
C13 -C12 -C11	121.6(5)	H12 -C12 -C11	119.3
C14 -C13 -C12	119.8(5)	H12 -C12 -C13	119.1
C15 -C14 -C13	120.0(5)	H13 -C13 -C12	120.3
C16 -C15 -C14	120.8(4)	H13 -C13 -C14	119.9
C15 -C16 -C11	120.1(4)	H14 -C14 -C13	120.1
C22 -C21 -N3	121.4(4)	H14 -C14 -C15	119.9
C26 -C21 -N3	121.0(4)	H15 -C15 -C14	119.7
C26 -C21 -C22	117.6(4)	H15 -C15 -C16	119.5
C23 -C22 -C21	120.5(4)	H16 -C16 -C11	120.2
C24 -C23 -C22	121.5(5)	H16 -C16 -C15	119.7
C25 -C24 -C23	118.7(4)	H22 -C22 -C21	120.1
C26 -C25 -C24	120.6(4)	H22 -C22 -C23	119.5
C25 -C26 -C21	121.2(4)	H23 -C23 -C22	119.1
C35 -C31 -C32	108.7(5)	H23 -C23 -C24	119.4
C36 -C31 -C32	126.5(5)	H24 -C24 -C23	120.4
C36 -C31 -C35	124.5(6)	H24 -C24 -C25	120.9
C33 -C32 -C31	107.8(5)	H25 -C25 -C24	119.0
C37 -C32 -C31	125.1(5)	H25 -C25 -C26	120.4
C37 -C32 -C33	127.1(5)	H26 -C26 -C21	119.7
C34 -C33 -C32	107.7(4)	H26 -C26 -C25	119.2

Table IX. (Continued)

	Angle(°)
H36A –C36 –C31	108.5
H36B –C36 –C31	108.5
H36C –C36 –C31	108.4
H36B –C36 –H36A	110.6
H36C –C36 –H36A	110.4
H36C –C36 –H36B	110.4
H37A –C37 –C32	108.3
H37B –C37 –C32	107.0
H37C –C37 –C32	108.1
H37B –C37 –H37A	110.1
H37C –C37 –H37A	112.0
H37C –C37 –H37B	111.1
H38A –C38 –C33	107.8
H38B –C38 –C33	108.0
H38C –C38 –C33	107.5
H38B –C38 –H38A	111.7
H38C –C38 –H38A	110.5
H38C –C38 –H38B	111.2
H39A –C39 –C34	108.7
H39B –C39 –C34	108.5
H39C –C39 –C34	108.1
H39B –C39 –H39A	111.0
H39C –C39 –H39A	110.4
H39C –C39 –H39B	110.0
H40A –C40 –C35	108.2
H40B –C40 –C35	108.3
H40C –C40 –C35	108.4
H40B –C40 –H40A	110.6
H40C –C40 –H40A	110.5
H40C –C40 –H40B	110.7

Table X. Assigned Hydrogen Atom Parameters for $Cp^*Ta(=NPh)(NHPh)_2$ (32).

x, y and $z \times 10^4$

Atom	x	y	z	B
HN2	4685	609	4366	6.0
HN3	2525	−844	5010	5.4
H2	2039	3394	4037	6.3
H3	790	4576	4051	8.4
H4	−860	4300	4408	8.6
H5	−1243	2822	4798	8.5
H6	9	1630	4804	6.6
H12	5716	1745	3733	6.4
H13	6630	3150	3989	7.2
H14	6191	4219	4946	7.8
H15	4796	3901	5627	7.2
H16	3886	2488	5402	6.1
H22	3090	1312	6186	5.3
H23	3440	1498	7774	5.9
H24	3304	277	8711	6.1
H25	2806	−1169	8037	6.1
H26	2438	−1380	6441	5.3
H36A	3075	−1781	3794	10.3
H36B	2028	−2106	2950	10.3
H36C	1856	−1823	3889	10.3
H37A	4275	19	2554	14.1
H37B	3811	−975	2297	14.1
H37C	4378	−696	3345	14.1
H38A	2274	1956	2104	12.6
H38B	2301	1275	1316	12.6
H38C	3393	1411	2194	12.6
H39A	−289	1262	2665	8.4
H39B	−262	1174	1644	8.4
H39C	529	1883	2332	8.4
H40A	325	−778	3939	8.4
H40B	−284	−1094	2907	8.4
H40C	−489	−108	3215	8.4

Table XI. Crystal and Intensity Collection Data for $Cp^*Ta(OCONPh)(\eta^2\text{-}OCONHPh)_2$ (**36**).

chemical formula	$C_{31}H_{36}N_3O_6Ta \cdot 2(C_4H_8O)$
crystal dimensions, mm	0.36 X 0.42 X 0.47
crystal system	monoclinic
space group	$P2_1/n$
a,Å	12.2094 (12)
b,Å	15.8783 (13)
c, Å	19.7276 (12)
β, deg	102.329 (6)
V, Å^3	3736.3 (5)
ρ_{calc}, g cm^{-3}	1.543
Z	4
λ,Å	0.711
μ, mm^{-1}	2.960
temp, K	163
2θ rang, deg	4-55
no. of reflections measured, total	11,846
R	0.047
GOF	1.49

Table XII. Final Heavy Atom Parameters for
$Cp^*Ta(OCONPh)(\eta^2\text{-}OCONHPh)_2$ (**36**).
Atomic Coordinates (X 10^5)
Equivalent isotropic displacement coefficients ($Å^2$ X 10^4)

	x	y	z	U(eq)
Ta(1)	9718(2)	18548(1)	11502(1)	270(1)
O(1)	6933(30)	19515(20)	1084(17)	294(11)
O(2)	-9673(34)	16902(22)	-6205(17)	345(13)
O(3)	8942(32)	5265(22)	8363(17)	322(12)
O(4)	5170(31)	9179(21)	18184(16)	295(11)
O(5)	3092(34)	25231(22)	19156(17)	341(13)
O(6)	4473(33)	31913(21)	9806(17)	307(11)
N(1)	-7224(36)	17233(25)	5971(21)	276(13)
N(2)	2033(37)	-4654(26)	14557(20)	306(14)
N(3)	-3527(42)	38624(27)	17966(22)	364(16)
C(1)	27295(47)	25059(36)	10385(31)	391(19)
C(2)	28561(46)	16270(37)	9855(30)	367(18)
C(3)	28401(49)	12748(36)	16424(31)	401(19)
C(4)	26762(53)	19313(37)	20859(32)	442(20)
C(5)	26136(49)	26941(35)	17129(30)	392(19)
C(6)	27884(60)	31351(39)	4810(37)	536(24)
C(7)	30132(56)	11601(46)	3555(35)	560(26)
C(8)	30673(59)	3707(39)	18542(40)	577(26)
C(9)	26310(65)	18265(44)	28357(33)	583(26)
C(10)	25560(61)	35759(40)	19987(37)	585(26)
C(11)	-4110(46)	17798(29)	-269(26)	288(16)
C(12)	-17534(44)	14577(31)	7061(26)	299(16)
C(13)	-26136(50)	11211(36)	1816(30)	407(20)
C(14)	-36043(58)	8663(45)	3359(35)	539(24)
C(15)	-37881(50)	9197(44)	10011(36)	511(24)
C(16)	-29645(54)	12475(40)	15092(33)	471(22)
C(17)	-19618(51)	15238(37)	13705(29)	385(19)

Table XII. (Continued)

C(18)	5334(45)	3184(31)	13757(25)	294(16)
C(19)	-1675(45)	-8236(32)	20315(26)	309(16)
C(20)	-1738(50)	-17008(34)	20528(30)	382(19)
C(21)	-4383(57)	-21048(40)	26244(32)	466(22)
C(22)	-7083(61)	-16305(42)	31519(33)	519(24)
C(23)	-7205(59)	-7650(41)	31182(31)	490(23)
C(24)	-4474(49)	-3487(36)	25589(27)	385(19)
C(25)	1266(49)	32029(32)	15454(26)	336(17)
C(26)	-5271(48)	46808(32)	15136(26)	343(17)
C(27)	-12157(64)	51979(40)	17962(32)	518(24)
C(28)	-13809(70)	60196(43)	15672(35)	627(29)
C(29)	-8878(61)	63339(37)	10645(30)	500(23)
C(30)	-2119(53)	58127(37)	7753(31)	444(21)
C(31)	-258(51)	49751(36)	9981(29)	402(20)
O(7)	55337(46)	87802(36)	18136(24)	649(20)
C(32)	65750(78)	87093(57)	16367(48)	792(37)
C(33)	66838(94)	78084(72)	15143(65)	1119(56)
C(34A)	56545(242)	73795(155)	14133(124)	964(109)
C(34B)	55007(230)	76595(130)	10335(96)	864(93)
C(35)	48241(79)	81380(71)	14526(41)	913(46)
O(8)	59560(46)	39920(32)	1792(28)	722(22)
C(36)	63872(87)	46831(55)	-1299(58)	1041(49)
C(37)	71949(82)	44014(53)	-4950(50)	848(39)
C(38)	74885(77)	35143(50)	-2412(47)	769(36)
C(39)	68350(66)	33975(46)	3008(41)	604(28)

* Equivalent isotropic U defined as one third of the trace of the orthogonalized U_{ij} tensor

Table XIII. Complete Distances for $Cp^*Ta(OCONPh)(\eta^2\text{-}OCONHPh)_2$ (**36**).

Ta(1)-O(1)	2.016(3)	Ta(1)-O(3)	2.195(3)
Ta(1)-O(4)	2.138(3)	Ta(1)-O(5)	2.140(4)
Ta(1)-O(6)	2.221(3)	Ta(1)-N(1)	2.133(4)
Ta(1)-C(1)	2.434(6)	Ta(1)-C(2)	2.418(6)
Ta(1)-C(3)	2.459(6)	Ta(1)-C(4)	2.472(6)
Ta(1)-C(5)	2.465(6)	Ta(1)-C(11)	2.566(5)
Ta(1)-C(18)	2.557(5)	Ta(1)-C(25)	2.569(6)
Ta(1)-Cnt	2.137		

O(1)-C(11)	1.345(7)	O(2)-C(11)	1.230(6)
O(3)-C(18)	1.279(7)	O(4)-C(18)	1.295(6)
O(5)-C(25)	1.296(6)	O(6)-C(25)	1.258(7)
N(1)-C(11)	1.367(7)	N(1)-C(12)	1.387(7)
N(2)-C(18)	1.328(7)	N(2)-C(19)	1.428(7)
N(3)-C(25)	1.345(7)	N(3)-C(26)	1.412(7)
C(1)-C(2)	1.410(8)	C(1)-C(5)	1.400(9)
C(1)-C(6)	1.499(9)	C(2)-C(3)	1.415(9)
C(2)-C(7)	1.494(10)	C(3)-C(4)	1.403(9)
C(3)-C(8)	1.504(8)	C(4)-C(5)	1.411(8)
C(4)-C(9)	1.501(9)	C(5)-C(10)	1.517(9)
C(12)-C(13)	1.412(7)	C(12)-C(17)	1.392(8)
C(13)-C(14)	1.370(10)	C(14)-C(15)	1.381(10)
C(15)-C(16)	1.363(8)	C(16)-C(17)	1.382(9)
C(19)-C(20)	1.394(7)	C(19)-C(24)	1.386(8)
C(20)-C(21)	1.394(9)	C(21)-C(22)	1.380(10)
C(22)-C(23)	1.376(9)	C(23)-C(24)	1.387(9)
C(26)-C(27)	1.376(9)	C(26)-C(31)	1.376(9)
C(27)-C(28)	1.381(9)	C(28)-C(29)	1.360(11)
C(29)-C(30)	1.376(10)	C(30)-C(31)	1.404(8)

Table XIII. (Continued)

O(7)-C(32)	1.393(12)	O(7)-C(35)	1.426(11)
C(32)-C(33)	1.461(15)	C(33)-C(34A)	1.406(31)
C(33)-C(34B)	1.568(26)	C(34A)-C(35)	1.587(29)
C(34B)-C(35)	1.495(27)	O(8)-C(36)	1.411(12)
O(8)-C(39)	1.411(9)	C(36)-C(37)	1.412(16)
C(37)-C(38)	1.512(12)	C(38)-C(39)	1.476(13)

* Cnt is the centroid of the C(1)–C(5) ring.

Table XIV. Complete Angles for $Cp^*Ta(OCONPh)(\eta^2\text{-}OCONHPh)_2$ (36).

O(1)-Ta(1)-O(3)	78.3(1)	O(1)-Ta(1)-O(4)	132.2(1)
O(3)-Ta(1)-O(4)	60.3(1)	O(1)-Ta(1)-O(5)	132.4(1)
O(3)-Ta(1)-O(5)	132.5(1)	O(4)-Ta(1)-O(5)	73.9(1)
O(1)-Ta(1)-O(6)	78.1(1)	O(3)-Ta(1)-O(6)	151.9(1)
O(4)-Ta(1)-O(6)	130.8(1)	O(5)-Ta(1)-O(6)	59.5(1)
O(1)-Ta(1)-N(1)	63.4(2)	O(3)-Ta(1)-N(1)	77.5(1)
O(4)-Ta(1)-N(1)	84.0(1)	O(5)-Ta(1)-N(1)	86.4(2)
O(6)-Ta(1)-N(1)	78.4(1)	Cnt-Ta(1)-O(1)	104.7
Cnt-Ta(1)-O(3)	100.2	Cnt-Ta(1)-O(4)	105.2
Cnt-Ta(1)-O(5)	103.3	Cnt-Ta(1)-O(6)	100.3
Cnt-Ta(1)-N(1)	168.0		

Ta(1)-O(1)-C(11)	97.5(3)	Ta(1)-O(3)-C(18)	90.9(3)
Ta(1)-O(4)-C(18)	93.0(3)	Ta(1)-O(5)-C(25)	93.5(3)
Ta(1)-O(6)-C(25)	90.8(3)	Ta(1)-N(1)-C(11)	91.6(3)
Ta(1)-N(1)-C(12)	139.8(3)	C(11)-N(1)-C(12)	126.6(4)
C(18)-N(2)-C(19)	128.6(4)	C(25)-N(3)-C(26)	127.7(5)
C(2)-C(1)-C(5)	108.5(5)	C(2)-C(1)-C(6)	125.6(6)
C(5)-C(1)-C(6)	125.8(5)	C(1)-C(2)-C(3)	107.4(5)
C(1)-C(2)-C(7)	126.0(6)	C(3)-C(2)-C(7)	126.5(6)
C(2)-C(3)-C(4)	108.0(5)	C(2)-C(3)-C(8)	126.4(6)
C(4)-C(3)-C(8)	125.3(6)	C(3)-C(4)-C(5)	108.2(6)
C(3)-C(4)-C(9)	124.9(6)	C(5)-C(4)-C(9)	126.9(6)
C(1)-C(5)-C(4)	107.9(5)	C(1)-C(5)-C(10)	124.9(5)
C(4)-C(5)-C(10)	126.9(6)	O(1)-C(11)-O(2)	122.6(5)
O(1)-C(11)-N(1)	107.1(4)	O(2)-C(11)-N(1)	130.3(5)
N(1)-C(12)-C(13)	124.0(5)	N(1)-C(12)-C(17)	118.5(4)
C(13)-C(12)-C(17)	117.5(5)	C(12)-C(13)-C(14)	120.2(6)
C(13)-C(14)-C(15)	121.6(6)	C(14)-C(15)-C(16)	118.6(6)
C(15)-C(16)-C(17)	121.4(6)	C(12)-C(17)-C(16)	120.7(5)

Table XIV. (Continued)

O(3)-C(18)-O(4)	115.4(4)	O(3)-C(18)-N(2)	120.6(5)
O(4)-C(18)-N(2)	124.1(5)	N(2)-C(19)-C(20)	115.3(5)
N(2)-C(19)-C(24)	123.5(5)	C(20)-C(19)-C(24)	121.2(5)
C(19)-C(20)-C(21)	119.2(6)	C(20)-C(21)-C(22)	119.5(6)
C(21)-C(22)-C(23)	120.7(6)	C(22)-C(23)-C(24)	120.8(6)
C(19)-C(24)-C(23)	118.5(5)	O(5)-C(25)-O(6)	116.0(5)
O(5)-C(25)-N(3)	118.5(5)	O(6)-C(25)-N(3)	125.5(5)
N(3)-C(26)-C(27)	116.3(5)	N(3)-C(26)-C(31)	123.5(5)
C(27)-C(26)-C(31)	120.2(5)	C(26)-C(27)-C(28)	119.4(7)
C(27)-C(28)-C(29)	121.9(7)	C(28)-C(29)-C(30)	118.7(6)
C(29)-C(30)-C(31)	120.8(6)	C(26)-C(31)-C(30)	119.0(6)

C(32)-O(7)-C(35)	107.9(7)	O(7)-C(32)-C(33)	103.9(8)
C(32)-C(33)-C(34A)	112.8(14)	C(32)-C(33)-C(34B)	98.2(11)
C(33)-C(34A)-C(35)	100.8(16)	C(33)-C(34B)-C(35)	97.8(12)
O(7)-C(35)-C(34A)	103.9(11)	O(7)-C(35)-C(34B)	106.9(11)
C(36)-O(8)-C(39)	104.7(7)	O(8)-C(36)-C(37)	109.9(7)
C(36)-C(37)-C(38)	105.6(8)	C(37)-C(38)-C(39)	103.3(8)
O(8)-C(39)-C(38)	107.6(6)		

Table XV. Assigned Hydrogen Atom Parameters for $Cp^*Ta(OCONPh)(\eta^2\text{-}OCONHPh)_2$ (**36**).
H-Atom coordinates (X 10^4)
Isotropic displacement coefficients ($Å^2$ X 10^4)

	x	y	z	U
H(2A)	213	-817	1099	800
H(3A)	-594	3771	2191	800
H(6A)	3550	3316	523	800
H(6B)	2525	2882	34	800
H(6C)	2328	3612	529	800
H(7A)	3797	1116	354	800
H(7B)	2700	606	362	800
H(7C)	2635	1452	-54	800
H(8A)	3856	298	2034	800
H(8B)	2663	218	2203	800
H(8C)	2833	18	1454	800
H(9A)	3373	1873	3119	800
H(9B)	2163	2259	2962	800
H(9C)	2325	1284	2906	800
H(10A)	3303	3767	2193	800
H(10B)	2210	3948	1631	800
H(10C)	2125	3572	2353	800
H(13A)	-2500	1077	-284	800
H(14A)	-4177	630	-23	800
H(15A)	-4489	747	1104	800
H(16A)	-3079	1284	1975	800
H(17A)	-1395	1756	1736	800
H(20A)	5	-2019	1677	800
H(21A)	-444	-2709	2646	800
H(22A)	-883	-1907	3548	800
H(23A)	-917	-447	3489	800
H(24A)	-462	255	2533	800
H(27A)	-1580	4987	2148	800

Table XV. (Continued)

H(28A)	-1856	6380	1770	800
H(29A)	-1013	6907	912	800
H(30A)	143	6025	420	800
H(31A)	443	4613	792	800
H(32A)	7160	8907	2008	800
H(32B)	6597	9021	1223	800
H(33A)	7161	7562	1915	800
H(33B)	7023	7717	1124	800
H(34A)	5622	6961	1759	800
H(34B)	5480	7121	963	800
H(34C)	5302	7074	981	800
H(34D)	5451	7910	585	800
H(35A)	4454	8322	998	800
H(35B)	4267	7974	1705	800
H(36A)	6727	5075	224	800
H(36B)	5784	4965	-438	800
H(37A)	7841	4762	-409	800
H(37B)	6882	4391	-985	800
H(38A)	8277	3473	-45	800
H(38B)	7291	3105	-605	800
H(39A)	6535	2837	276	800
H(39B)	7297	3481	754	800

Chapter 4

Polymerization and Heterolytic Cleavage Reactions with Zirconium Borollide Complexes

Abstract: The preparation and reactivity of several zirconium complexes with the borollide ligand, $(C_4H_4BN^iPr_2)^{2-}$, is described. The ligand is introduced by treating Cp^*ZrCl_3 with one equivalent of $Li_2(C_4H_4BN^iPr_2)\cdot THF$ to generate $Cp^*(C_4H_4BN^iPr_2)ZrCl\cdot LiCl$. This complex contains a η^5-coordinated borollide ligand, as shown by an X-ray crystal structure analysis. Alkylation and arylation with trimethylsilylmethyllithium, benzylpotassium or phenyllithium yielded $Cp^*(C_4H_4BN^iPr_2)ZrR$ complexes. These catalysts polymerizes ethylene, but only oligomerizes α-olefins. In addition, $Cp^*(C_4H_4BN^iPr_2)ZrCl\cdot LiCl$ has been found to exhibit the formal heterolytic cleavage of HCl and CH_3I, affording $Cp^*(C_4H_4BNH^iPr_2)ZrCl_2$ and $Cp^*(C_4H_4BN(CH_3)^iPr_2)ZrCl(I)$, respectively. Finally, treatment of $Cp^*(C_4H_4BN^iPr_2)ZrCl\cdot LiCl$ with $LiNH^tBu$ generated the zwitterionic complex, $Cp^*(C_4H_4BNH^iPr_2)Zr{=}N^tBu$.

Introduction

The cyclopentadienyl (Cp) ligand and its analogues have been the foundation for the synthesis of many organometallic complexes.[1] With electron-donating groups, the ligand is capable of stabilizing high oxidation states (see Chapters 2 and 3) and substitution on the Cp ring allows for catalytic stereoselectivity.[2] Furthermore, many cyclopentadienyl complexes serve as catalysts for various organic transformations, including hydrogenation,[3] hydroamination,[4] and hydroboration[5] of olefins and imines.

One area in which metallocene complexes have proved especially successful is Ziegler-Natta polymerization. Nearly forty years ago, Ziegler discovered that zirconium acetylacetonate in the presence of the co-catalyst, triethylaluminum, readily polymerized ethylene.[6] Subsequent work by Natta extended this process to propylene polymerizations.[7] Today, over 8 billion pounds of polyethylene is produced yearly using catalysts consisting of $TiCl_4$ with trialkylaluminum as a co-catalyst and $MgCl_2$ or SiO_2 as a support.[8] The activity of these systems approach one million grams of polymer per one gram of $TiCl_4$; however, these heterogeneous systems are not amenable to mechanistic study. When Sinn and Kaminsky found that metallocene dichlorides in the presence of methylalumoxane (MAO) resulted in an active polymerization catalyst, it provided the opportunity for studies with homogeneous systems.[9]

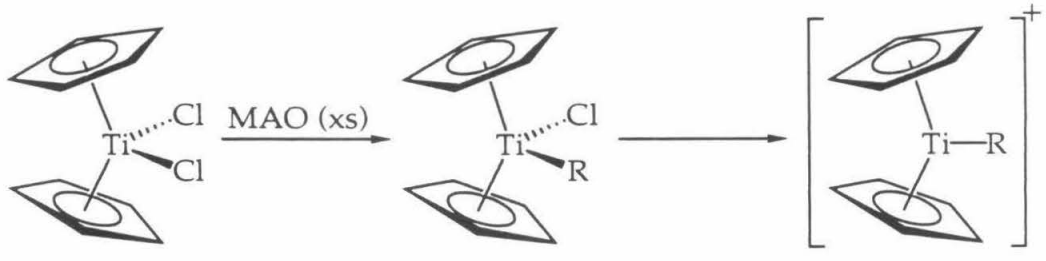

1 **2** **3**

This result and the work of Breslow[10] suggested that the role of the aluminum cocatalyst is to alkylate the transition metal to $Cp_2M(R)Cl$ (**2**) and then abstract a halogen to afford $[Cp_2MR]^+$, (**3**).[11] This 14 electron species is presumed to be the active polymerization catalyst.

Homogeneous group IV cationic metallocenes have been studied extensively as a model for the heterogeneous process.[12] However, choosing

the proper counterion can be crucial to its successful isolation, as the P-F and C-H bonds of both $[PF_6]^-$ and $[B(C_6H_5)_4]^-$ counterions are activated by these catalysts.[13] Recently, it has been found that the tetrakis-perfluorophenylborate anion, $[B(C_6F_5)_4]^-$, is an inert non-coordinating counter-anion.[14] This anion can be easily introduced by protonation of **4** with an anilinium salt[15] or by methyl anion abstraction from **4** with the trityl salt[16] or by the neutral $B(C_6F_5)_3$ to afford the related $[CH_3B(C_6F_5)_3]^-$ anion.[17] (Scheme I) Both cations **5** and **6** have been found to be active ethylene and propylene polymerization catalysts.

Scheme I

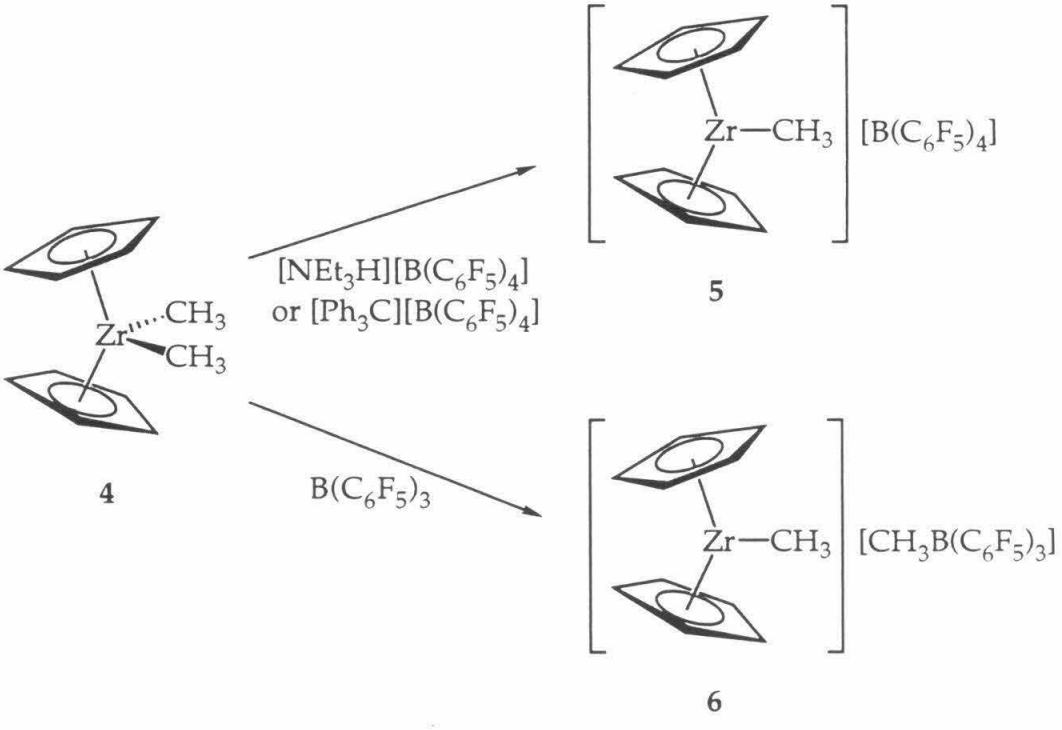

For the last ten years, homogeneous catalysts of group III, lanthanide and group IV metals have been prepared as models of the heterogeneous polymerization systems. Early on, Watson demonstrated that a neutral lanthanide metallocene system performs many of the key reactions in olefin polymerization.[18]

Scheme II

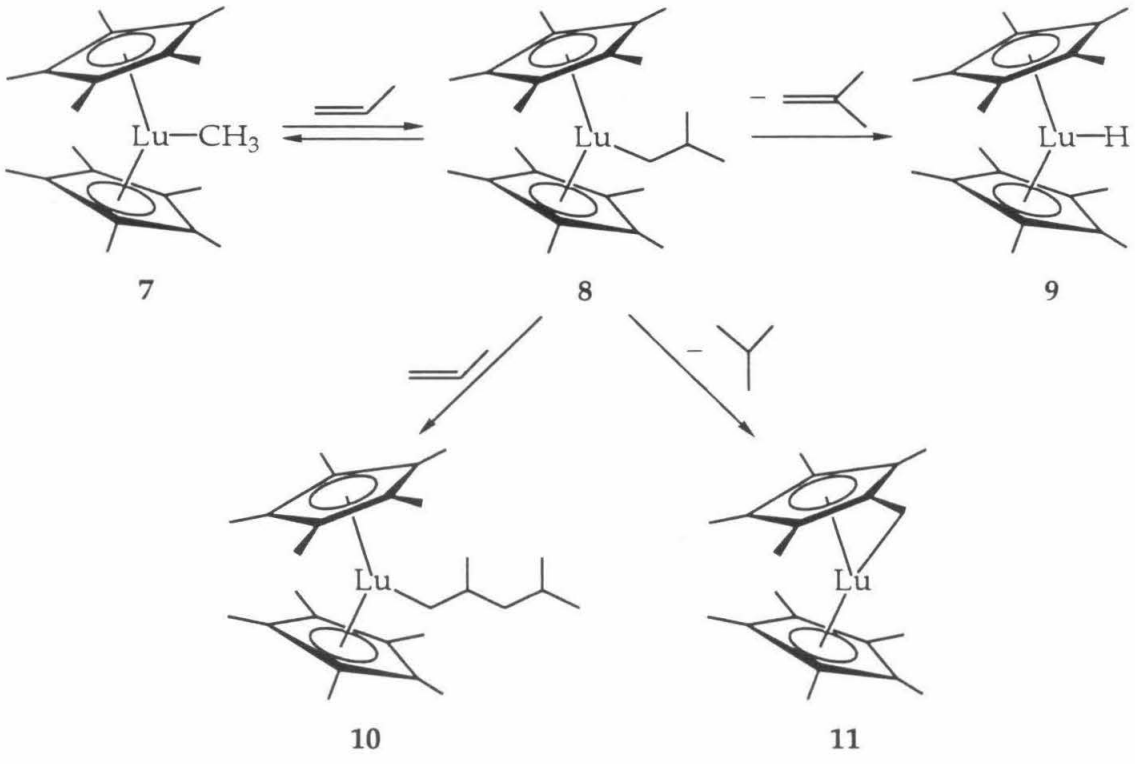

Exposure of the methyl complex (**7**) to excess propene afforded the isobutyl complex (**8**). Subsequent studies demonstrated that **8** undergoes β-H elimination to **9**, β-CH_3 elimination to **7**, olefin insertion to **10**, and σ bond metathesis of the Lu-R bond to **11**, all of which serve as chain termination pathways. (Scheme II)

Marks and Schumann have provided a method of preparing halide-free lanthanide polymerization catalysts.[19] Treatment of $[Li(ether)_2][Cp^*_2MCl_2]$ (M = La, Nd, Lu) with the bulky bis-trimethylsilylmethyllithium resulted in the isolation of **12**. This technique is now often used to obtain halide-free early transition metal catalysts.

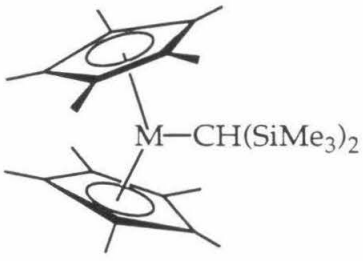

12a, M = La
b, M = Nd
c, M = Lu

Hydrogenation of **12** affords the corresponding hydride complexes, which are active ethylene polymerization catalysts.

Previous work by Bercaw[20] on scandocene complexes and their derivatives show that the group III metallocenes are also amenable to the study of insertion chemistry. The scandocene alkyl complexes (**13**) readily polymerize ethylene and a detailed study on the propagation and termination steps has been carried out.[21]

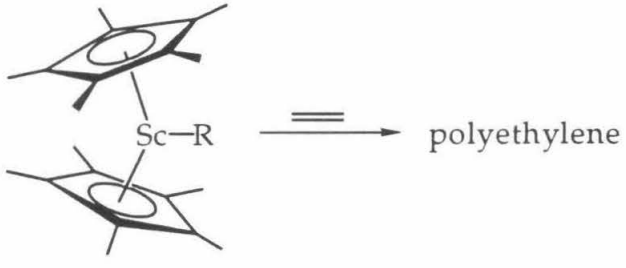

13a, R = CH_3
b, R = CH_2CH_3
c, R = $CH_2CH_2CH_3$

Due to the steric bulk of the Cp* rings, these formally 14 electron alkyl complexes (**13**) are monomeric and can be prepared free of solvent. However, the steric bulk also retards the insertion of α-olefins, as exposure of **13** to α-olefins results in the exclusive isolation of scandium alkenyl complexes, due to a σ-bond metathesis pathway.

In order to create more reactive species, the cyclopentadienyl rings were linked using a dimethylsilyl unit, resulting in more space at the metallocene wedge.[22]

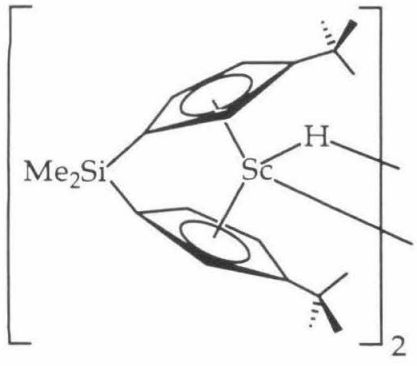

14

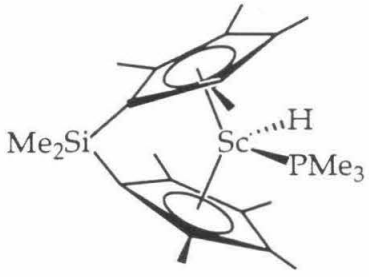

15

The polymerization reactivity of both hydrides **14** and **15** exceeded that for the permethylscandocene complexes. The dimerization of α-olefins in a "head-to-tail" fashion and cyclization of α-ω-dienes are both observed using these catalysts.

In order to achieve a truly "living" Ziegler-Natta olefin polymerization system, the steric crowding around the metal was further reduced in order to decrease competing reactions. Therefore, the linked [(Cp*SiNR)Sc] complexes (**16** and **17**) were prepared.[23]

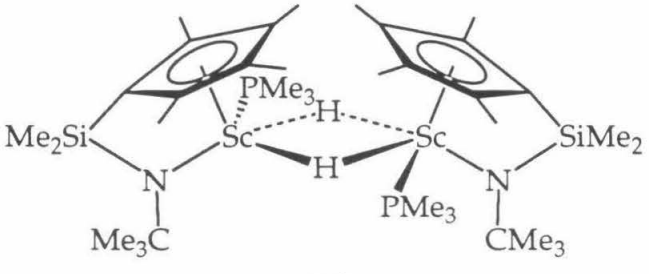

16

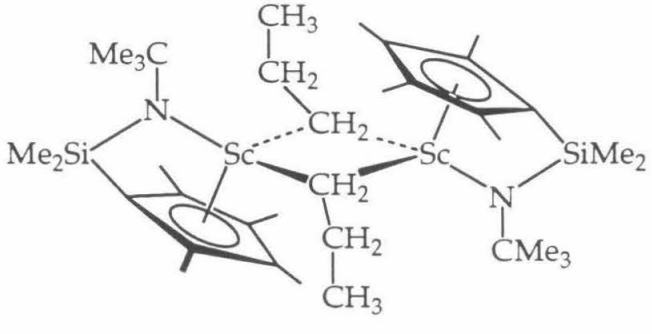

17

Complex **16** readily polymerizes α-olefins, requiring the loss of PMe_3 to achieve the active 12 electron species.[24] In addition, the molecular weight distribution of the oligomers at low conversion indicates that nearly all of the scandium centers are active sites. The propyl dimer (**17**) was found to be even more active toward α-olefins.[25]

Diverse chemistry has been exhibited by the metallocene systems with regard to insertion, polymerization, and C-H activation processes. In order to prepare complexes with different metal and charge distributions, dianionic ligands have been used to replace cyclopentadienyl groups. For example, the dicarbollide ligand, $[C_2B_9H_{11}]^{2-}$, has been complexed to group III, IV, and V metals. Jordan has prepared both zirconium and hafnium alkyl analogues.

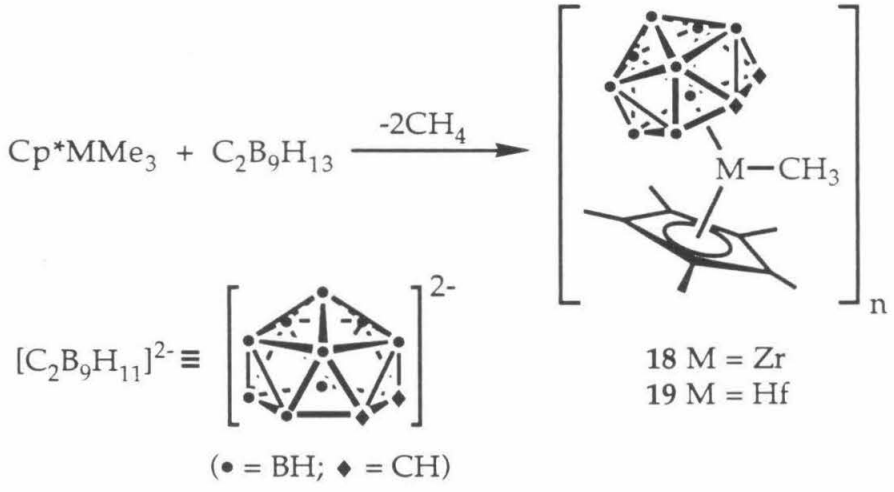

The complexes exhibit pentahapto dicarbollide coordination and display reaction chemistry similar to that of the bent metallocene systems. The electrophilic nature of **18** and **19** was demonstrated by their coordination of donor ligands to form adducts **20** and **21**. Insertion of 2-butyne into the methyl complex **18** resulted in **22** with a β-CH_3 agostic interaction, which further demonstrates the electrophilicity of the metal center. Polyethylene was produced when **18** was exposed to ethylene; 2-methyl-1-pentene and 2, 4-dimethyl-1-heptene were isolated when **18** was exposed to propene. (Scheme III)

Scheme III

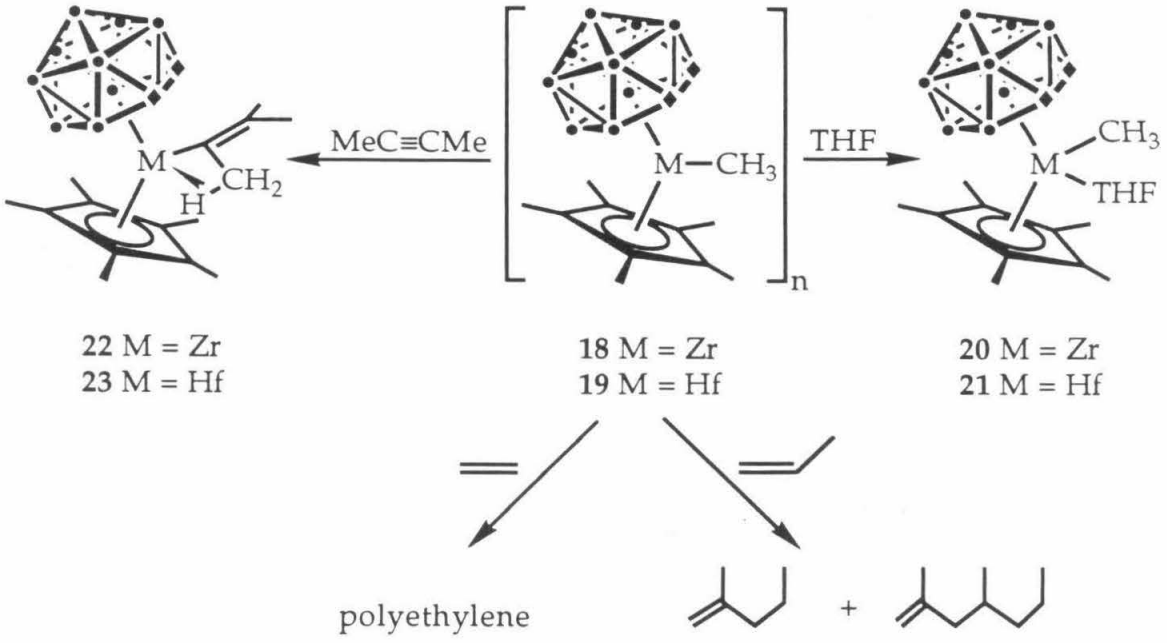

22 M = Zr
23 M = Hf

18 M = Zr
19 M = Hf

20 M = Zr
21 M = Hf

Group five analogs can also be easily prepared by two methods. Treatment of $Cp'TaCl_4$ ($Cp' = \eta^5\text{-}C_5H_4Me$) with one equivalent of the dilithium carbollide followed by alkylation with methylmagnesium bromide affords **24**. Alternatively, treatment of $TaCl_5$ with one equivalent of the dilithium carbollide followed by methylmagnesium bromide yields **25**. The polymerization chemistry of these complexes has not been reported.

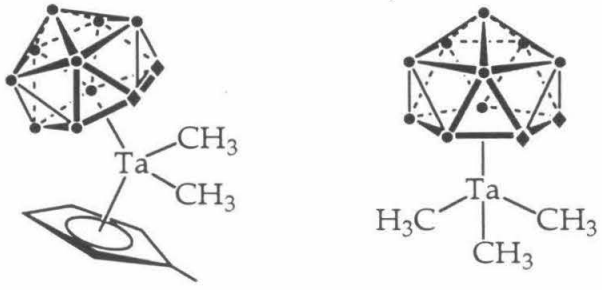

24 **25**

Previous work in the Bercaw group has demonstrated that the dicarbollide ligand is easily introduced to the [Cp*Sc] fragment. However, with the dicarbollide ligand, crystal structures of several complexes, including **26**, have shown interactions between the B-H bond of one dicarbollide with

the metal center of a second dicarbollide ligand.[26] This B-H agostic interaction provides electron density to the electrophilic metal, thus reducing the activity of the complex.[27]

$[Li(THF)]_2 \cdot 3/2(C_6H_5CH_3)$ 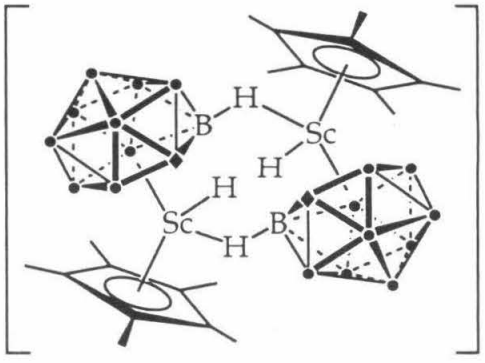

26

As mentioned earlier, group IV industrial catalyst are successfully modelled by neutral group III and group IV metallocenes. Ideally, however, the polymerization catalyst would not require counterions, would not possess β-H agostic interactions, and would not dimerize. In order to achieve such a catalyst, complexes with the dianionic borollide, $(C_4H_4BN^iPr_2)^{2-}$,[28] have been prepared.

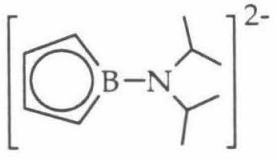

The borollide ligand is expected to be similar to both the dicarbollide and the cyclopentadienyl analogues in its coordination to various transition metal centers.[29]

The neutral zirconium and hafnium borollide complexes would be isoelectronic to the neutral group III (**13a**) and cationic group IV (**5**) metallocene complexes. (Scheme IV). Therefore, zirconium borollide complexes were considered extremely likely to serve as Ziegler-Natta polymerization catalysts.

Scheme IV

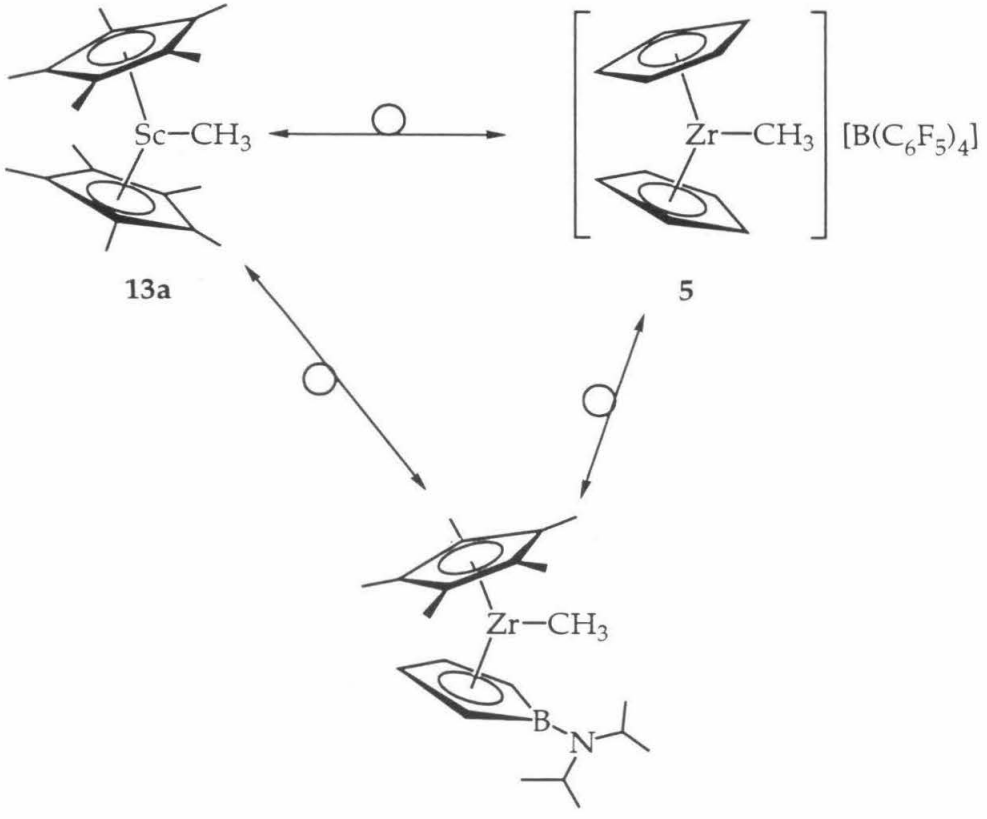

This chapter recounts the synthesis of the borollide complexes and their properties as polymerization catalysts. In addition, the amine nitrogen on the borollide permits study of the unique situation of an electrophilic center and a basic center that are in close proximity, yet not directly bonded to each other (Chapters 2 and 3). This aspect will be explored in the potential of the borollide complexes in the heterolytic activation of H-X (X = Cl, OR, NHR, CR_3) bonds.

Results and Discussion

A zirconium compound with the borollide ligand was first prepared by treating Cp^*ZrCl_3 with $Li_2(C_4H_4BN^iPr_2)\cdot THF$. The reaction in toluene afforded a polymeric complex with LiCl, **28**. This product is insoluble in benzene, but recrystallized from toluene/petroleum ether to afford pure **28** in 57% yield. When the reaction was carried out in diethyl ether, a burgundy monomeric complex with LiCl and diethyl ether (**27**) was isolated. (Scheme V)

Scheme V

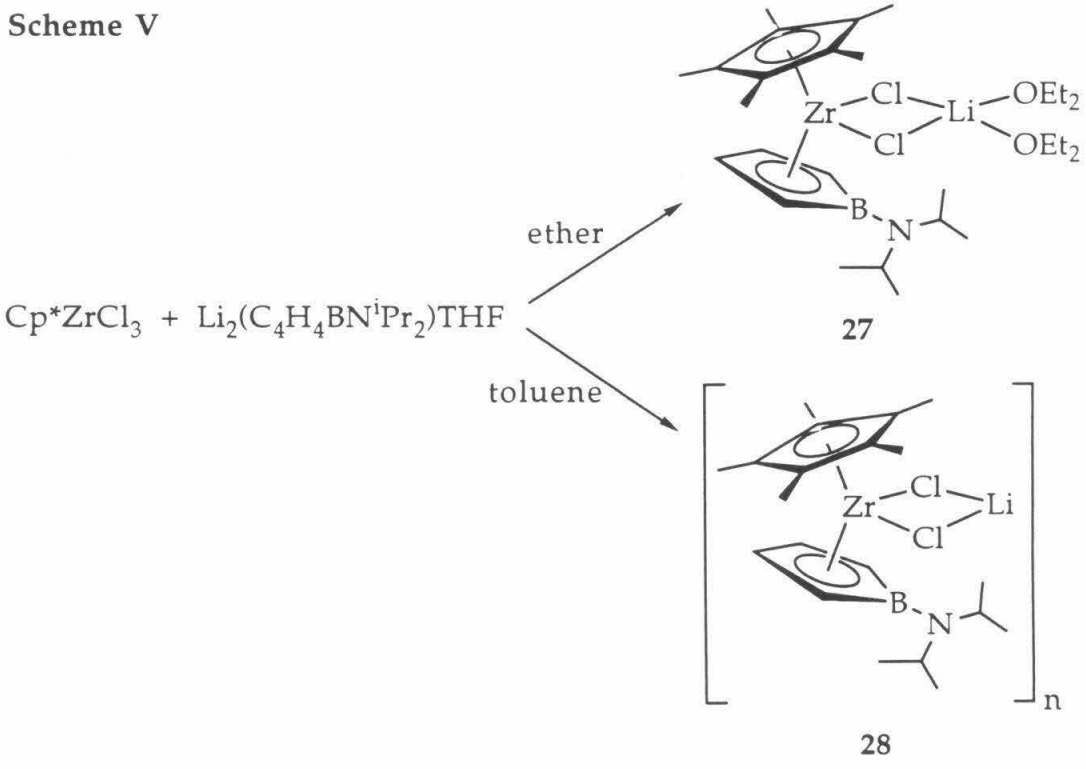

27 **28**

Slow cooling of a concentrated solution of **27** in diethyl ether afforded crystals which were submitted for X-ray diffraction studies with the ORTEP diagram shown in figure 1. Inspection of the atom-atom bond distances around the borollide suggested that the zirconium center is η^5-bonded to the borollide ligand (Figure 2).

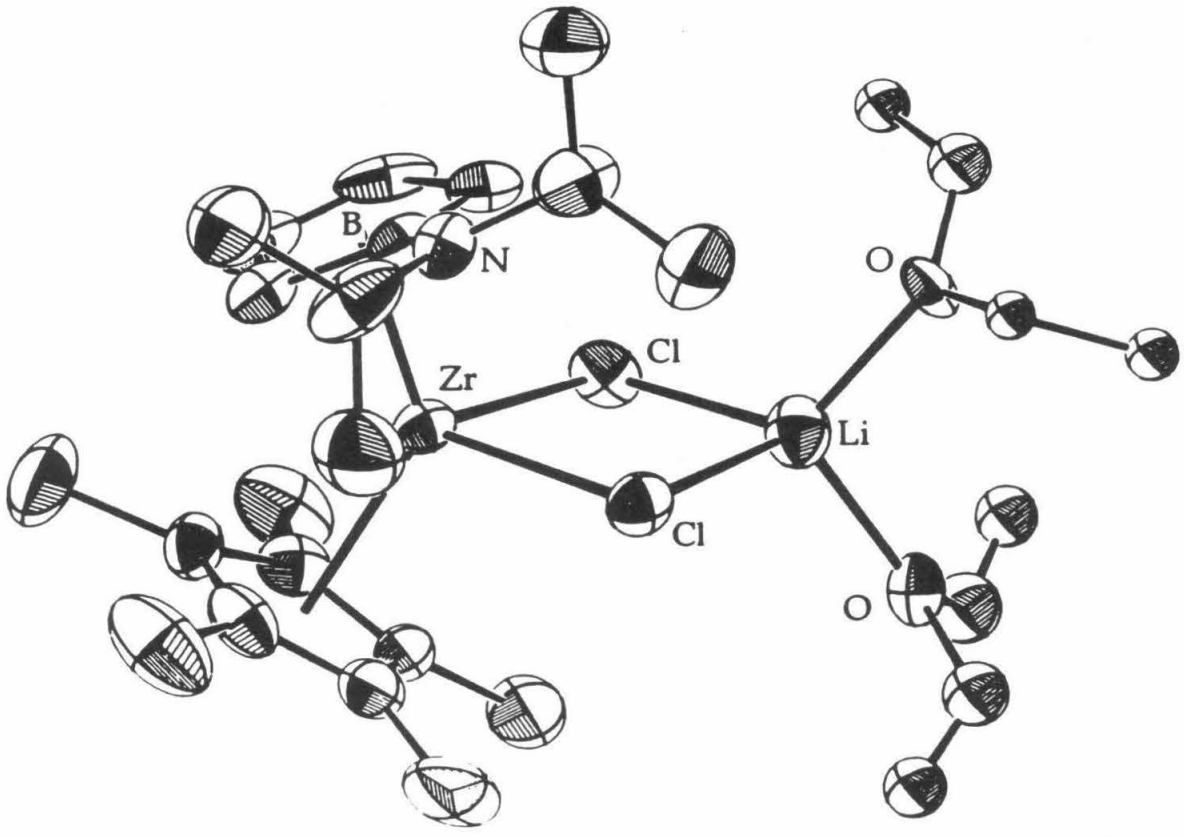

Figure 1. ORTEP diagram of $Cp^*(C_4H_4BN^iPr_2)ZrCl{\cdot}LiCl(Et_2O)_2$ (**27**)

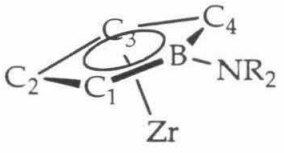

Bond distances (Å)		Angles (°)	
Zr-C_1	2.405	C_1-B-N	129.9
Zr-C_2	2.354	C_4-B-N	128.5
Zr-C_3	2.439	C_1-B-C_4	101.6
Zr-C_4	2.518		
Zr-B	2.714		
C_1-C_2	1.404		
C_2-C_3	1.377		
C_3-C_4	1.423		
B-C_1	1.526		
B-C_4	1.520		

η^5-Zr^{IV}, d^0 η^4-Zr^{II}, d^2

Figure 2. Hapticity of the zirconium borollide.

Therefore, the ring does not have η^4-character which is in sharp contrast to $(C_4H_4BN^iPr_2)_2Cr(CO)_2$ (**29**) and $(C_4H_4BN^iPr_2)_2MnCO$ (**30**). In both of these compounds, the borollide bonds in a fashion characteristic of a diene.[30]

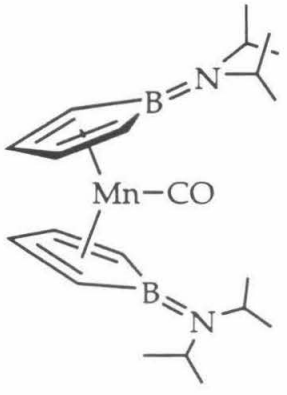

29

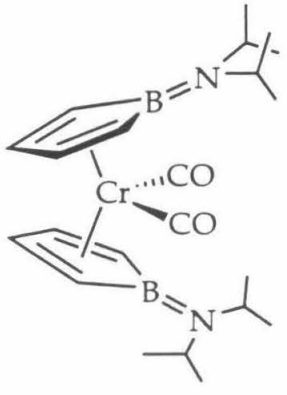

30

Furthermore, in **27**, the boron atom, the two adjacent carbon atoms to boron, and the nitrogen atom of the isopropyl group are coplanar. In the crystal structures of **29** and **30** a dative bond between the boron and nitrogen is suggested by the B-N distances of 1.42Å and 1.40Å, respectively. In **27** , the

B-N distance is 1.43Å, which would apparently suggest a dative bond between the boron and nitrogen atoms. However, with an η^5-borollide, the planarity of the amine nitrogen can be accounted for by the localization of the lone pair in an orbital that is primarily p in character.[31]

As mentioned above, all of the zirconium borollide complexes are intensely colored. This result was intriguing since the expected dianionic nature of the borollide predicted d^0 metal centers and therefore, preclude the intense colors observed. However, ligand-to-metal charge transfer events can explain the observed colors. In order to test this hypothesis, the UV-visible spectrum of **28** was taken in THF. Also, the electrochemical properties of **28** was determined in order to compare it to the charge transfer energy value calculated from the spectroscopic study. The UV-visible spectrum exhibited a peak at 570 nm. Using $E_{CT} = hc/\lambda(N_A)$ (where h is Planck's constant, λ is the wavelength of the peak, c is speed of light, and N_A is Avogadro's number), the charge transfer energy is calculated to be 50 kcal/mole. The cyclic voltammogram exhibited an oxidative wave at -320 mV and a reductive wave at -2.12 V. Using E = -96.5X (where X is the difference in the oxidative and reductive wave potentials), the charge transfer energy is calculated to be 56 kcal/mole. These results are consistent with a LMCT event which is responsible for the intense colors observed for the complexes.

Derivitization of **27** is readily accomplished with benzylpotassium, trimethylsilylmethyllithium and phenyllithium to afford **31**, **32**, and **33**, respectively.

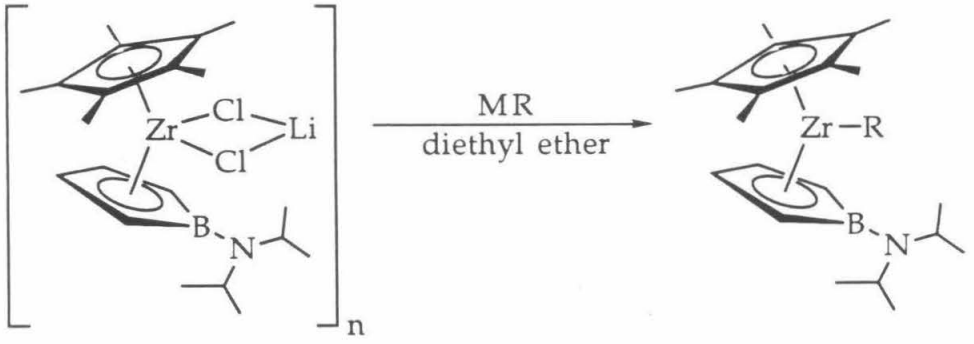

MR = $LiCH_2TMS$, LiPh, KCH_2Ph

R = CH_2TMS **(31)**
= Ph **(32)**
= CH_2Ph **(33)**

Interestingly, the ^1H NMR spectra for these three complexes exhibit four borollide resonances, which indicates that in solution, the borollide ring rotates slowly or not at all on the NMR time scale. Treatment of **27** with smaller alkylating agents such as methyllithium resulted in a mixture of species, presumably mono- and dialkylated products.

The behavior of $Cp^*(C_4H_4BN^iPr_2)ZrPh$ and $Cp^*(C_4H_4BN^iPr_2)ZrCH_2Ph$ as Ziegler-Natta polymerization catalysts was examined.

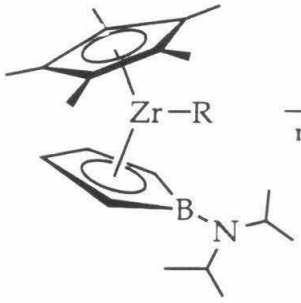

$\xrightarrow[\text{methylcyclohexane}]{=}$ polyethylene

	R = Ph	R = CH_2Ph
PDI	6.06	3.20
M_n	119,900	69,679

$Cp^*(C_4H_4BN^iPr_2)ZrPh$ catalyzes the polymerization of $CH_2{=}CH_2$, but the reaction is slow. On the other hand, $Cp^*(C_4H_4BN^iPr_2)ZrCH_2Ph$ rapidly polymerized ethylene with the formation of a polymer apparent within minutes under conditions where $Cp^*(C_4H_4BN^iPr_2)ZrPh$ required 12 hours. This result was anticipated since the initiation of $Cp^*(C_4H_4BN^iPr_2)ZrPh$ requires breaking a relatively strong Zr-C(sp^2) bond. With a weaker Zr-C(sp^3) bond, initiation is more facile with $Cp^*(C_4H_4BN^iPr_2)ZrCH_2Ph$. Though $Cp^*(C_4H_4BN^iPr_2)ZrCH_2Ph$ is an active ethylene polymerization catalyst, attempts to polymerize propylene met with little success. Small scale reactions in NMR tubes revealed that $Cp^*(C_4H_4BN^iPr_2)ZrCH_2Ph$ underwent only several propylene insertions, affording small oligomers. Interestingly, CO did not insert into the Zr-C bond of $Cp^*(C_4H_4BN^iPr_2)ZrCH_2TMS$.

These alkyl and aryl complexes are 14 electron species; therefore, they might be expected to coordinate a donor solvent or ligand. Interestingly, preparation of these complexes in diethyl ether resulted in donor-free products. These results indicate that the 14 electron species might dimerize in solution. However, a solution molecular weight determination showed that $Cp^*(C_4H_4BN^iPr_2)ZrCH_2TMS$ is monomeric in a benzene solution.

In an attempt to increase the reactivity of the borollide complexes, a cyclopentadienyl complex was prepared. This compound was predicted to

have less steric blockage in the wedge of the metallocene and, hence, be a better catalyst for α-olefin polymerization. Therefore, $CpZrCl_3(DME)$ was treated with one equivalent of $Li_2(C_4H_4BN^iPr_2)\cdot THF$ to afford $Cp(C_4H_4BN^iPr_2)ZrCl\cdot LiCl(DME)$, **34**, as a green solid.

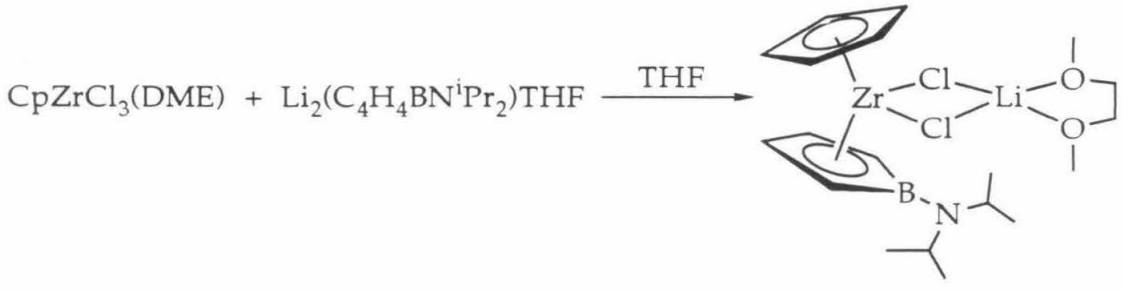

34

Reaction of **34** with either bis-trimethylsilylmethyllithium or benzylpotassium resulted in an ill-defined mixture of products. This result was not unpredicted, since other complexes with dimethoxyethane or tetramethylethylenediamine as LiCl adducts are also unreactive.[32] It is possible that alkylation of $CpZrCl_3(DME)$ prior to the introduction of the borollide ligand will result in a DME-free complex, $Cp(C_4H_4BN^iPr_2)ZrCl\cdot LiCl$.

In addition to the studies of Ziegler-Natta polymerization, the borollide complexes also provide a unique opportunity to study the ramifications of an electrophilic center in close proximity to a basic site. This situation sharply contrasts the complexes in the previous two chapters; in those complexes an electrophilic center is directly attached to a basic site (oxo or imido group). When **28** was treated with one equivalent of HCl, a yellow solid was isolated, and the number of resonances in the ^1H NMR spectrum suggests that the proton is hydrogen-bonded to both of the chloride atoms in the metallocene wedge.[33,34] Complex **35** can be envisioned as the formal heterolytic cleavage of the H-Cl bond by **28.** The hafnium analogue has also been prepared and the symmetry of the ^1H NMR spectrum also suggested a complex isostructural to **35**.

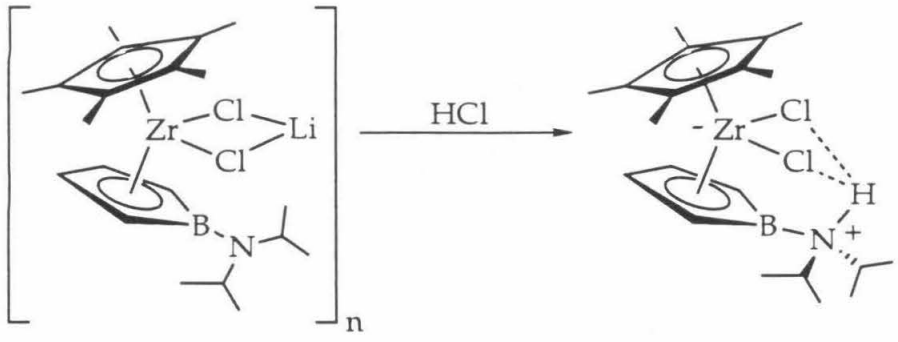

28 **35**

However, an X-ray diffraction study of the hafnium analogue showed that the amine hydrogen is *not* located between the two chlorine atoms. Instead there is hydrogen-bonding to only one of the chloride atoms.[35]

The reactions between **28** and other heterolytic cleavage substrates, including CpH,*tert*-butylacetylene, and CH_3OH were explored; however, no reaction occurred, suggesting that these C-H bonds are not sufficiently acidic to effect heterolytic cleavage. In a related reaction, **28** was treated with one equivalent of methyl iodide, and **36** was isolated as an orange solid.

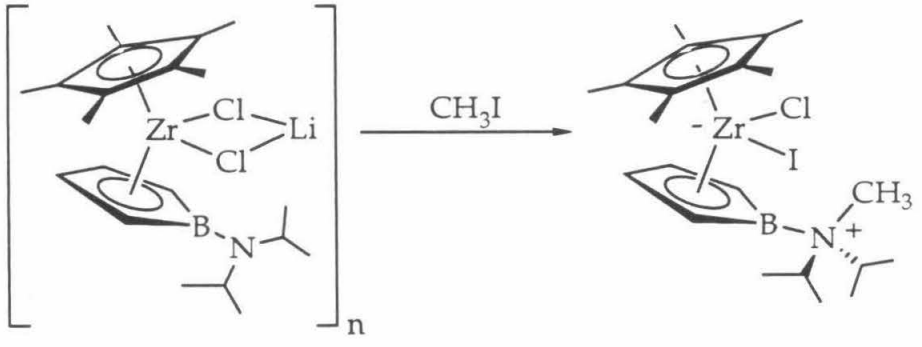

28 **36**

This type of chemistry is precedented by the reaction of $(\eta^5\text{-}C_5H_5NMe_2)_2Fe$ with two equivalents of CH_3I to afford $[(\eta^5\text{-}C_5H_5NMe_3)_2Fe]I_2$.[36]

An example of an intramolecular proton transfer to the borollide ligand was found upon the treatment of **28** with lithium *tert*-butylamide in benzene to afford **37** as a tan product (Scheme VI).

Scheme VI

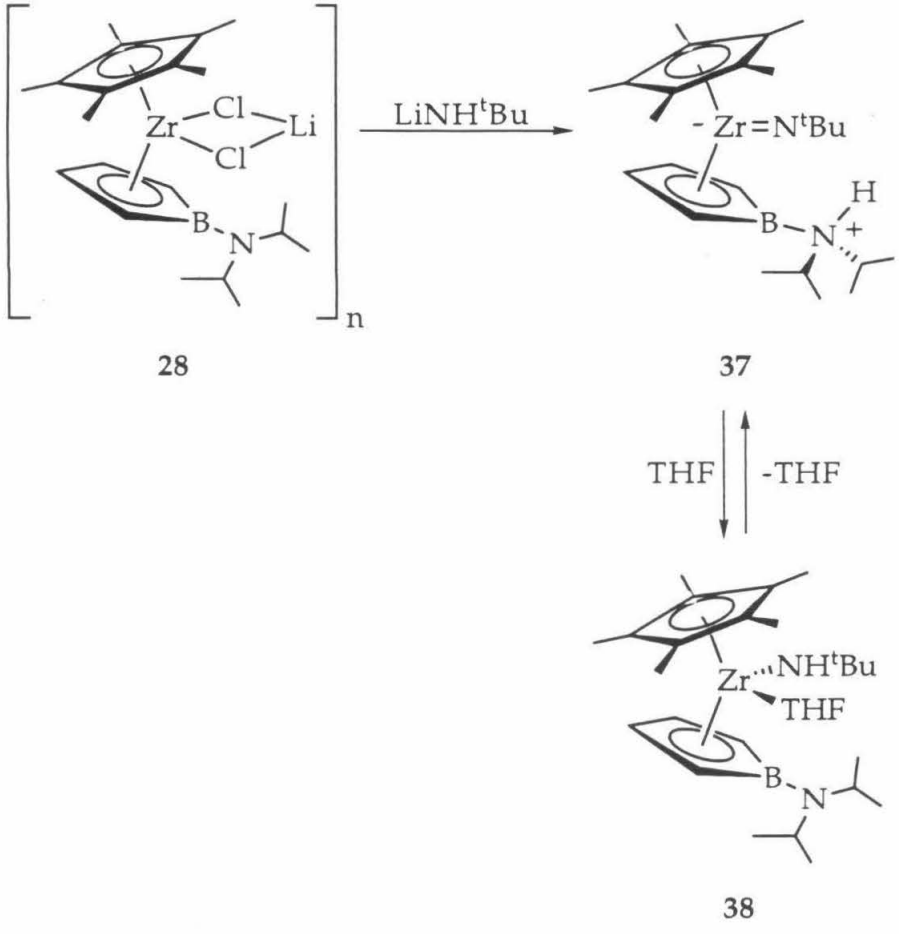

28 **37** **38**

It is intriguing that the amino group is capable of abstracting the proton from the amide , but not from CpH (pK_a ~ 15) or ^{t}BuC≡CH (pK_a ~ 25). Isolation of the zwitterionic complex **37** can be attributed to the formation of a strong zirconium imido bond upon proton transfer. This conjecture was substantiated by the appearance in the solid state IR spectrum of an absorbance at 1200 cm^{-1} for the Zr imido stretch. However, in the presence of coordinating solvents, the proton moves from the diisopropylamino group on the borollide to the zirconium imido group, which results in **38** (Scheme VI). These results are consistent with the earlier proposal that a ligand-to-metal charge transfer is responsible for the intense colors of these compounds; the zwitterionic **37** would not be expected to contain a low energy ligand to metal charge transfer transition. In order to probe whether the proton transfer to the amino group is exclusive for the amido group,

$Cp^*(C_4H_4BN^iPr_2)ZrCH_2TMS$ (**31**) was used to determine whether a markedly less acidic proton could be transferred to the diisopropylamino group. However, heating **31** in solution resulted only in its decomposition.

The availability of **38** provided an opportunity to prepare the anionic imido species, $[Cp^*(C_4H_4BN^iPr_2)Zr{=}N^tBu]^-$, and study its reaction chemistry. However, deprotonation of **38** with alkyllithiums yielded only a mixture of products. When **38** was treated with lithium *tert*-butylamide, the bis-amido anion (**39**) was the product.

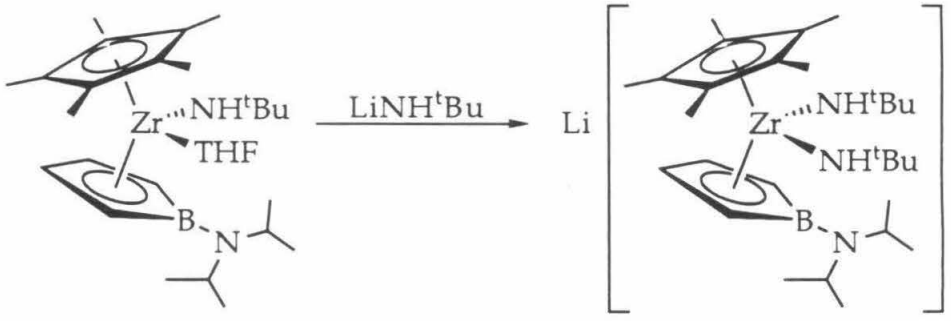

38 **39**

Similar reactivity was observed when **28** was treated with one and two equivalents of lithium anilide to yield **40** and **41**, respectively.

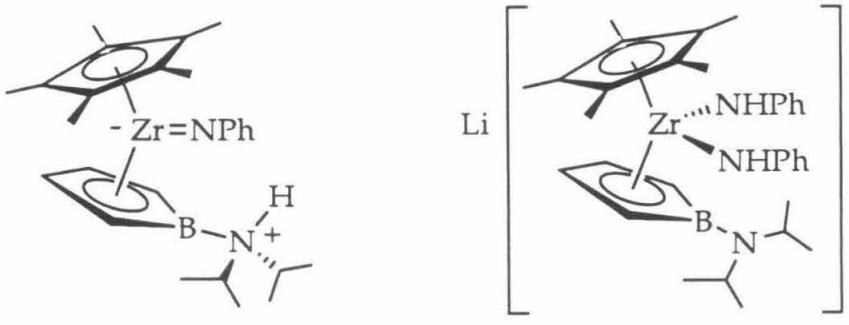

40 **41**

Conclusion

The borollide ligand, $[C_4H_4BN^iPr_2]^{2-}$, provides a unique opportunity to prepare neutral group IV Ziegler-Natta polymerization catalysts. Though the alkyl complexes are 14 electron species, there is no indication that the borollide amine unit is capable of acting as a two electron donor to the electrophilic metal center. In fact, the crystal structure of

$Cp^*(C_4H_4BN^iPr_2)ZrCl{\cdot}LiCl(Et_2O)_2$ shows that the nitrogen is not a donor and that the borollide is η^5-coordinated to the zirconium center. The zirconium alkyl and aryl complexes are ethylene polymerization catalysts, but they catalyze only the oligomerization of α-olefins. Furthermore, the borollide ligand, with a basic group, exhibited interesting cleavage chemistry. When exposed to HCl, CH_3I, and $LiNH^tBu$, $Cp^*(C_4H_4BN^iPr_2)ZrCl{\cdot}LiCl$ affords $Cp^*(C_4H_4BNH^iPr_2)ZrCl_2$ and $Cp^*(C_4H_4BN(CH_3I)^iPr_2)ZrCl(I)$ and $Cp^*(C_4H_4BNH^iPr_2)Zr(=N^tBu)$. In conclusion, the dianionic borollide ligand, $(C_4H_4BN^iPr_2)^{2-}$, has provided a unique opportunity to study new metal/charge combinations in Ziegler-Natta polymerization chemistry. In addition, initial studies indicate that this basic ligand allows for interesting reaction chemistry, the full scope of which is just beginning to be surveyed.

Experimental

General Considerations. All manipulations were performed using glovebox or high vacuum line techniques.[37] Solvents were dried over $LiAlH_4$ or Na/benzophenone and stored under vacuum over "titanocene."[38] Benzene-d_6 and tetrahydrofuran-d_8, were dried over activated molecular sieves (4Å, Linde) and stored over "titanocene" or Na/benzophenone. Argon and nitrogen gases were passed over MnO on vermiculite and activated sieves. $CpZrCl_3(DME)$,[39] $Li_2(C_4H_4BN^iPr_2)\cdot THF$,[28] were prepared as previously described.

Many reactions were monitored by NMR spectroscopy. Any experiment described in this chapter but not explicitly listed below was carried out in a sealed NMR tube using ~0.7 mL of the NMR solvent with the appropriate reagents.

$Cp^*(C_4H_4BN^iPr_2)ZrCl\cdot LiCl$ (28). A 100 mL round bottom flask was charged with 2.50 g (7.51 mmol) Cp^*ZrCl_3 and 1.87 g (7.51 mmol) $Li_2(C_4H_4BN^iPr_2)\cdot THF$. A swivel frit assembly was attached to the reaction vessel. Approximately 60 mL toluene was then condensed onto the solids at -78°C. Even at -78°C, the reaction commenced and the resultant purple solution was stirred for 24 hours. The LiCl precipitate was removed by filtration and the volatiles were removed *in vacuo* . Petroleum ether (20 mL) was then condensed on the solid at -78°C. After warming to room temperature all of the solid dissolved. The solution was slowly cooled to -78°C and filtration afforded a purple product (2.01 g, 4.28 mmol). Yield = 57%. Analysis : Calculated (Found) C: 56.53 (53.15); H: 7.83 (7.17); N: 3.30 (2.71).

$Cp^*(C_4H_4BN^iPr_2)ZrCH_2TMS$ (31). A 50 mL round bottom flask was charged with 943 mg (2.02 mmol) $Cp^*(C_4H_4BN^iPr_2)ZrCl\cdot LiCl$ and 209 mg (2.22 mmol) trimethylsilylmethyllithium. A swivel frit assembly was then attached. Approximately 25 mL toluene was condensed on the solids at -78°C, resulting in a red solution. The resultant solution was allowed to warm slowly to room temperature and was stirred overnight. LiCl was removd by filtration and the volatiles were removed *in vacuo*. The solid was washed with petroluem ether to yield 900 mg (1.89 mmol) of a red-brown product. Yield = 93%. Analysis : Calculated (Found) C: 60.47 (59.29); H: 9.30 (8.91); N: 2.94 (2.32).

$Cp^*(C_4H_4BN^iPr_2)ZrPh$ (32). A 100 mL round bottom flask was charged with 1.01 g (2.16 mmol) $Cp^*(C_4H_4BN^iPr_2)ZrCl{\cdot}LiCl$ and 200 mg (2.38 mmol) phenyllithium. A swivel frit assembly was then attached. Approximately 50 mL toluene was condensed on the solids at -78°C, and the resultant solution was allowed to warm slowly to room temperature. The solution was stirred overnight and then filtered to remove LiCl. The volatiles were removed *in vacuo*, and then 20 mL diethyl ether was condensed on the solid. Concentration, cooling, and filtration of the solution afforded 552 mg (1.18 mmol) of a red-brown solid. Yield = 55%. Analysis : Calculated (Found) C: 66.92 (62.34); H: 8.21 (7.78); N: 3.00 (2.19).

$Cp^*(C_4H_4BN^iPr_2)ZrCH_2Ph$ (33). A 50 mL round bottom flask was charged with 670 mg (1.43 mmol) $Cp^*(C_4H_4BN^iPr_2)ZrCl{\cdot}LiCl$ and 206 mg (1.58 mmol) benzyl potassium. A swivel frit assembly was then attached. Approximately 25 mL diethyl ether was then condensed onto the solids at -78°C. The resultant solution was allowed to warm to room temperature slowly and then stirred for 30 minutes. Precipitated LiCl was then removed by filtration and the volatiles were removed *in vacuo* to afford a fluffy orange solid. The residue was washed with petroleum ether and 587 mg (1.22 mmol) of an orange-red solid was isolated. Yield = 85%. Analysis : Calculated (Found) C: 67.47 (62.89); H: 8.39 (7.88); N: 2.91 (2.22).

$Cp(C_4H_4BN^iPr_2)ZrCl{\cdot}LiCl(DME)$ (34). A 100 mL round bottom flask was charged with 1.12 g (3.19 mmol) $CpZrCl_3(DME)$ and 800 mg (3.19 mmol) $Li_2(C_4H_4BN^iPr_2){\cdot}THF$. A swivel frit assembly was then attached. Approximately 50 mL of THF was condensed on the solids at -78°C, and the solution was allowed to warm slowly to room temperature and then stirred overnight. The volatiles were removed *in vacuo* and 15 mL diethyl ether was then condensed on the solid. The LiCl was then filtered away and the volatiles were removed again *in vacuo*. The residue was washed with petroleum ether to afford 1.06 g (2.17 mmol) of a green product. Yield = 68%. Analysis : Calculated (Found) C: 46.81 (46.97); H: 6.82 (6.72); N: 2.86 (2.83).

$Cp^*(C_4H_4BNH^iPr_2)ZrCl_2$ (35). A 50 mL round bottom flask was charged with 427 mg (1.00 mmol) $Cp^*(C_4H_4BN^iPr_2)ZrCl{\cdot}LiCl$. A swivel frit assembly was attached. Approximately 25 mL toluene was then condensed on the solid at

-78°C. One equivalent HCl was added using a gas bulb and the resultant solution was stirred for 9 hours. The volatiles were removed *in vacuo*,, leaving a yellow residue which was extracted with diethyl ether to afford a yellow solution. The ether was removed *in vacuo* to yield a yellow solid (130 mg, 0.28 mmol). Yield = 28%. Analysis : Calculated (Found) C: 47.68 (52.06); H: 6.60 (7.43); N: 2.78 (3.03). IR spectroscoy (KBr, cm^{-1}): 3424.2, 2972.7, 2905.7, 1389.3, 1375.7, 1317.3, 1256.1, 806.9.

$Cp^*(C_4H_4BN(CH_3)^iPr_2)ZrI(Cl)$ (36). A 50 mL round bottom flask was charged with 500 mg (1.07 mmol) $Cp^*(C_4H_4BN^iPr_2)ZrCl\cdot LiCl$. A swivel frit assembly was then attached. Approximately 25 mL toluene was condensed on the solid at -78°C, and then 1 equivalent CH_3I was added using a gas bulb. The purple solution was stirred for one hour. A small amount of THF (5 mL) was then added at -78°C and the solution was allowed to warm to room temperature. The resultant orange solution was stirred overnight, and the volatiles were then removed *in vacuo*. Toluene was condensed on the solid, and the orange solution was filtered. The volatiles were removed *in vacuo*, resulting in an orange solid (179 mg, 0.03 mmol). Yield = 30%. Analysis : Calculated (Found) C: 44.49 (40.30); H: 6.41 (5.56); N: 2.47 (1.95).

$Cp^*(C_4H_4BN^iPr_2)ZrNH^tBu$ (38). A 100 mL round bottom flask was charged with 1.0 g (2.14 mmol) $Cp^*(C_4H_4BN^iPr_2)ZrCl\cdot LiCl$ and 160 mg (2.05 mmol) lithium *tert*-butylamide. Attached swivel frit assembly. Approximately 50 mL benzene was condensed on the solids at -78°C. The solution was stirred overnight at room temperature. Then the volatiles were removed *in vacuo* and diethyl ether was condensed in the flask. A white solid (LiCl) was filtered. Removed the volatiles to afford 710 mg (1.54 mmol) of a tan solid. Yield = 72%.

X-Ray Crystal Structure Determination of $Cp^*(C_4H_4BN^iPr_2)ZrCl\cdot LiCl(OEt_2)_2$.

The ORTEP drawing of $Cp^*(C_4H_4BN^iPr_2)ZrCl\cdot LiCl(OEt_2)_2$ is shown in figure 1. To obtain the structure a burgundy plate, which was obtained by cooling a diethyl ether solution of the complex, was mounted in a greased capillary. The crystal was then centered on a CAD-4 diffractometer. Unit cell parameters and an orientation matrix were obtained by a least squares calculation from the setting angles of 25 reflections with $16^o < \theta < 18^o$.

Coordinates of the zirconium atom were obtained from a Patterson map; locations of the other non-hydrogen atoms were determined from successive structure factor-Fourier calculations. Calculations were done with programs of the CRYM Crystallographic Computing System and ORTEP with scattering factors and corrections for anamalous scattering taken from a standard reference.[40]

Table I. ^{1}H NMR Spectral Data (Bo = ($C_4H_4BN^iPr_2$)) for complexes **28 - 38**.

Compound	Assignment	δ in ppm (m)	J (Hz)
Cp*BoZrCl·LiCl **(28)**	N-CH-(CH_3)$_2$	1.07 (d)	6.7
in THF-d_8	C_5(CH_3)$_5$	1.86 (s)	
	N-CH-CH_3	3.47 (p)	6.9
	CH_2CH_2B	3.70 (t)	3.9
	CH_2CH_2B	5.21 (t)	3.6
Cp*BoZrCl·LiCl **(28)**	N-CH-(CH_3)$_2$	1.31 (d)	6.7
in C_6D_6/THF-d_8	C_5(CH_3)$_5$	1.99 (s)	
	N-CH-CH_3	3.74 (m)	6.7
	CH_2CH_2B	4.48 (t)	3.7
	CH_2CH_2B	5.77 (t)	3.8
Cp*BoZrCH$_2$TMS **(31)**	CH_2Si(CH_3)$_3$	-0.70 (br)	
in C_6D_6	CH_2Si(CH_3)$_3$	-0.32 (br)	
	CH_2Si(CH_3)$_3$	0.41 (s)	
	N-CH-(CH_3)$_2$	1.42 (br)	
	C_5(CH_3)$_5$	1.95 (s)	
	N-CH-(CH_3)$_2$	3.59 (m)	
	CH_2CH_2B	4.18 (br)	
	CH_2CH_2B	5.13 (br)	
	CH_2CH_2B	5.57 (br)	
	CH_2CH_2B	6.39 (br)	
Cp*BoZrPh **(32)**	N-CH-(CH_3)$_2$	1.06 (d)	6.6
in THF-d_8	C_5(CH_3)$_5$	1.68 (s)	
	CH_2CH_2B	3.33 (d of t)	^{3}J = 4.5
			^{4}J = 2.1
	N-CH-(CH_3)$_2$	3.46 (sept)	6.6
	CH_2CH_2B	3.70 (d of t)	^{3}J = 5.1
			^{4}J = 2.4
	CH_2CH_2B	4.40 (m)	
	CH_2CH_2B	5.84 (m)	
	para-C_6H_5	6.58 (t)	7.2
	meta-C_6H_5	6.71 (t)	7.2
	ortho-C_6H_5	7.43 (d)	6.3

Table I. (Continued) ^{1}H NMR Spectral Data for complexes **28 - 38**.

Cp*BoZrCH$_2$Ph **(33)** in THF-d_8	CH_2Ph	0.89 (d)	9.3
	N-CH-(CH_3)$_2$	1.02 (d)	6.6
	CH_2Ph	1.58 (d)	9.3
	C$_5$(CH_3)$_5$	1.85 (s)	
	CH_2CH$_2$B	3.10 (d of t)	^{4}J = 4.8
			^{3}J = 2.4
	CH_2CH$_2$B	3.28 (d of t)	^{4}J = 4.5
			^{3}J = 2.4
	N-CH-(CH$_3$)$_2$	3.33 (sept)	6.9
	CH$_2$CH_2B	4.38 (m)	
	CH$_2$CH_2B	5.21 (m)	
	aromatic	6.30-6.90	
CpBoZrCl·LiCl(DME) **(34)** in C$_6$D$_6$	N-CH-(CH_3)$_2$	1.40 (br)	
	CH_2-O-CH$_3$	2.62 (s)	
	CH$_2$-O-CH_3	2.94 (s)	
	N-CH-CH$_3$	3.83 (br)	
	CH_2CH$_2$B	4.45 (br)	
	C$_5H_5$	6.47 (s)	
	CH$_2$CH_2B	6.55 (br)	
Cp*BoZrCl·HCl **(35)** in C$_6$D$_6$	N-CH-(CH_3)$_2$	0.86 (d)	6.6
	N-CH-(CH_3)$_2$	0.89 (d)	6.9
	C$_5$(CH_3)$_5$	1.99 (s)	
	N-CH-CH$_3$	3.19 (m)	6.9
	CH_2CH$_2$B	4.78 (t)	4.2
	CH$_2$CH_2B	5.92 (t)	3.6
	NH-CH-(CH$_3$)$_2$	6.43 (s)	

Table I. (Continued) ^{1}H NMR Spectral Data for complexes **28 - 38**.

Cp*BoZrCl(CH_3I) **(36)** in THF-d_8	N-CH-(CH_3)$_2$	1.17 (m)	
	N-CH_3	2.07 (s)	
	$C_5(CH_3)_5$	2.02 (s)	
	N-C*H*-CH_3	3.23 (sept)	6.6
	N-C*H*-CH_3	3.35 (sept)	6.6
	CH_2CH_2B	3.90 (br)	
	CH_2CH_2B	4.83 (br)	
	CH_2CH_2B	5.71 (br)	
	CH_2CH_2B	6.26 (br)	
Cp*BoZrNH^{t}Bu **(38)** in C_6D_6/ THF-d_8	N-CH-(CH_3)$_2$	1.22 (d)	
	N-C(CH_3)$_3$	1.32 (s)	
	$C_5(CH_3)_5$	2.00 (s)	
	N-C*H*-CH_3	3.34 (br)	
	CH_2CH_2B	4.17 (br)	
	N-*H*	4.63 (s)	
	CH_2CH_2B	4.79 (br)	
	CH_2CH_2B	5.51 (br)	
	CH_2CH_2B	6.52 (br)	

Table II. ^{13}C NMR Spectral Data (Bo = $(C_4H_4BN^iPr_2)$) for complexes **28 - 38**.

Compound	Assignment	δ (ppm)
Cp*BoZrCl·LiCl **(28)**	$C_5(CH_3)_5$	12.27
in C_6D_6/THF-d_8	N-CH-CH_3	24.00
	N-CH-CH_3	47.31
	CH_2-CH_2-B	97.71
	$C_5(CH_3)_5$	119.65
	CH_2-CH_2-B	124.51
Cp*BoZrCH_2TMS **(31)**	CH_2-Si-$(CH_3)_3$	4.74
in C_6D_6	CH_2-Si-$(CH_3)_3$	12.30
	$C_5(CH_3)_5$	12.44
	N-CH-CH_3	24.16
	N-CH-CH_3	47.50
	CH_2-CH_2-B	93.20
	CH_2-CH_2-B	96.74
	CH_2-CH_2-B	109.40
	CH_2-CH_2-B	112.99
	$C_5(CH_3)_5$	119.00
Cp*BoZrPh **(32)**	$C_5(CH_3)_5$	9.67
in THF-d_8	N-CH-CH_3	21.41
	N-CH-CH_3	44.82
	CH_2-CH_2-B	85.06
	CH_2-CH_2-B	92.40
	CH_2-C_6H_5	104.71
	CH_2-C_6H_5	112.92
	$C_5(CH_3)_5$	118.99
	CH_2-C_6H_5	122.24
	CH_2-CH_2-B	123.55
	CH_2-CH_2-B	137.15
	CH_2-C_6H_5	195.06

Table II (Continued) ^{13}C NMR spectra for complexes **28 - 38**.

Cp*BoZrCH$_2$Ph **(33)** in THF-d_8	$C_5(CH_3)_5$	9.56
	N-CH-CH_3	21.50
	N-CH-CH_3	44.77
	CH_2-Ph	50.28
	CH_2-CH_2-B	86.03
	CH_2-CH_2-B	90.53
	CH_2-C_6H_5	106.90
	CH_2-C_6H_5	112.78
	CH_2-C_6H_5	114.99
	$C_5(CH_3)_5$	119.15
	CH_2-CH_2-B	123.95
	CH_2-CH_2-B	125.01
	CH_2-C_6H_5	155.40
CpBoZrCl·LiCl(DME) **(34)** in C_6D_6	N-CH-CH_3	23.96
	N-CH-CH_3	47.69
	CH_2-O-CH_3	59.11
	CH_2-O-CH_3	70.05
	CH_2-CH_2-B	93.76
	C_5H_5	113.78
	CH_2-CH_2-B	126.39
Cp*BoZrCl·HCl **(35)** in C_6D_6	$C_5(CH_3)_5$	12.28
	N-CH-CH_3	20.16
	N-CH-CH_3	20.54
	N-CH-CH_3	51.01
	CH_2-CH_2-B	104.66
	$C_5(CH_3)_5$	116.54
	CH_2-CH_2-B	121.09

Table II (Continued) ^{13}C NMR spectra for complexes **28 - 38**.

Cp*BoZrCl(CH_3I) **(36)** in THF-d_8	$C_5(CH_3)_5$	12.62
	$N(CH_3)CH(CH_3)_2$	17.89
	N-CH-CH_3	21.50
	N-CH-CH_3	22.24
	N-CH-CH_3	22.67
	N-CH-CH_3	23.20
	N-CH-CH_3	23.57
	N-CH-CH_3	24.08
	N-CH-CH_3	45.38
	N-CH-CH_3	53.78
	CH_2-CH_2-B	94.02
	CH_2-CH_2-B	119.48
	$C_5(CH_3)_5$	124.01
	CH_2-CH_2-B	131.28
	CH_2-CH_2-B	140.27

References

1. (a) Marks, T. J. *Prog. Inorg. Chem.* **1979**, *25*, 223. (b) Marks, T. J. *Prog. Inorg. Chem.* **1978**, *24*, 51. (c) Collman, J. P.; Hegedus, L. S.; Norton, J. R.; Finke, R. G. *Principle and Applications of Organotransition Metal Chemistry*. University Science Books., Mill Valley, California, 1987. (c) Coville, N. J.; du Plooy, K. E.; Pickl, W. *Coord. Chem. Rev.* **1992**, *116*, 1. (d) Halterman, R. L. *Chem. Rev.* **1992**, *92*, 965. (e) Janiak, C.; Schumann, H. *Adv. Organomet. Chem.* **1991**, *33*, 291. (f) Poli, R. *Chem. Rev.* **1991**, *91*, 509.

2. Recent work include: (a) Coughlin, E. B.; Bercaw, J. E. *J. Am. Chem. Soc.* **1992**, *114*, 7606. (b) Erker, G.; Aulbach, M.; Knickmeier, M.; Wingbermühle, Krüger, C.; Nolte, M.; Werner, S. *J. Am. Chem. Soc.* **1993**, *115*, 4590. (c) Krauledat, H.; Brintzinger, H. H. *Angew. Chem. Int. Ed. Engl.* **1990**, *29*, 1412. (d) Collins, S.; Hong, Y.; Ramachandran, R.; Taylor, N. J. *Organometallics* **1991**, *10*, 2349. (e) Colletti, S. L.; Halterman, R. L. *Organometallics* **1991**, *10*, 3438.

3. (a) Willoughby, C. A.; Buchwald, S. L. *J. Am. Chem. Soc.* **1992**, *114*, 7562. (b) Schofield, P. A.; Adams, H.; Bailey, N. A.; Cesarotti, E.; White, C. *J. Organomet. Chem.* **1991**, *412*, 273.

4. Gagné, M. R.; Brard, L.; Conticello, V. P.; Giardello, M. A.; Stern, C. L.; Marks, T. J. *Organometallics* **1992**, *11*, 2003.

5. (a) Harrison, K. N.; Marks, T. J. *J. Am. Chem. Soc.* **1992**, *114*, 9220. (b) Pearson, A. J.; Mallik, S.; Pinkerton, A. A.; Adams, J. P.; Zheng, S. *J. Org. Chem.* **1992**, *57*, 2910.

6. Ziegler, K.; Holzkamp, E.; Breil, H.; Martin, H. *Angew. Chem.* **1955**, *67*, 541.

7. Natta, G.; Pino, P.; Corradini, P.; Danusso, F.; Mantica, E.; Mazzanti, G.; Moraglio, G. *J. Am. Chem. Soc.* **1955**, *77*, 1708.

8. *Chemical and Engineering News*, April, 1992.

9. Sinn, H.; Kaminsky, W. *Adv. Organomet. Chem.* **1980**, *18*, 99.

10. Long, W. P.; Breslow, D. S. *Liebigs. Ann. Chem.* **1975**, 463.

11. For a review of Ziegler-Natta polymerizations, see: (a) Boor, J. Jr. *Ziegler-Natta Catalysts and Polymerizations*. Academic Press, London, 1979. (b) Tait, P. J. T. *Comprehensive Polymer Science* Pergamon Press,

Oxford, 1989.

12. (a) Jordan R. F. *Advances in Organometallic Chemistry* **1991**, *32*, 325. (b) Bochmann reference (c) Teuben reference

13. (a) Jordan, R. F.; Dasher, W. E.; Echols, S. F. *J. Am. Chem. Soc.* **1986**, *108*, 1718. (b) Hlatky, G. G.; Turner, H. W.; Eckman, R. R. *J. Am. Chem. Soc.* **1989**, *111*, 2728.

14. Strauss, S. H. *Chem. Rev.* **1993**, *93*, 927.

15. (a) Hlatky, G. G.; Turner, H. W.; Eckman, R. R. *J. Am. Chem. Soc.* **1989**, *111*, 2728. (b) Turner, H. W. *European Patent Application* **1988** *277* 004. (c) Hlatky, G. G.; Turner, H. W. *European Patent Application* 1988 *277* 003.

16. Chien, J. C. W.; Tsai, W-M.; Raush, M. D. *J. Am. Chem. Soc.* **1991**, *113*, 8570.

17. Xinmin, Y.; Stern, C. L.; Marks, T. J. *J. Am. Chem. Soc.* **1991**, *113*, 3623.

18. (a) Watson, P. L. *J. Am. Chem. Soc.* **1982**, *104*, 337. (b) Watson, P. L.; Roe, D. C. *J. Am. Chem. Soc.* **1982**, *104*, 6471.

19. Jeske, G.; Lauke, H.; Mauermann, H.; Swepston, P. N.; Schumann, H.; Marks, T. J. *J. Am. Chem. Soc.* **1985**, *107*, 8091.

20. Thompson, M. E.; Baxter, S. M.; Bulls, A. R.; Burger, B. J.; Nolan, M. C.; Santarsiero, B. D.; Schaefer, W. P.; Bercaw, J. E. *J. Am. Chem. Soc.* **1987**, *109*, 203.

21. Burger, B. J.; Thompson, M. E.; Cotter, W. D.; Bercaw, J. E. *J. Am. Chem. Soc.* **1990**, *112*, 1566.

22. (a) Piers, W. E.; Shapiro, P. J.; Bunel, E. E.; Bercaw, J. E. *Synlett* **1990**, *2*, 74. (b) Bunel, E. E. Ph. D. theis, California Institute of Technology, 1989.

23. Shapiro, P. J.; Bunel, E.; Schaefer, W. P.; Bercaw, J. E. *Organometallics* **1990**, *9*, 867.

24. Shapiro, P. J.; Cotter, W. D.; Bercaw, J. E. Manuscript in preparation.

25. Shapiro, P. J. Ph. D. Thesis, California Institute of Technology, 1990.

26. Behnken, P. E.; Marder, T. B.; Baker, R. T.; Knober, C. B.; Thompson, M. R.; Hawthorne, M. F. *J. Am. Chem. Soc.* **1985**, *107*, 932.

27. Brookhart, M.; Green, M. L. H.; Wong, L.-L. *Prog. Inorg. Chem.* **1988**, *36*, 1.

28. (a) Herberich, G. E.; Boveleth, W.; Heβner, B.; Hostalek, M.; Köffer, D. P. J.; Ohst, H.; Söhnen, D. *Chem. Ber.* **1986**, *119*, 420. (b) Herberich, G. E.; Ohst, H. *Z. Naturforsch* **1983**, *B38*, 1388.

29. (a) Herberich, G. E.; Negele, M.; Ohst, H. *Chem. Ber.* **1991**, *124*, 25. (b) Herberich, G. E.; Hessner, B.; Ohst, H.; Raap, I. A. *J. Organomet. Chem.* **1988**, *348*, 305.

30. Herberich, G. E.; Hessner, B.; Ohst, H. *J. Organomet. Chem.* **1988**, *348*, 305.

31. Kiely, A. F.; Bercaw, J. E. Unpublished results. $Cp^*(C_4H_4BNH^iPr_2)HfCl_2$ exhibits a B-N bond distance of 1.58 Å in which there is no dative interaction between the boron and the nitrogen.

32. Coughlin, E. B. Ph. D. Thesis, California Institute of Technology, 1994.

33. Herberich, G. E.; Negele, M.; Ohst, H. *Chem. Ber.* **1991**, *124*, 25.

34. A variable temperature NMR study showed no changes in the spectra from that obtained at room temperature.

35. Kiely, A. F.; Bercaw, J. E. Unpublished results.

36. Stahl, K-P.; Boche, G.; Massa, W. *J. Organomet. Chem.* **1984**, *277*, 113. It was found that $(\eta^5\text{-}C_5H_4NMe_2)_2Fe$ reacts with two equivalents of CH_3I to afford $[(\eta^5\text{-}C_5H_4NMe_3)_2Fe]I_2$.

37. Burger, B.J.; Bercaw, J. E. In *Experimental Organometallic Chemistry*; Wayda, A. L., Darensbourg, M. Y. Eds.; ACS Symposium Series 357; American Chemical Society, Washington, D. C. 1987.

38. Marvich, R. H.; Brintzinger, H. H. *J. Am. Chem. Soc.* **1971**, *93*, 2046.

39. Lund, E. C.; Livinghouse, T. *Organometallics* **1990**, *9*, 2426.

40. International Tables for X-ray Crystallography, Volume IV, p. 71, p. 147; Birmingham, Kynoch Press, 1974.

Appendix 3. X-ray crystal structure data for $Cp^*(C_4H_4BN^iPr_2)ZrCl{\cdot}LiCl(Et_2O)_2$ (**27**).

Table III. Crystal and Intensity Collection Data for $Cp^*(C_4H_4BN^iPr_2)ZrCl{\cdot}LiCl(Et_2O)_2$ (**27**).

chemical formula	$C_{28}H_{53}BCl_2NO_2ZrLi$
crystal dimension, mm	0.11 X 0.30 X 1.15
crystal system	monoclinic
space group	$P2_1/n$
a,Å	11.013 (5)
b,Å	21.440 (11)
c, Å	14.462 (5)
β, deg	95.91 (3)
V, Å^3	3396.6 (26)
ρ_{calc}, g cm^{-3}	1.20
Z	4
λ,Å	0.711
μ, cm^{-1}	4.98
temp, ^oC	23
2θ rang, deg	2-42
no. of reflections measured, total	7997
R	0.036
GOF	2.44

Table IV. Final Heavy Atom Parameters for $Cp^*(C_4H_4BN^iPr_2)ZrCl\cdot LiCl(Et_2O)_2$ (27).

	x, y, z and $U_{eq}{}^a \times 10^4$			
Atom	x	y	z	U_{eq} or B
Zr	2170(.7)	2008(.3)	4209(.4)	533(2)
Cl1	672(2)	2046(1)	2760(1)	637(5)
Cl2	1212(2)	958(1)	4571(1)	686(6)
Cp1	4481(7)	2048(5)	4480(6)	674(25)
Cp2	4172(8)	2310(4)	3607(7)	746(28)
Cp3	3687(7)	1841(5)	3013(5)	706(27)
Cp4	3654(7)	1298(4)	3518(7)	740(27)
Cp5	4157(7)	1423(4)	4437(6)	646(25)
Cp6	5267(9)	2364(5)	5283(7)	1327(38)
Cp7	4521(9)	2948(5)	3305(8)	1394(39)
Cp8	3365(9)	1913(6)	1972(6)	1513(47)
Cp9	3318(9)	648(5)	3155(7)	1384(39)
Cp10	4355(8)	945(5)	5202(7)	1144(33)
C1	2313(7)	3022(4)	4924(5)	665(23)
C2	2481(9)	2563(5)	5618(6)	878(33)
C3	1397(11)	2255(4)	5687(6)	862(34)
C4	466(7)	2478(4)	5013(5)	667(23)
B	956(8)	3063(4)	4589(5)	544(25)
N	308(6)	3512(3)	3991(4)	599(19)
C5	−1002(10)	3498(4)	3810(7)	1003(34)

Table IV. (Continued)

C6	−1551(9)	3341(5)	2886(7)	1392(41)
C7	−1699(9)	3871(5)	4417(6)	1243(36)
C8	876(11)	4046(4)	3621(7)	1103(40)
C9	1301(9)	4540(4)	4244(7)	1201(35)
C10	1500(10)	3920(5)	2802(8)	1289(39)
Li	−258(12)	1107(6)	3240(9)	737(40)
O1	−1956(5)	1212(3)	3426(4)	1191(23)
C11	−2729(12)	1520(6)	2645(9)	11.7(3) *
C12	−3458(12)	1070(6)	2120(9)	13.8(4) *
C13	−2589(16)	1095(8)	4145(14)	19.3(6) *
C14	−2060(13)	934(6)	4978(10)	14.7(4) *
O2	−182(6)	436(3)	2306(5)	1179(23)
C15	−394(19)	604(9)	1282(15)	20.5(8) *
C16	361(17)	724(8)	897(12)	18.1(6) *
C17	−84(22)	−197(12)	2488(15)	24.6(9) *
C18	−622(17)	−404(8)	3015(13)	18.8(6) *

[a] $U_{eq} = \frac{1}{3}\sum_i \sum_j [U_{ij}(a_i^* a_j^*)(\vec{a}_i \cdot \vec{a}_j)]$

* Isotropic displacement parameter, B

Table V. Anisotropic Displacement Parameters for $Cp^*(C_4H_4BN^iPr_2)ZrCl{\cdot}LiCl(Et_2O)_2$ (**27**).

Atom	U_{11}	U_{22}	U_{33}	U_{12}	U_{13}	U_{23}
Zr	606(5)	574(5)	417(4)	42(5)	46(3)	−6(5)
Cl1	689(13)	706(13)	501(11)	17(13)	−8(10)	58(11)
Cl2	669(15)	711(14)	680(14)	21(12)	81(11)	166(11)
Cp1	533(51)	689(64)	774(63)	70(53)	−64(44)	−169(58)
Cp2	594(61)	643(61)	1017(77)	−69(50)	166(56)	178(62)
Cp3	540(56)	1012(81)	574(57)	−14(54)	92(45)	44(58)
Cp4	643(61)	729(67)	880(72)	−125(51)	230(55)	−393(59)
Cp5	628(58)	656(62)	657(63)	162(49)	87(48)	59(50)
Cp6	945(79)	1600(94)	1330(89)	130(69)	−399(69)	−720(73)
Cp7	987(78)	1039(78)	2216(117)	141(74)	455(79)	414(85)
Cp8	949(75)	3052(146)	562(58)	−47(93)	192(54)	167(83)
Cp9	1005(82)	1312(89)	1921(108)	−257(68)	560(78)	−1024(80)
Cp10	855(72)	1309(82)	1267(82)	351(64)	107(64)	427(68)
C1	800(62)	660(52)	518(48)	105(54)	−12(43)	−89(47)
C2	1040(87)	1044(79)	519(62)	436(68)	−62(62)	−166(56)
C3	1357(98)	900(75)	376(52)	432(69)	308(63)	94(46)
C4	756(63)	680(58)	592(53)	146(50)	202(50)	−78(45)
B	701(69)	495(62)	433(50)	116(61)	37(49)	−105(52)
N	672(51)	465(42)	639(43)	42(38)	−40(38)	−5(34)
C5	869(81)	1283(87)	820(71)	404(69)	−90(63)	−150(62)
C6	1078(89)	1883(113)	1176(88)	−62(78)	−73(74)	−587(77)
C7	952(77)	1749(102)	1038(78)	171(75)	153(65)	−343(72)
C8	1929(117)	547(63)	839(75)	−111(72)	165(75)	−142(58)
C9	1306(91)	857(71)	1479(91)	−216(66)	335(75)	−417(68)
C10	1323(97)	1090(85)	1507(103)	−194(73)	406(82)	−49(74)
Li	664(98)	659(92)	870(100)	18(76)	−13(82)	−49(78)
O1	791(47)	1721(64)	1068(51)	−180(44)	134(41)	459(47)
O2	1215(56)	937(49)	1326(59)	−148(42)	−150(46)	243(43)

$U_{i,j}$ values have been multiplied by 10^4

The form of the displacement factor is:

$$\exp -2\pi^2(U_{11}h^2a^{*2} + U_{22}k^2b^{*2} + U_{33}\ell^2c^{*2} + 2U_{12}hka^*b^* + 2U_{13}h\ell a^*c^* + 2U_{23}k\ell b^*c^*)$$

Table VI. Complete Distances and Angles for $Cp^*(C_4H_4BN^iPr_2)ZrCl{\cdot}LiCl(Et_2O)_2$ (**27**).

		Distance(Å)			Distance(Å)
Zr	-Cl1	2.531(2)	N	-C8	1.434(12)
Zr	-Cl2	2.563(2)	C5	-C6	1.448(14)
Zr	-Cp	2.236	C5	-C7	1.463(14)
Zr	-Cp1	2.535(8)	C8	-C9	1.437(14)
Zr	-Cp2	2.536(9)	C8	-C10	1.454(14)
Zr	-Cp3	2.550(9)	O1	-C11	1.496(14)
Zr	-Cp4	2.515(9)	O1	-C13	1.334(19)
Zr	-Cp5	2.514(8)	C11	-C12	1.423(18)
Zr	-Cb	2.165	C13	-C14	1.33(2)
Zr	-C1	2.405(8)	O2	-C15	1.52(2)
Zr	-C2	2.354(10)	O2	-C17	1.38(3)
Zr	-C3	2.439(10)	C15	-C16	1.08(3)
Zr	-C4	2.518(8)	C17	-C18	1.10(3)
Zr	-B	2.714(9)	Cp6	-Hp1A	0.946
Li	-Cl1	2.393(13)	Cp6	-Hp1B	0.955
Li	-Cl2	2.405(13)	Cp6	-Hp1C	0.948
Li	-O1	1.930(14)	Cp7	-Hp2A	0.956
Li	-O2	1.982(15)	Cp7	-Hp2B	0.945
Cp1	-Cp2	1.390(12)	Cp7	-Hp2C	0.944
Cp1	-Cp5	1.387(12)	Cp8	-Hp3A	0.954
Cp1	-Cp6	1.533(13)	Cp8	-Hp3B	0.947
Cp2	-Cp3	1.393(13)	Cp8	-Hp3C	0.947
Cp2	-Cp7	1.497(14)	Cp9	-Hp4A	0.932
Cp3	-Cp4	1.376(12)	Cp9	-Hp4B	0.951
Cp3	-Cp8	1.520(13)	Cp9	-Hp4C	0.959
Cp4	-Cp5	1.412(12)	Cp10	-Hp5A	0.948
Cp4	-Cp9	1.520(13)	Cp10	-Hp5B	0.949
Cp5	-Cp10	1.508(13)	Cp10	-Hp5C	0.954
C1	-C2	1.404(12)	C1	-H1	0.952
C1	-B	1.526(12)	C2	-H2	0.952
C2	-C3	1.377(14)	C3	-H3	0.953
C3	-C4	1.423(12)	C4	-H4	0.954
C4	-B	1.520(12)	C5	-H5	0.955
B	-N	1.433(11)	C6	-H6A	0.949
N	-C5	1.440(11)	C6	-H6B	0.949

Table VI. (Continued)

C6	-H6C	0.937	Cl1	-Zr	-Cl2	87.1(1)
C7	-H7A	0.945	Cp	-Zr	-Cb	132.7
C7	-H7B	0.940	Cp	-Zr	-Cl1	109.3
C7	-H7C	0.950	Cp	-Zr	-Cl2	105.8
C8	-H8	0.954	Cb	-Zr	-Cl1	106.2
C9	-H9A	0.950	Cb	-Zr	-Cl2	106.3
C9	-H9B	0.941	Cl1	-Li	-Cl2	94.1(5)
C9	-H9C	0.951	Cl1	-Li	-O1	113.1(6)
C10	-H10A	0.937	Cl1	-Li	-O2	111.3(6)
C10	-H10B	0.954	Cl2	-Li	-O1	119.1(6)
C10	-H10C	0.942	Cl2	-Li	-O2	112.1(6)
C11	-H11A	0.949	O1	-Li	-O2	106.8(7)
C11	-H11B	0.947	Zr	-Cl1	-Li	89.7(3)
C12	-H12A	0.949	Zr	-Cl2	-Li	88.7(3)
C12	-H12B	0.942	Cp5	-Cp1	-Cp2	108.2(8)
C12	-H12C	0.942	Cp6	-Cp1	-Cp2	125.2(8)
C13	-H13A	0.975	Cp6	-Cp1	-Cp5	125.7(8)
C13	-H13B	0.920	Cp3	-Cp2	-Cp1	108.1(8)
C14	-H14A	0.947	Cp7	-Cp2	-Cp1	125.9(8)
C14	-H14B	0.970	Cp7	-Cp2	-Cp3	125.0(8)
C14	-H14C	0.916	Cp4	-Cp3	-Cp2	108.3(8)
C15	-H15A	0.997	Cp8	-Cp3	-Cp2	125.0(8)
C15	-H15B	0.920	Cp8	-Cp3	-Cp4	126.5(8)
C15	-H16B	1.598	Cp5	-Cp4	-Cp3	108.0(8)
C16	-H16A	0.969	Cp9	-Cp4	-Cp3	127.6(8)
C16	-H16B	0.954	Cp9	-Cp4	-Cp5	123.9(8)
C16	-H16C	0.888	Cp4	-Cp5	-Cp1	107.5(7)
C17	-H17A	1.007	Cp10	-Cp5	-Cp1	127.4(8)
C17	-H17B	0.911	Cp10	-Cp5	-Cp4	125.1(8)
C18	-H18A	0.955	B	-C1	-C2	108.7(7)
C18	-H18B	0.973	C3	-C2	-C1	109.7(8)
C18	-H18C	0.883	C4	-C3	-C2	111.0(8)
			B	-C4	-C3	107.0(7)
			C4	-B	-C1	101.6(7)
			N	-B	-C1	129.9(7)

Table VI. (Continued)

N	-B	-C4	128.5(7)	Hp4B	-Cp9	-Cp4	107.8
C5	-N	-B	121.6(7)	Hp4C	-Cp9	-Cp4	107.5
C8	-N	-B	123.5(7)	Hp4B	-Cp9	-Hp4A	111.8
C8	-N	-C5	114.6(7)	Hp4C	-Cp9	-Hp4A	111.2
C6	-C5	-N	119.2(8)	Hp4C	-Cp9	-Hp4B	109.5
C7	-C5	-N	117.2(8)	Hp5A	-Cp10	-Cp5	108.7
C7	-C5	-C6	119.1(9)	Hp5B	-Cp10	-Cp5	108.8
C9	-C8	-N	118.7(8)	Hp5C	-Cp10	-Cp5	108.5
C10	-C8	-N	114.6(8)	Hp5B	-Cp10	-Hp5A	110.6
C10	-C8	-C9	119.8(9)	Hp5C	-Cp10	-Hp5A	110.2
C13	-O1	-C11	111.7(10)	Hp5C	-Cp10	-Hp5B	110.0
C12	-C11	-O1	110.4(10)	H1	-C1	-C2	125.6
C14	-C13	-O1	122.7(15)	H1	-C1	-B	125.8
C17	-O2	-C15	114.8(13)	H2	-C2	-C1	125.5
C16	-C15	-O2	120.7(19)	H2	-C2	-C3	124.8
C18	-C17	-O2	119.1(22)	H3	-C3	-C2	124.6
Hp1A	-Cp6	-Cp1	108.8	H3	-C3	-C4	124.4
Hp1B	-Cp6	-Cp1	108.3	H4	-C4	-C3	126.2
Hp1C	-Cp6	-Cp1	108.7	H4	-C4	-B	126.8
Hp1B	-Cp6	-Hp1A	110.2	H5	-C5	-N	99.7
Hp1C	-Cp6	-Hp1A	110.7	H5	-C5	-C6	93.9
Hp1C	-Cp6	-Hp1B	110.1	H5	-C5	-C7	97.7
Hp2A	-Cp7	-Cp2	108.0	H6A	-C6	-C5	108.1
Hp2B	-Cp7	-Cp2	108.4	H6B	-C6	-C5	108.6
Hp2C	-Cp7	-Cp2	108.7	H6C	-C6	-C5	108.9
Hp2B	-Cp7	-Hp2A	110.1	H6B	-C6	-H6A	109.7
Hp2C	-Cp7	-Hp2A	110.3	H6C	-C6	-H6A	110.7
Hp2C	-Cp7	-Hp2B	111.2	H6C	-C6	-H6B	110.7
Hp3A	-Cp8	-Cp3	108.4	H7A	-C7	-C5	108.5
Hp3B	-Cp8	-Cp3	108.6	H7B	-C7	-C5	108.8
Hp3C	-Cp8	-Cp3	108.7	H7C	-C7	-C5	108.6
Hp3B	-Cp8	-Hp3A	110.2	H7B	-C7	-H7A	110.7
Hp3C	-Cp8	-Hp3A	110.1	H7C	-C7	-H7A	109.9
Hp3C	-Cp8	-Hp3B	110.8	H7C	-C7	-H7B	110.3
Hp4A	-Cp9	-Cp4	109.0	H8	-C8	-N	100.6

Table VI. (Continued)

H8	-C8	-C9	93.8	H14C	-C14	-H14B	110.7
H8	-C8	-C10	102.1	H15A	-C15	-O2	100.5
H9A	-C9	-C8	109.2	H15B	-C15	-O2	104.8
H9B	-C9	-C8	109.2	H16B	-C15	-O2	103.9
H9C	-C9	-C8	108.7	H15A	-C15	-C16	105.8
H9B	-C9	-H9A	110.2	H15B	-C15	-C16	115.5
H9C	-C9	-H9A	109.4	H16B	-C15	-C16	35.5
H9C	-C9	-H9B	110.1	H15B	-C15	-H15A	107.9
H10A	-C10	-C8	109.2	H16B	-C15	-H15A	141.2
H10B	-C10	-C8	107.8	H16B	-C15	-H15B	94.4
H10C	-C10	-C8	108.5	H16A	-C16	-C15	103.4
H10B	-C10	-H10A	110.2	H16B	-C16	-C15	103.6
H10C	-C10	-H10A	111.3	H16C	-C16	-C15	113.2
H10C	-C10	-H10B	109.8	H16B	-C16	-H16A	107.6
H11A	-C11	-O1	109.1	H16C	-C16	-H16A	113.3
H11B	-C11	-O1	109.1	H16C	-C16	-H16B	114.8
H11A	-C11	-C12	109.1	H17A	-C17	-O2	101.7
H11B	-C11	-C12	109.3	H17B	-C17	-O2	107.2
H11B	-C11	-H11A	109.9	H17A	-C17	-C18	103.7
H12A	-C12	-C11	108.1	H17B	-C17	-C18	115.8
H12B	-C12	-C11	108.7	H17B	-C17	-H17A	107.9
H12C	-C12	-C11	108.8	H18A	-C18	-C17	104.8
H12B	-C12	-H12A	110.2	H18B	-C18	-C17	101.6
H12C	-C12	-H12A	110.2	H18C	-C18	-C17	113.6
H12C	-C12	-H12B	110.8	H18B	-C18	-H18A	107.2
H13A	-C13	-O1	103.3	H18C	-C18	-H18A	115.1
H13B	-C13	-O1	106.7	H18C	-C18	-H18B	113.3
H13A	-C13	-C14	103.9				
H13B	-C13	-C14	109.7				
H13B	-C13	-H13A	109.9				
H14A	-C14	-C13	107.7				
H14B	-C14	-C13	105.7				
H14C	-C14	-C13	111.7				
H14B	-C14	-H14A	108.1				
H14C	-C14	-H14A	112.7				

Table VII. Assigned Hydrogen Atom Parameters for $Cp^*(C_4H_4BN^iPr_2)ZrCl\cdot LiCl(Et_2O)_2$ (**27**).

	x, y and $z \times 10^4$			
Atom	x	y	z	B
HM1A	6096	2340	5167	12.1
HM1B	5146	2149	5844	12.1
HM1C	5017	2785	5321	12.1
HM2A	3888	3095	2856	12.4
HM2B	5264	2917	3035	12.4
HM2C	4600	3213	3829	12.4
HM3A	3206	2343	1841	13.7
HM3B	2661	1671	1791	13.7
HM3C	4035	1775	1664	13.7
HM4A	2590	526	3378	12.6
HM4B	3972	376	3359	12.6
HM4C	3232	669	2489	12.6
HM5A	4844	1124	5711	10.3
HM5B	4751	592	4972	10.3
HM5C	3580	827	5385	10.3
H1	2943	3268	4702	5.9
H2	3228	2475	5986	8.0
H3	1284	1935	6128	7.8
H4	−319	2295	4863	6.0
H5	−1161	3098	4062	9.1
H6A	−983	3097	2591	12.6
H6B	−2268	3105	2941	12.6
H6C	−1737	3710	2554	12.6
H7A	−1217	3930	4990	11.2
H7B	−1891	4256	4128	11.2
H7C	−2423	3651	4515	11.2
H8	175	4272	3365	10.1
H9A	798	4560	4739	10.8
H9B	2115	4460	4479	10.8
H9C	1248	4923	3911	10.8
H10A	1112	3588	2471	11.5

Table VII. (Continued)

H10B	1455	4288	2429	11.5
H10C	2322	3826	2997	11.5
H11A	−3247	1816	2894	13.5
H11B	−2216	1723	2253	13.5
H12A	−3934	1282	1633	15.8
H12B	−2938	779	1872	15.8
H12C	−3969	872	2514	15.8
H13A	−2973	1494	4253	22.4
H13B	−3176	806	3945	22.4
H14A	−2685	880	5375	17.1
H14B	−1688	530	4895	17.1
H14C	−1484	1219	5203	17.1
H15A	−718	201	1016	16.0
H15B	−1027	887	1242	16.0
H16A	−24	797	274	15.8
H16B	626	1118	1151	15.8
H16C	935	432	924	15.8
H17A	−461	−382	1886	28.8
H17B	727	−293	2548	28.8
H18A	−428	−838	3016	20.9
H18B	−221	−227	3587	20.9
H18C	−1409	−316	2924	20.9